NTNU
Norwegian University of
Science and Technology

Earthquake Response Analysis of Pile Supported Structures

Correspondence of PLAXIS 2D with Eurocode 8

Mohsin Ara Toma

Geotechnics and Geohazards
Submission date: June 2017
Supervisor: Gudmund Reidar Eiksund, IBM

Norwegian University of Science and Technology
Department of Civil and Environmental Engineering

NORGES TEKNISK-
NATURVITENSKAPELIGE UNIVERSITET
INSTITUTT FOR BYGG OG MILJØTEKNIKK

Thesis title:	Date: **18.06.2017**	
Earthquake Response Analysis of Pile Supported Structures:	Total page number (inc. appendices): **138**	
Correspondence of PLAXIS 2D with Eurocode 8	Master Thesis	x
Name: Mohsin Ara Toma		
Professor in charge/supervisor: Gudmund Reidar Eiksund		

Abstract:

Earthquake response of a structure on relatively soft soil is influenced by the soil material properties and type of foundation i.e. shallow or deep foundation. The design recommendations of Eurocode 8 provide a conservative method to determine seismic loads for spectral analysis approach assuming a fixed base structure. This thesis attempts to evaluate the influence of the piles on the response of a structure in terms of acceleration and base shear force. The shear force induced at the shallow base is determined using finite element program PLAXIS 2D and compared with the calculation based on Eurocode 8. The aim is to investigate the correspondence of numerical analysis in PLAXIS 2D with simplified analysis method of Eurocode 8 (NS-EN 1998-1:2004+A1:2013+NA:2014).

A representative soil model is constructed with proper boundary conditions for dynamic analysis in PLAXIS 2D based on previous researches and recommendations. The choice of boundary conditions is tested with a simpler material model and a harmonic motion and verified with theoretical solution of amplitude factor. The next step is to perform a free field site response analysis of the main soil model for an input motion of 0.1g to evaluate the soil behavior during earthquake. The results are compared with one dimensional ground response analysis in DEEPSOIL and reasonable agreement is observed.

The soil model is then provided with the structures to evaluate the effect of the piles. Four cases consisting of two different structures with two different foundation systems (shallow foundation and piled raft) are simulated on the given soil condition. Free vibration analyses are carried out for all the cases to determine natural frequencies or period of vibration of the structures. The obtained results are compared with logarithmic decrement and Eurocode 8. The resulting natural period of vibrations are 0.33 seconds for the single-story structure and 0.6 seconds for the four-story structure. This indicates that the numerical analysis results are consistent with theory and Eurocode 8.

Results of full dynamic analyses show that the foundation type has considerable influence on seismic response of a structure. For a single-story structure, the acceleration increases over 40% and the for the four-story structure it is over 45%. Calculated shear force at the bottom of the rigid base is increased by almost 100% due to the piles for both structures. This highlights the fact that specific analysis for design base shear is required for pile supported structures to ensure safety against earthquakes. However, the obtained values of base shear for all the cases are lower than the values calculated based on Eurocode 8 as expected. Although for shallow foundation, Eurocode 8 provides overestimation which may not be cost effective. Therefore, it can be inferred that the numerical analysis using PLAXIS 2D demonstrates reasonable correspondence with Eurocode 8. Further studies can be conducted to obtain spectral behavior for different kinds of foundations.

Key words:

1. Earthquake
2. Pile foundation
3. Eurocode 8
4. PLAXIS 2D

Mohsin Ara Toma

(sign.)

NTNU
Faculty of Engineering Science and Technology
Institute of Civil and Environmental Engineering

MASTER DEGREE THESIS

Mohsin Ara Toma

Earthquake Response Analysis of Pile Supported Structures:
Correspondence of PLAXIS 2D with Eurocode 8

BACKGROUND

Pile foundations are mainly provided to increase load bearing capacity. The design of pile foundations usually considers the load bearing under static condition. In case of an earthquake, the loading condition become dynamic and the behavior of structure supported by the piles may change. For this reason, it is necessary to study how the presence of pile influences the response of a structure.

When compared to the global scale, Norway is less vulnerable to seismic actions. For this reason, seismic design considerations and related studies are limited. However, the design recommendation introduced by Eurocode 8 requires strict control of earthquake load effect. There are design specifications to calculated in seismic load by a simplified method according to Eurocode 8. This thesis attempts to observe to what extent this method corresponds with the values that is obtained from numerical analysis.

TASK

The aim of this thesis is to evaluate the effect of the piles on earthquake response of a structure and examine the correspondence with Eurocode 8. To achieve this goal, a detailed seismic analysis is performed for two structures with different natural frequencies on a specific soil condition, first with shallow and then with pile foundations. The numerical analysis is carried out in the FEM program PLAXIS 2D and the shear force induced at the interface of the rigid basement is compared with the calculation based on Eurocode 8. The effect of piles on the earthquake response is discussed in terms of change in acceleration and shear force at the base that is induced by the earthquake. The concerning part of Eurocode is Eurocode 8; div. NS-EN 1998-1:2004+A1:2013+NA:2014, Part 1 (General Rules, Seismic Loads and Rules for Buildings).

Task description

- Free field site response analysis to evaluate the behavior of soil profile during earthquake and comparing the result with one dimensional analysis in DEEPSOIL.
- Free vibration analysis to determine natural frequency of the structures.
- Seismic response analysis of the structures with shallow and pile foundations and evaluating the effect of the piles.
- Calculation of base shear force based on simplified method recommended by Eurocode 8.
- Shear force calculation on the rigid base of the structure from PLAXIS output and evaluating the correspondence with the calculation based on Eurocode 8.

NTNU
Faculty of Engineering Science and Technology
Institute of Civil and Environmental Engineering

Objective and purpose

The thesis will attempt to answer:

1) How piles change the seismic response of structure.
2) To what extent the base shear calculated from FEM analysis in PLAXIS 2D corresponds with the simplified method suggested by Eurocode 8.

Professor in charge: Gudmund Reidar Eiksund

Department of Civil and Transport Engineering, NTNU

Date: 15.06.2017

Professor in charge (signature)

PREFACE

This thesis is submitted to the Department of Civil and Environmental Engineering, Norwegian University of Science and Technology (NTNU), in the partial fulfillment for the Master of Science (MSc) degree in Geotechnics and Geohazards. The study was carried out in the spring semester of 2017 under supervision of professor Gudmund Reidar Eiksund.

I would like to express my sincere gratitude to my supervisor, Gudmund Reidar Eiksund, for his continuous support and guidance throughout the thesis period. He always had an open door for discussions and patiently guided me at every stage of the research, starting from the numerical modeling in PLAXIS 2D to the interpretation of the results. It was a great experience to work under his supervision.

I would also like to thank Amir M. Kaynia for his valuable suggestions. I am also grateful to Steinar Nordal and Arnfinn Emdal for helping me to have a deeper insight towards my results.

Finally, I would like to thank my family and friends for their continuous support and love and everyone who supported me during this period.

Mohsin Ara Toma

Mohsin Ara Toma
Trondheim, 18 June 2017

ABSTRACT

Earthquake response of a structure on relatively soft soil is influenced by the soil material properties and type of foundation i.e. shallow or deep foundation. The design recommendations of Eurocode 8 provide a conservative method to determine seismic loads for spectral analysis approach assuming a fixed base structure. This thesis attempts to evaluate the influence of the piles on the response of a structure in terms of acceleration and base shear force. The shear force induced at the shallow base is determined using finite element program PLAXIS 2D and compared with the calculation based on Eurocode 8. The aim is to investigate the correspondence of numerical analysis in PLAXIS 2D with simplified analysis method of Eurocode 8 (NS-EN 1998-1:2004+A1:2013+NA:2014).

A representative soil model is constructed with proper boundary conditions for dynamic analysis in PLAXIS 2D based on previous researches and recommendations. The choice of boundary conditions is tested with a simpler material model and a harmonic motion and verified with theoretical solution of amplitude factor. The next step is to perform a free field site response analysis of the main soil model for an input motion of 0.1g to evaluate the soil behavior during earthquake. The results are compared with one dimensional ground response analysis in DEEPSOIL and reasonable agreement is observed.

The soil model is then provided with the structures to evaluate the effect of the piles. Four cases consisting of two different structures with two different foundation systems (shallow foundation and piled raft) are simulated on the given soil condition. Free vibration analyses are carried out for all the cases to determine natural frequencies or period of vibration of the structures. The obtained results are compared with logarithmic decrement and Eurocode 8. The resulting natural period of vibrations are 0.33 seconds for the single-story structure and 0.6 seconds for the four-story structure. This indicates that the numerical analysis results are consistent with theory and Eurocode 8.

Results of full dynamic analyses show that the foundation type has considerable influence on seismic response of a structure. For a single-story structure, the acceleration increases over 40% and the for the four-story structure it is over 45%. Calculated shear force at the bottom of the rigid base is increased by almost 100% due to the piles for both structures. This highlights the fact that specific analysis for design base shear is required for pile supported structures to ensure safety against earthquakes. However, the obtained values of base shear

for all the cases are lower than the values calculated based on Eurocode 8 as expected. Although for shallow foundation, Eurocode 8 provides overestimation which may not be cost effective. Therefore, it can be inferred that the numerical analysis using PLAXIS 2D demonstrates reasonable correspondence with Eurocode 8. Further studies can be conducted to obtain spectral behavior for different kinds of foundations.

TABLE OF CONTENTS

Preface i
Abstract iii
Table of Contents v
List of Figures vii
List of Tables xi
List of Symbols xiii
1 Introduction 1
1.1 Background 1
1.2 Research Objective 2
1.3 Approach 3
1.4 Research Boundaries 4
1.5 Thesis Outline 5
2 Literature Review 7
2.1 Geotechnical Earthquake Engineering 7
2.1.1 Seismic Wave Propagation 7
2.1.2 Equation of Motion 9
2.1.3 Damping 11
2.1.4 Free Vibration 12
2.1.5 Non-linear Stress-Strain Behavior of Soil 13
2.1.6 Site Response Analysis 13
2.1.7 Response Spectrum Analysis 21
2.1.8 Typical Pile Foundation Damage During Earthquake 24
2.2 FEM Analysis In PLAXIS 25
2.2.1 Material Models 26
2.2.2 Dynamic Analysis 29
2.2.3 Modelling Pile in PLAXIS 2D 31
2.3 Eurocode 8 38
2.3.1 Identification of Ground Types 39
2.3.2 Basic Representation of Seismic Action 40
2.3.3 Base Shear Force Calculation 44
3 Construction of FEM Models and Parameters 47
3.1 Concept and Geometry 47
3.2 Material Properties 50

3.2.1 Shear Wave Velocity and Soil Type 53
3.2.2 Damping Parameters 56
3.3 Construction of Pile Using Embedded Beam Row 57
3.4 Dynamic Analysis in PLAXIS 2D 59
3.4.1 Mesh generation 59
3.4.2 Stage Construction 59
3.4.3 Loading and Boundary Condition 60
3.4.4 Test on Boundary Condition 61
4 Analysis and Results 63
4.1 Free Field Analysis 63
4.1.1 Two-Dimensional Analysis in PLAXIS 64
4.1.2 One Dimensional Analysis in DEEPSOIL 66
4.1.3 Summary and Discussion 68
4.1.4 Additional Information 70
4.2 Free Vibration Analysis 72
4.2.1 Summary and Discussion 72
4.3 Seismic Response Analysis in PLAXIS 75
4.3.1 Single Story Structure with shallow foundation 75
4.3.2 Single Story Structure with Piled raft 76
4.3.3 Four Story Structure with shallow foundation 78
4.3.4 Four Story Structure with Piled Raft 79
4.3.5 Summary and Discussion 80
4.4 Calculation of Shear Force at The Shallow Base 82
4.4.1 Eurocode 8 82
4.4.2 PLAXIS 2D 85
4.4.3 Summary and Discussion 89
5 Discussion and Conclusion 91
5.1 Summary 91
5.2 Discussion and Conclusion 92
6 Recommendation for Further Work 95
Bibliography 97
Acronyms 101
Appendices 103

LIST OF FIGURES

Figure 2-1 (a) P-wave (b) S-wave (Kramer, 1996) *8*
Figure 2-2 (a) Rayleigh wave (b) Love wave (Kramer, 1996) *8*
Figure 2-3 One dimensional wave propagation in a constraint infinite rod (Kramer, 1996). *9*
Figure 2-4 Earthquake excitation on a simple SDOF system (Clough & Penzien, 1993) *10*
Figure 2-5 Effect of damping on free vibration (Chopra, 2007) *13*
Figure 2-6 Schematic representation of stress-strain model used in equivalent-linear model. (Bardet et. al.,2000) *14*
Figure 2-7 Hysteretic behavior of soil under cyclic loading (Laera & Brinkgreve 2015) *15*
Figure 2-8 shear modulus, G, as the resistance to shear deformation γ because of shear force τ (Brandt, 2014) *16*
Figure 2-9 (a) Back-bone curve (b) Modulus reduction curve (Kramer, 1996) *16*
Figure 2-10 Vucetic & Dobry (1991) G/Gmax - γc and ξ - γc curves equations (charts from Guerreiro et al. (2012)) *17*
Figure 2-11 Wave propagation in a linear elastic uniform layer (Kramer, 1996) *18*
Figure 2-12 Amplification of a damped uniform layer (Kramer, 1996) *19*
Figure 2-13 Displacement patterns for waves at first (n=0), second (n=1) and third (n=2) natural frequency (Kramer, 1996) *19*
Figure 2-14 Iteration toward strain compatible shear modulus and damping ratio (Kramer, 1996) *20*
Figure 2-15 Construction of the response spectrum from ("QuakeManager Wiki," 2015) after Stensløkken (2016) *22*
Figure 2-16 Pile foundation damage due to strong earthquakes (Hamada 1991; Mizuno 1987) figure from (Teguh, 2006) *24*
Figure 2-17 Estimation of bending moment in piles caused by ground deformation (J. Hamada, 2015) *25*
Figure 2-18 Triangular element with 6 and 15 nodes (Nordal, 2016) *26*
Figure 2-19 Definition of stiffness parameters (a) for drained triaxial test result (b) oedometer test result ("PLAXIS 2D Material Models Manual," 2016) *27*
Figure 2-20 Secant and tangent shear modulus reduction curve ("PLAXIS 2D Material Models Manual," 2016) *29*

Figure 2-21 Embedded beam in 3D mesh and elastic zone around the beam (Kwaak, 2015) 33
Figure 2-22 Soil structure interaction by special interface elements, concept of embedded beam (row) after Sluis (2012) 34
Figure 2-23 Principle of interface by (Sluis et al., 2014) 34
Figure 2-24 Application areas of PLAXIS 2D and 3D modelling a pile row with various structural elements (Sluis, 2012) 36
Figure 2-25 Deformation of pile (left) and soil around a pile (right) under active lateral load (Fleming et al., 2008) 36
Figure 2-26 Bearing resistance of pile (Eiksund, 2016) 37
Figure 2-27 Recommended horizontal elastic response spectra in Norway for ground type A to E (Figure NA.3(903) in NS-EN 1998-1:2004+A1:2013+NA:2014) 41
Figure 2-28 Effect of behavior factor on the shape of design response spectrum (Bisch et al., 2012) 44
Figure 3-1 Schematic presentation of the model concept with single story structure. 48
Figure 3-2 Model 1: Soil profile without structure 48
Figure 3-3 Model 2: Single-story structure with shallow foundation 48
Figure 3-4 Model 3: Single-story structure with piled raft 49
Figure 3-5 Model 4: Four-story structure with shallow foundation 49
Figure 3-6 Model 5: Four-story structure with piled raft 49
Figure 3-7 Cu parameter compared to MC formula 51
Figure 3-8 Modulus reduction curve for (a) clay and (b) sand, damping cure for (c) clay and (d) sand 52
Figure 3-9 Small strain stiffness of clay layer 54
Figure 3-10 Shear wave velocity of clay layer 54
Figure 3-11 Small strain stiffness of sand layer 55
Figure 3-12 Shear wave velocity of sand layer 55
Figure 3-13 Rayleigh damping curve obtained from PLAXIS 56
Figure 3-14 side friction resistance along pile length (sharp change indicates change in soil layer) 58
Figure 3-15 Lateral resistance along pile length 58
Figure 3-16 Time history of input motion from SIMQKE 61

Figure 3-17 Deformed mesh and selected nodes of the test model *62*
Figure 3-18 Acceleration at point A and Point B for f=3 Hz *62*
Figure 3-19 Amplification factor over frequency ratio *62*
Figure 4-1 Generated mesh with selected nodes *64*
Figure 4-2 Free field response in terms of acceleration *65*
Figure 4-3 Deformation pattern of free field motion at dynamic time 10.01s (when maximum acceleration occurs at the surface). Scaled up 500 times. *65*
Figure 4-4 : PSA response spectrum at point B on the surface *65*
Figure 4-5 One dimensional site response in terms of acceleration *67*
Figure 4-6 : (a) Input profile in DEEPSOIL (b) PSA response spectrum at point B on the surface *67*
Figure 4-7 Acceleration from DEEPSOIL and PLAXIS at the surface *68*
Figure 4-8 PSA response spectra from DEEPSOIL and PLAXIS at the surface *69*
Figure 4-9 FFT at the top and bottom of the mesh *71*
Figure 4-10 Relative displacement response spectrum *71*
Figure 4-11 Free vibration of single story structure *72*
Figure 4-12 Free vibration of four story structure *72*
Figure 4-13 Natural period of vibration of four story structure *73*
Figure 4-14 Natural period of vibration of single story structure with shallow foundation . *74*
Figure 4-15 deformed mesh at maximum acceleration at t =10.03s. *75*
Figure 4-16 Time-acceleration curve of single-story structure *76*
Figure 4-17 Time-displacement curve of single-story structure *76*
Figure 4-18 deformed mesh at maximum acceleration at t =10.65s. *77*
Figure 4-19 Time acceleration curve of Single-story Structure with Piled raft *77*
Figure 4-20 Time-displacement curve of single story structure with piled raft *77*
Figure 4-21 deformed mesh at maximum acceleration on the top at t= 10.03s scaled up 100 times *78*
Figure 4-22 Time-acceleration curve of four story structure *78*
Figure 4-23 Time-displacement curve of four story structure *79*
Figure 4-24 Deformed mesh at maximum acceleration *79*
Figure 4-25 Time-acceleration curve for four story structure with piled raft *80*
Figure 4-26 Time-displacement curve of four story structure with piled raft *80*

Figure 4-27 Time-acceleration curve of single story structure *81*

Figure 4-28 Time-acceleration curve of four story structure *81*

Figure 4-29 Horizontal component of design response spectra for given seismic action and soil type *83*

Figure 4-30 Calculation of shear force at the base *85*

Figure 4-31 Pile arrangement and shear force in the reference pile *87*

Figure 4-32 Calculation of shear force at the pile head *87*

LIST OF TABLES

Table 2-1 Different available options for modeling pile in PLAXIS 2D *31*
Table 2-2 Input parameters for an embedded beam row element *32*
Table 2-3 Seismic Importance Classes according to NS-EN 1998-1, NA.4 (901) *39*
Table 2-4 Recommended parameters for elastic response spectrum (Table NA.3.3 in NS-EN 1998-1:2004+A1:2013+NA:2014) *41*
Table 3-1 Soil parameters for HSsmall model *50*
Table 3-2 Material Properties of basement, slab and wall of the structures (set type: Plate) *53*
Table 3-3 Weights of different parts of the structure in kN/m/m *53*
Table 3-4 Material Properties of columns (set type: Node to node anchor) *53*
Table 3-5 Input parameters of embedded beam row *57*
Table 3-6 Average element sizes for different distributions *59*
Table 3-7 Stage construction for Model 1 ..... *59*
Table 3-8 Stage construction for Model 2 to 4 ..... *60*
Table 3-9 Properties of input motion *61*
Table 4-1 Co-ordinates of selected nodes *64*
Table 4-2 Result summary of free field analysis *68*
Table 4-3 Summary of obtained natural frequency *74*
Table 4-4 Co-ordinates of selected nodes *75*
Table 4-5 The summary of input parameters for design spectrum *82*
Table 4-6 Calculated base shears at different peak accelerations *86*
Table 4-7 Calculated base shears at different peak accelerations *88*
Table 4-8 Calculated base shears at different peak accelerations *88*
Table 4-9 Calculated base shears at different peak accelerations *88*
Table 4-10 Obtained base shear for single story structure in KN/m *89*
Table 4-11 Obtained base shear for four story structure in KN/m *89*

LIST OF SYMBOLS

α	Rayleigh co-efficient
α	Normalized side friction of clay
α_N	Newmark co-efficient
β	Rayleigh co-efficient
β	Lower bound factor of horizontal design spectrum
β_N	Newmark co-efficient
γ	Shear strain
γ_1	Seismic classes
δ	Logarithmic decrement
δ_t	Time discretization
η	Viscosity
η	Modification factor
ν	Poisson's ratio
ξ	Damping ratio
ρ	Density
σ_1'	Major effective principal stress
σ_3'	Minor effective principal stress
σ_v'	Vertical effective stress
τ	Shear stress
φ	Friction angle
ψ	Dilatancy angle
ω	Angular frequency
a	Attraction
a_g	Ground acceleration
a_{gR}	Reference peak ground acceleration
A	Cross-sectional area of a pile
c	Cohesion
C	Damping matrix
c_u	Undrained shear strength
d_g	Design ground displacement

D	Diameter of a pile
E	Young's modulus
E_d	Dissipated energy
E_s	Accumulated Energy
E_{50}	Triaxial stiffness
E_{oed}	Oedometer stiffness
E_{ur}	Unloading/ reloading stiffness
EA	Axial stiffness
EI	Inertial stiffness
f	frequency
f_n	Natural frequency
F_b	Base shear
F_{max}	Maximum tip resistance of pile
g	Gravity
G_0	Shear modulus for small strain
G	Shear modulus
G_s	Secant shear modulus
G_t	Tangent shear modulus
G_{ur}	Unloading/reloading stiffness
G^*	Complex shear modulus
I	Moment of Inertia
k^*	complex wave number
K	Stiffness matrix
K_F	Base spring stiffness of pile
$l_{spacing}$	Out-of-the-plane spacing of the piles
m	mass
M	mass matrix
n	number of nodes
P_u	Lateral skin resistance of pile
q	Behavior factor
r	Roughness ratio

R_S	Axial spring stiffness
R_N	Lateral spring stiffness
S	Soil factor
S_D	Maximum deformation
S_A	Pseudo acceleration
S_V	Pseudo velocity
S_d (T)	Design elastic response spectra
S_{De} (T)	Elastic Displacement response spectra
S_e (T)	Horizontal elastic response spectra
S_{ve} (T)	Vertical elastic response spectra
T	Period of vibration
T_B	Lower limit of the period of the constant spectral acceleration branch
T_C	Upper limit of the period of the constant spectral acceleration branch
T_D	The value defining the beginning of the constant displacement
T_d	Damped natural period
T_n	Undamped Natural Period
T_{skin}	Axial skin resistance of pile
T_{lat}	Lateral skin resistance of pile
$u\ (t)$	Displacement
$\dot{u}\ (t)$	Velocity
$\ddot{u}\ (t)$	Acceleration
V_s	Shear wave velocity
$V_{s,30}$	Shear wave velocity of top 30m soil
z	Depth

1 INTRODUCTION

1.1 BACKGROUND

Pile foundations are often essential for load bearing in various structures such as multi story buildings, bridge abutments, offshore structures. The design of pile foundation usually considers the load bearing under static condition. In case of an earthquake, the loading condition become dynamic and the behavior of structure supported by pile may change. It is required to analyze the effect of piles in case of an earthquake according to Eurocode 8. Pile supported structure under earthquake loading should be designed accordingly. For this reason, it is essential to study how the presence of piles influences the response of a structure when it is subjected to a strong earthquake motion and how it corresponds to the calculation method recommended by Eurocode 8. If the impact can be predicted it will be easier to introduce design criteria. A representative FEM model is required to incorporate the effect of foundation type under seismic loading.

Although Norway has low seismicity compared to global scale, the updated design recommendations introduced by Eurocode 8 requires control of earthquake load effect more strictly. Based on Rønnquist et al. (2012) one of the reasons for this new standard with new load factors and updated load actions was to update the reliability based design of structures in order to ensure that structures can withstand up to an earthquake of magnitude 6.5 on the Richter scale.

This thesis performs a detailed seismic analysis of two structures with different natural frequencies, first with shallow and then with pile foundations, in the FEM program PLAXIS 2D and compares the shear force which is induced at the interface of a shallow rigid basement on a layered soil system with calculated based on Eurocode 8. The effect of piles on the earthquake response is discussed in terms of change in acceleration and shear force at the base that is induced by the earthquake. The concerning part of Eurocode is Eurocode 8; NS-EN 1998-1:2004+A1:2013+NA:2014.

1.2 RESEARCH OBJECTIVE

The main objective of the study is to determine the influence of the piles on seismic response of a structure and evaluate the correspondence of numerical analysis in PLAXIS 2D with the simplified method of Eurocode 8. The influence of the piles on the response of a structure is obtained in terms of acceleration and seismic loads in compared to a shallow foundation. Eurocode 8 recommends a conservative method of seismic load analysis for spectral analysis approach assuming fixed base structure. The shear force obtained from this methos is compared with the numerical calculation from FEM analysis in PLAXIS 2D to examine the correspondence.

To obtain this goal, a representative model of two layered soil system is simulated in PLAXIS 2D. The soil type is determined depending on the calculated shear wave velocity from the given ranges in Eurocode 8 (Appendix A-1). Before analyzing the response of the structure, the soil behavior under free field condition is analyzed and compared with equivalent linear analysis in DEEPSOIL.

There are number of sub objectives that are formed to obtain the goal of the study which are enlisted as following:

- Free field site response analysis to evaluate the behavior of soil profile during earthquake and comparing the result with one dimensional analysis in DEEPSOIL.
- Free vibration analysis to determine natural frequency of the structures.
- Seismic response analysis of the structures with shallow and pile foundations and evaluating the effect of the piles.
- Calculation of base shear force based on simplified method recommended by Eurocode 8, NS-EN 1998-1:2004+A1:2013+NA:2014.
- Shear force calculation on the rigid base of the structure from PLAXIS output and evaluating the correspondence with the calculation based on Eurocode 8.

1.3 APPROACH

To achieve the goals stated above, the problem is simulated by the following stages:

Stage 1: Construction of material model: A representative soil profile is simulated with HSsmall model in PLAXIS 2D. Shear wave velocity is of the profile is calculated to determine the soil type from Eurocode guideline. Dynamic boundary conditions are selected based on previous research and recommendations. The chosen boundary condition is then tested for a simple material model and a harmonic motion. After that, the simulated soil profile is subjected to a strong motion that is artificially generated by SIMQKE software.

Stage 2: Free field analysis of the soil profile: A free field analysis of the soil profile is performed. The purpose of this analysis is to observe the response of the top layer in free field condition to the earthquake provided at bedrock. The obtained results from PLAXIS 2D is compared with a one-dimensional ground response analysis in DEEPSOIL.

Stage 3: Construction of the structure and free vibration analysis: A simple single story and a four story structure with wall, slab and shallow base are constructed. Same structures are modeled with pile foundation as well. The piles are added to the shallow foundation and the foundation system acts as a piled-raft. Then a free vibration analysis is performed to determine the natural frequency of the structures. The effect of piles is also observed on the results.

Stage 4: Dynamic analysis of the structure and examining the correspondence with Eurocode: The structures are then subjected to the strong motion and the response is observed. The resulting shear force at the interface of the base is determined from PLAXIS 2D. The base shear force is validated with the hand calculation based on Eurocode 8. The result is compared to evaluate the influence of pile on the seismic performance of the structures. For this calculation, the design spectrum for elastic analysis according to Norwegian National Annex is considered.

1.4 RESEARCH BOUNDARIES

As described in the previous section, the goal of the thesis is to conduct earthquake analysis of structures, evaluate the influence of pile foundations and correspondence with Eurocode 8. Earthquake analysis is a broad topic and there is a vast area in Eurocode 8 which can be taken into account. Due to practical limitations, such as time constraint, it is important to draw a boundary. Moreover, there are several assumptions and limitations in the calculations which are needed to be mentioned. Main research limitations are listed below:

- This thesis is limited to earthquake analysis for one input motion and one type of soil. Normally it is required perform several earthquake analyses to get a complete spectral overview.
- The soil material properties are assumed to represent a particular soil condition. No real boundary value problem is analyzed. Soil layer with two types of soil may not display a practical scenario.
- The piles are modeled as a 2D element while they are entirely 3D element. Embedded beam row element is used to simulate pile in 2D which assumes pile to be an elastic material on the mesh.
- Kinematic pile-soil-structure interaction and bending moment of the piles is not analyzed in this thesis. According to Eurocode 8: Part 5 (Fundaments, Support Structures and Geotechnical Conditions), piles should be designed to resist both inertial and kinematic forces and kinematic bending moment should be computed under certain condition.
- Liquefaction and ground water flow impacts are not taken into account.
- Only Rayleigh damping properties are used to define damping of soil, there is no geometric damping in plain strain model of PLAXIS 2D.
- Structural elements are modelled as fully elastic.

1.5 THESIS OUTLINE

This thesis contains six main chapters:

Chapter 1: Introduction: This chapter gives a general introduction to the thesis. It delineates research objectives, approach and limitations. An outline of thesis is provided for the readers to get an overview.

Chapter 2: Literature Review: A brief summary of all the relevant literatures and previous researches which are reviewed to perform the analysis is described in this chapter. The review of literature can be divided into three subclasses: 1) Literature regarding geotechnical earthquake engineering. 2) Literature and researches on finite element analysis method and the program. 3) Relevant part of Eurocode 8 which has been applied for further analysis.

Chapter 3: Construction of FEM Models and Parameters: This chapter describes the construction of models in PLAXIS and the material properties of soil and structural components that are used to simulate the problem. It describes the detail model construction procedure for dynamic analysis and also verification of chosen dynamic boundary conditions.

Chapter 4: Analysis and Result: In this section, results obtained from all the analyses is presented. The analyses are divided into four sections: 1) Free field analysis 2) Free vibration analysis 3) Seismic response analysis 4) Calculation of shear force at the rigid base. The results from each section is discussed.

Chapter 5: Discussion and Conclusion: Here a general summary, discussion and conclusion of the thesis based on its objectives are given.

Chapter 6: Recommendation for Further work: Recommendation on further scope of study is discussed in this chapter.

2 LITERATURE REVIEW

2.1 GEOTECHNICAL EARTHQUAKE ENGINEERING

Earthquakes are induced by the sudden release of stored deformational energy of the earth. Human induced earthquakes should also be considered, for example, gas extraction from rock causing stress reduction and collapse. The study of earthquake, process of occurrence and their effect of on ground motion is required to be carried out by geotechnical engineers for ensuring safety. Although earthquakes are complicated and unpredictable phenomena, the existing science provides good understanding of its mechanism. In this section, the relevant components of earthquake and corresponding behavior of soil and structures are discussed based on Kramer (1996), Chopra (2007), Clough and Penzien (1993) and other contributing authors.

2.1.1 Seismic Wave Propagation

The stress wave of earthquake starts to propagate through the earth's crust when the energy of an earthquake is released. Seismic waves are mainly divided into two types i.e. *body wave* and *surface wave*. *Body waves* consists *P-wave* and *S-wave* and propagates through the interior of the earth. *P- wave* or primary wave propagates by successive compression and rarefaction of the medium. *S-wave* or secondary wave causes shear deformation of the medium where the particle movement of the medium is perpendicular to the direction of the motion. The velocity of the propagation of these waves depends on the stiffness properties of the soil material. Since soil is stiffer in compression, P-wave moves faster. Surface waves on the hand is the result of interaction between body waves and the surficial layer of the earth. Surface waves consists of *Rayleigh waves* and *Love waves* and they travel along earth's surface. Surface waves are dominant in locations far from the source (Kramer, 1996).

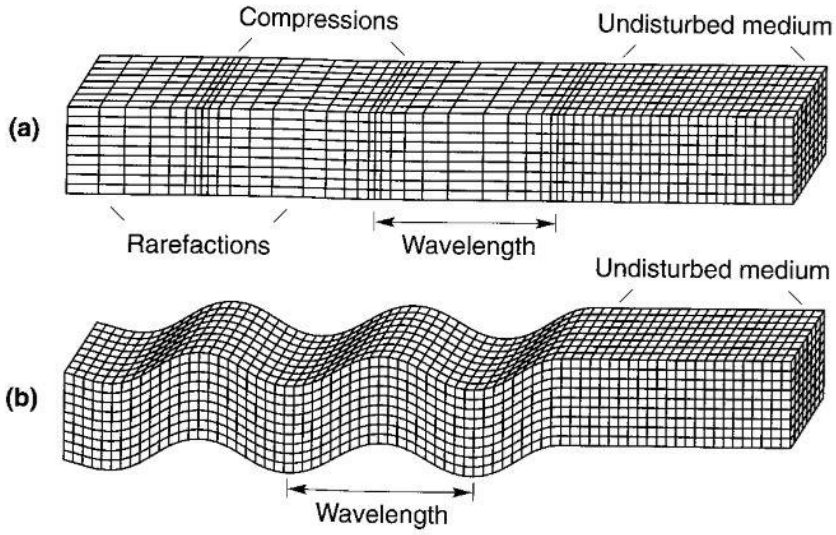

Figure 2-1 (a) P-wave (b) S-wave (Kramer, 1996)

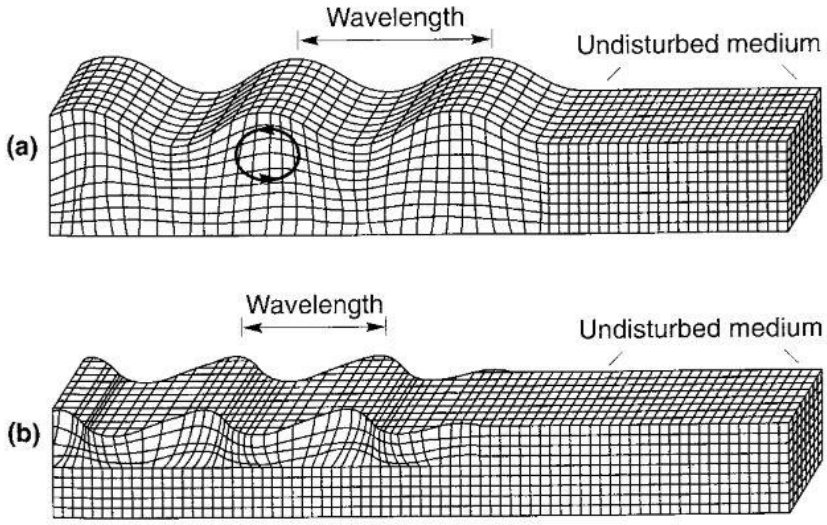

Figure 2-2 (a) Rayleigh wave (b) Love wave (Kramer, 1996)

A simple equation for propagation of wave can be derived by stress equilibrium assuming an infinite one dimensional unbounded medium. The differential equation given by Kramer (1996) is illustrated below:

$$\frac{\delta^2 u}{\delta t^2} = \frac{M}{\rho}\frac{\delta u}{\delta x^2}$$
$$\frac{\delta^2 v}{\delta t^2} = \frac{G}{\rho}\frac{\delta u}{\delta x^2}$$

Here *u* and *v* are the longitudinal and perpendicular particle motions respectively, E is Young's modulus, M and G are constrained and shear modulus and ρ is the density of material.

$$M = (1-\nu)\, E / (1+\nu)(1-2\nu)$$

$$G = E / 2(1+\nu)$$

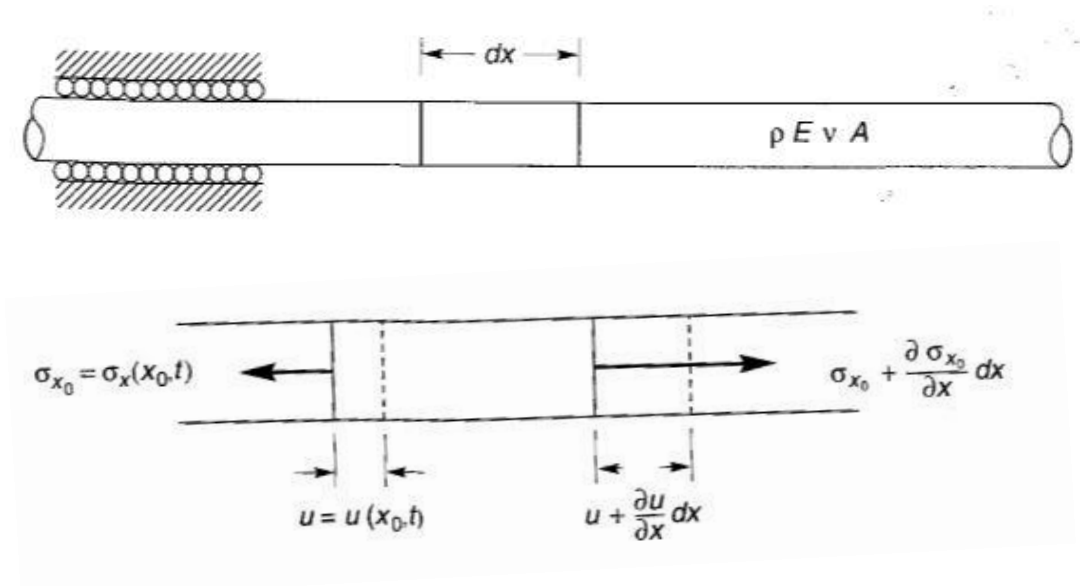

Figure 2-3 One dimensional wave propagation in a constraint infinite rod (Kramer, 1996)

Compression and shear wave velocity can be expressed as:

$$V_p = \sqrt{\frac{M}{\rho}} \quad and \quad V_s = \sqrt{\frac{G}{\rho}} \tag{2.1}$$

Thus, the differential equations can be expressed as:

$$\frac{\delta^2 u}{\delta t^2} = V_p \frac{\delta u}{\delta x^2}$$

$$\frac{\delta^2 v}{\delta t^2} = V_s \frac{\delta u}{\delta x^2}$$

2.1.2 Equation of Motion

To understand dynamic behavior of structures, equation of motion is usually explained for a simple *single-degree-of-freedom* (SDOF) structure. Chopra (2007) defined *degree-of-freedom* as "the number of independent displacements required to define the displaced positions of all masses relative to their original position". The equation of motion of a SDOF system for undamped free vibration can be expressed as:

$$m\ddot{u}(t) + ku(t) = 0 \tag{2.2}$$

In this equation, m and k are mass and stiffness of the system, $\ddot{u}$(t) is the acceleration and u(t) is displacement. Generally, more DOF is required to define a real problem and required to be expressed as *multiple-degree-of-freedom* system. In such cases, the parameters are provided as matrices in equation (2.2)

The behavior of structure changes when it is subjected to earthquake induced motion at the base. As explained in Clough and Penzien (1993), total displacement of the mass, $u_t(t)$ is sum of displacement of the ground $u_g(t)$ and relative displacement between mass and ground, $u(t)$. At each instant of time, the relation can be written as:

$$u_t(t)= u_g(t)+u(t) \tag{2.3}$$

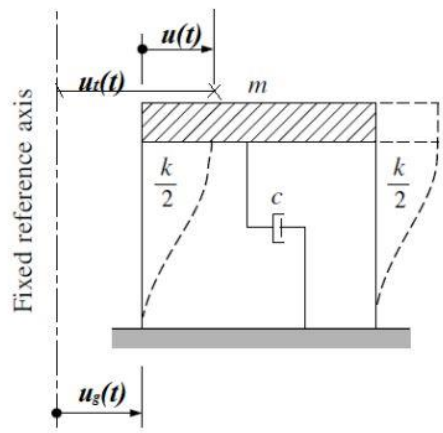

Figure 2-4 Earthquake excitation on a simple SDOF system (Clough & Penzien, 1993)

Ground acceleration and acceleration of structure (relative to ground acceleration) can be obtained by taking second order derivative, which gives the following equation:

$$m\ddot{u}_g(t)+m\ddot{u}(t)+ku(t)= 0 \tag{2.4}$$

Rearranging equation (2.4) gives:

$$m\ddot{u}(t)+ku(t)= -m\ddot{u}_g(t)= P(t) \tag{2.5}$$

Here, $- m\ddot{u}_g(t)$ or $P(t)$ is the external force due to earthquake. The response of the total system is obtained by taking step by step integration (Clough & Penzien, 1993)

2.1.3 Damping

Damping is the process by which free vibration steadily diminishes in amplitude. In other words, the energy of the vibrating system dissipates by one or more mechanisms (Chopra, 2007). When a viscus damper is assumed, equation 2.5 becomes:

$$m\ddot{u}(t)+ku(t)+c\dot{u}(t)= P(t) \tag{2.6}$$

In this equation c is co-efficient of damping and $\dot{u}(t)$ is velocity. Rayleigh damping provides a convenient damping measurement for dynamic analysis which lumps the damping effect within the mass and stiffness of the system. Rayleigh damping matrix C consists the α portion of mass matrix M and β portion of stiffness matrix K. The formula can be written as following where α and β are the Rayleigh coefficients ("PLAXIS 2D Reference Manual," 2016).

$$[C]= \alpha[M]+ \beta[K] \tag{2.7}$$

- The alpha parameter accounts for the influence of mass in damping of a system. More lower frequencies get damped as the alpha value gets higher.
- The beta parameter accounts for the stiffness influence on the damping of the system. More higher frequencies get damped as beta value increases.

However, in engineering practice, the damping is measured for the material and geometric damping which is given by damping ratio ξ. The coefficient α and β can be obtained from the following equation as a function of damping ratio ξ and angular frequency of vibration ω.

$$\alpha+\beta\omega_i^2 =2\omega_i \xi_i \tag{2.8}$$

This equation can be solved by setting at least two target frequencies for two corresponding damping ratios.

$$\alpha = 2\omega_1\omega_2 (\omega_1\xi_2- \omega_2\xi_1)/(\omega_1^2-\omega_2^2) \tag{2.9}$$

$$\beta = 2(\omega_1\xi_2- \omega_2\xi_1)/(\omega_1^2-\omega_2^2) \tag{2.10}$$

There are different methods for selecting appropriate Rayleigh parameters given by different authors. In this study, the method given by Hudson et al. (1994) will be followed. The first target frequency is the average natural frequency of the soil deposit and the second one is the next odd number of the ratio of fundamental frequency of the input motion to the natural frequency of the soil. Outside this range, the input signal is overdamped. The natural frequency of the soil is given by:

$$f = \frac{vs}{4H} \tag{2.11}$$

v_s is the shear wave velocity of the soil deposit and H is the thickness of the soil layer.

When the seismic wave propagates through a soil system, the wave energy also gets dissipated through the way. The shape and magnitude of the response of a soil-structure system is influenced by damping characteristics. The behavior of soil is irreversible even in the small deformation. The damping is caused by various factors. Some of those factors are (Kramer, 1996)

- Damping due to soil material property (stiffness/ strength properties)
- Damping at the interface of soil and structure.
- Damping due to soil radiation
- Refraction

2.1.4 Free Vibration

Free vibration of a structure is defined by Chopra (2007) as a phenomenon when the structure is disturbed from its static initial condition by an external load, then allowed to vibrate freely without any external action. This leads to a basis to determine natural period of vibration and damping ratio of a SDOF system.

For a viscously damped SDOF structure without any external load $P(t)$=0, equation (2.5) can be written as:

$$m\ddot{u}(t)+ku(t)+c\dot{u}(t)= 0 \tag{2.12}$$

Dividing this equation by mass m,

$$\ddot{u}(t)+ \omega_n^2 u(t)+2\zeta\omega_n\dot{u}(t)= 0 \tag{2.13}$$

Here, natural angular frequency, $\omega_n = \sqrt{k/m}$, and damping ratio, $\zeta = c/ 2m\omega_n = c/c_{cr}$

c_{cr} is critical damping coefficient and ζ is the damping ratio which is a dimensionless measure of damping. For $c \geq c_{cr}$ or $\zeta \geq 1$ the system does not oscillate and returns to its initial condition. Only if $c < c_{cr}$, or $\zeta < 1$, then the system oscillates and returns to its initial condition by gradual decrease of amplitude. This is called underdamped system. This kind of system is the concern of structural engineering because most of the structures have $\zeta < 1$, typically less than 0.1 (Chopra, 2007).

The natural period of a damped system T_D is related to natural period without damping T_n by,

$$T_D = T_n / \sqrt{1-\zeta^2} \tag{2.14}$$

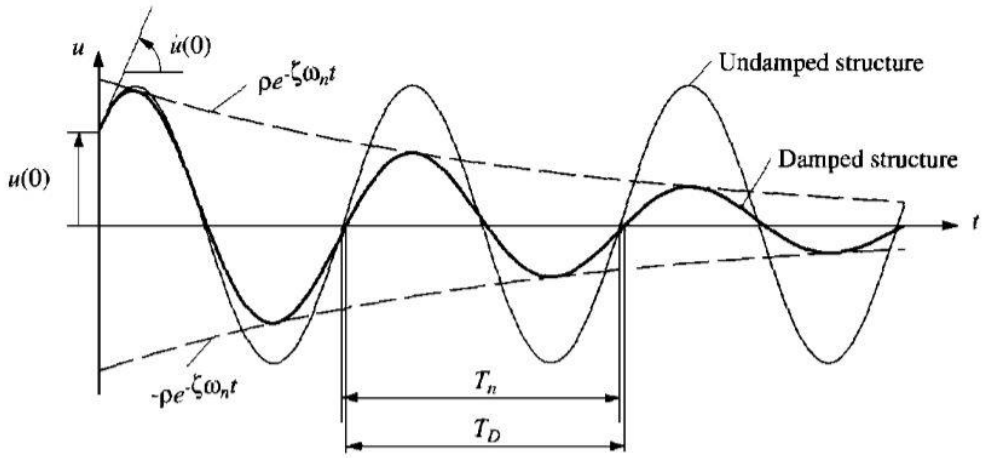

Figure 2-5 Effect of damping on free vibration (Chopra, 2007)

This relation can be used to determine undamped natural period by determining logarithmic decrement, δ which the logarithm of ratio of two successive peaks.

$$\delta = \ln \frac{u_i}{u_{i+1}} = \frac{2\pi\zeta}{\sqrt{1-\zeta^2}} \tag{2.15}$$

Over n cycles the displacement decreases from u_1 to u u_{n+1} then the equation becomes:

$$\delta = \frac{1}{n} \ln \frac{u_1}{u_{n+1}} \cong 2\pi\zeta \tag{2.16}$$

2.1.5 Non-linear Stress-Strain Behavior of Soil[1]

Soil behavior is non-linear and inelastic when it is under cyclic loading. It is important to understand the non-linear stress-strain behavior for determining failure mechanism. Since failure of soil under cyclic loading is beyond the scope of the thesis, only shear modulus and damping behavior of soil given by equivalent linear model will be discussed briefly in this section.

The stress-strain response in equivalent linear approach is governed by Kelvin -Voigt model i.e. a linear, visco-elastic material to incorporate some nonlinearities of soil. The relation between shear stress τ and shear strain γ and its rate ý are given as below (Bardet et al., 2000):

[1] This section is summarized from specialization project in autumn, 2016 semester (Toma, 2016)

$$\tau = G\,\gamma + \eta\,\acute{y} \tag{2.17}$$

where G= Shear Modulus and η= Viscosity. The shear strain and its rate are defined from the horizontal displacement u (z, t) at depth z and time t (in a one-dimensional shear beam column as explained in section 2.1.1):

$$\gamma = \frac{\partial u\,(z,t)}{\partial z} \text{ and } \acute{y} = \frac{\partial \gamma(z,t)}{\partial t} = \frac{\partial ^2 u\,(z,t)}{\partial z\,\partial t}$$

Stress-strain relation of soil under harmonic loading is given by the complex shear modulus G* and critical damping ratio ξ.

$$G^* = G(1+i2\xi). \tag{2.18}$$

Equation (2.8) shows that the complex shear modulus is frequency independent.

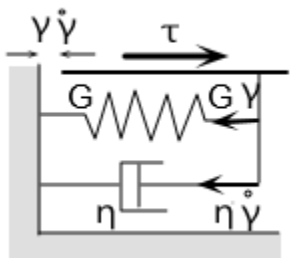

Figure 2-6 Schematic representation of stress-strain model used in equivalent-linear model. (Bardet et. al.,2000)

While under cyclic loading, a hysteretic loop generates due to the non-linear, dissipative, and irreversible behavior of soil (Figure 2.7). This loop has series of unloading reloading paths. Seismic motions create small stain condition in the soil with corresponding high shear stiffness G_0. The energy dissipation increases with increase of shear strain γ and the magnitude of G decreases. (Bardet et al., 2000).

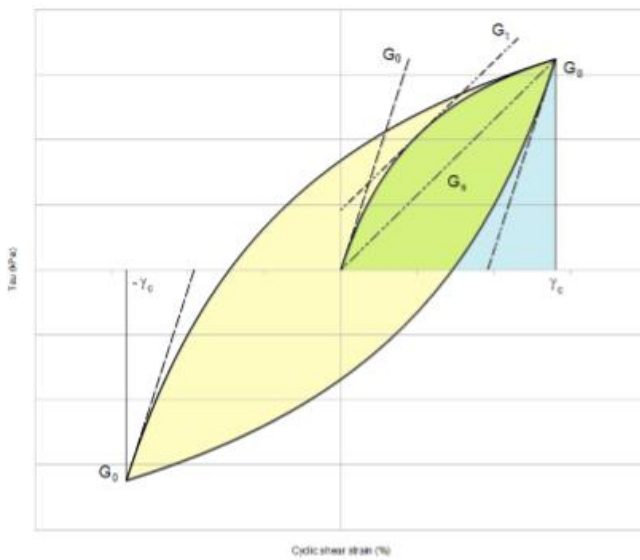

Figure 2-7 Hysteretic behavior of soil under cyclic loading (Laera & Brinkgreve 2015)

The stress-strain relationship in a strain controlled cycle can be written as:

$$G_s=\frac{\tau}{\gamma} \tag{2.19}$$

Where G_s is the secant shear stiffness which is the inclination of the loop.

Local hysteresis damping ratio is related to the area which is defined by the energy dissipated and energy accumulated. The damping ratio works until the material behavior remains inside the plastic range and shear modulus decreases with the increase of strain (Bardet et al., 2000)

$$\xi = \frac{Ed}{4\pi Es} \tag{2.20}$$

Where E_d is the dissipated energy, shown by the yellow area in Figure 2-7. The energy accumulated at the maximum strain is marked by the green and blue areas respectively.

<u>Shear modulus and damping ratio</u>

The measurement of soil resistance to shear deformation is called shear modulus, G. The relationship between shear stress and shear deformations can be shown by a simple illustration as given in figure 2-8 (Brandt, 2014). The shear modulus of a soil at small strains depends on several factors such as confining pressure, void ratio, over consolidation ratio, and plasticity index (Kramer, 1996).

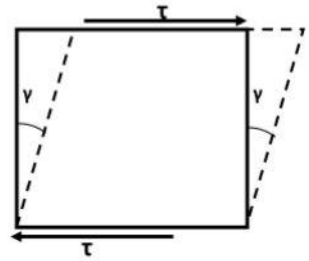

Figure 2-8 shear modulus, G, as the resistance to shear deformation γ because of shear force τ (Brandt, 2014)

The curve that represents the change of shear modulus with shear strain is called *Back-bone curve,* shown in figure 2-9 (a). The inclination of the backbone curve passing through the origin gives the maximum shear stiffness, G_{max}. The secant stiffness (G_{sec}) is obtained by taking a straight line from the origin to a specific point on the back-bone curve for a given shear strain. The ratio between the secant stiffness and the maximum stiffness is usually presented by modulus reduction curve (figure 2-9 (b)). Modulus reduction curves are often used to define material behavior in equivalent linear or non-linear analysis based on the proposal of different authors. Material properties defined by Vucetic and Dobry (1991) is used to calibrate the parameters of clay in DEEPSOIL and PLAXIS. Seed (1986) model is commonly used in case of sands (Hashash, 2012).

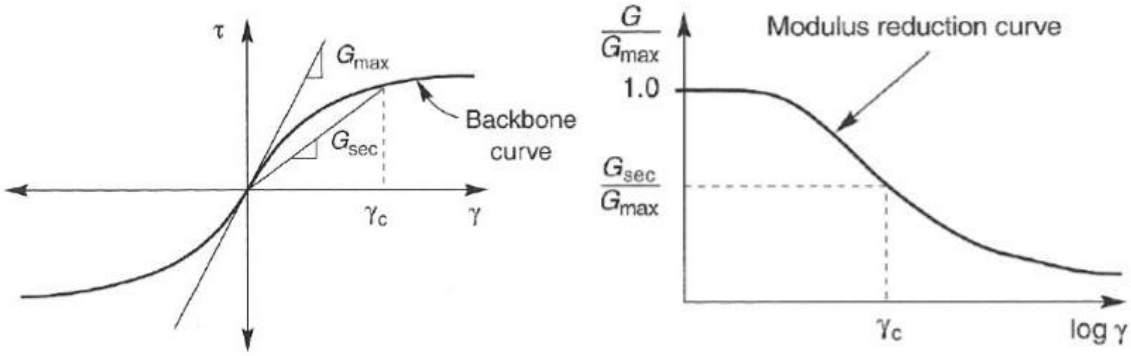

Figure 2-9 (a) Back-bone curve (b) Modulus reduction curve (Kramer, 1996)

Vucetic and Dobry (1991) provided the results of several different studies, which consists of different plasticity index, testing equipment and cyclic test types. Representative G/G_{max} and ξ curves were fitted graphically which was used to develop number of modulus reduction and damping ratio curves. The damping ratio is also dependent on the plasticity index.

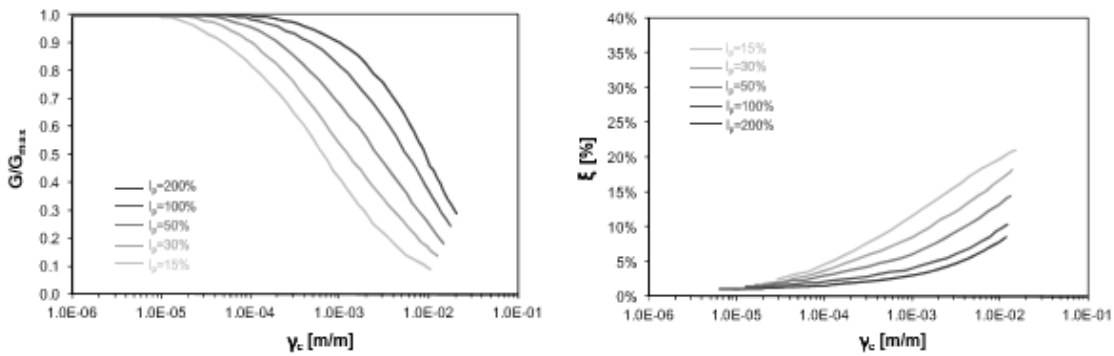

Figure 2-10 Vucetic & Dobry (1991) G/Gmax - γc and ξ - γc curves equations (charts from Guerreiro et al. (2012))

2.1.6 Site Response Analysis[2]

Site response analysis is the study to determine the response and local site effects of a soil deposit to a given seismic motion on the bedrock. As the wave propagates from the bedrock through the overlying deposit, it modifies the wave characteristics throughout the journey in terms of amplitude, duration, and frequency content. Thus, the response at the ground surface is different from the input action and dependent on the material properties of the overlying soil and characteristics of the wave. To perform a ground response analysis, information is required about characteristics of motion, dynamic properties of soil and computation of strong motion. Analysis approach can be one, two or three dimensional depending on the requirement. Available methods can be based on linear, equivalent linear and non-linear analysis (Imtiaz, 2009).

One dimensional analysis is the most common approach in the research are and the concept based on following assumptions (Govindaraju et al., 2004):

- The surface of the overlying soil deposit is perfectly horizontal.
- The soil deposit is extended infinitely in the horizontal direction.
- The response on the soil surface is the result of upward propagation of wave and it is spatially uniform.

Vertical one dimensional column is assumed for this kind of analysis. The soil properties do not change in a great extent in horizontal direction but in vertical direction. Earthquake energy

[2] Some parts of this section are summarized from specialization project in autumn, 2016 semester (Toma, 2016)

gets released from the source of a rupture and starts propagating in all direction and finally hits the surface. Due to increasingly stiffer medium with depth, the wave gets damped through the path and the undamped wave travels back to the rigid layer. This phenomenon keeps repeating until the wave is fully damped. Therefore, the vertically propagating shear waves in site response analysis is considered to be well argued (Imtiaz, 2009).

2.1.6.1 Amplification Factor

In a uniform linear elastic soil deposit, a harmonic horizontal motion of underlying bedrock will generate shear waves that propagates vertically as shown in figure 2-11, (Kramer, 1996). The equation of horizontal displacement can be expressed as:

$$U(z, t) = Ae^{i(\omega t+kz)} + B_e^{i(\omega t-kz)} \tag{2.21}$$

Where, ω is the angular frequency of the wave, k is wave number and t is time. A and B are the amplitude of wave travelling towards upward and downward direction.

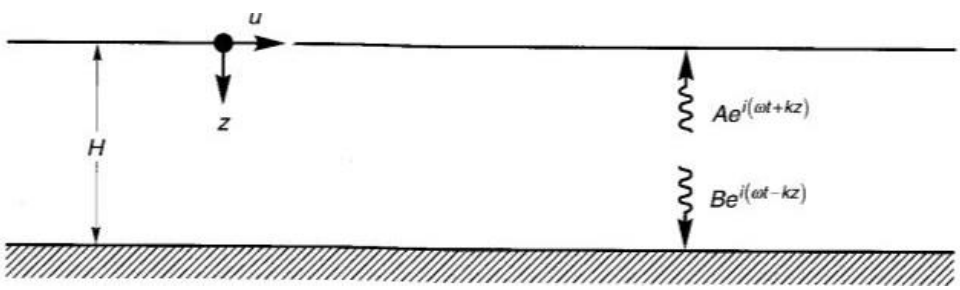

Figure 2-11 Wave propagation in a linear elastic uniform layer (Kramer, 1996)

Realistic results can be obtained by assuming the presence of damping in soil layer. If the soil has Kelvin-Voigt shearing characteristics, then the equation of wave can be expressed as:

$$\rho\frac{\delta^2 u}{\delta t^2} = G\frac{\delta u}{\delta x^2} + \eta\frac{\delta^3 u}{\delta x^2 \delta t} \tag{2.22}$$

Where U is expressed as: $U(z, t) = Ae^{i(\omega t+k^*z)} + B_e^{i(\omega t-k^*z)}$

Here, k* is a complex wave number which can be derived by complex shear modulus, $G^* = G(1+i2\xi)$.

Complex shear wave velocity, $v_s^* = \sqrt{\frac{G^*}{\rho}} = \sqrt{\frac{G(1+2i\xi)}{\rho}} = v_s(1+i\,\xi)$

For small ξ, complex wave number can be written as: $k^* = \omega / v_s^*$

Using these relations, the transfer function which is the ratio between surface motion and bedrock motion for damped soil over rigid rock can be expresses as:

$$|F(\omega)| \approx \frac{Umax\ (0,t)}{Umax\ (H,t)} = \frac{1}{\sqrt{cos^2\left(\frac{\omega H}{vs}\right)+\left[\xi\left(\frac{\omega H}{vs}\right)\right]^2}} \tag{2.23}$$

Amplification factor F(ω) depends on frequency of the wave and reaches maximum when the frequency of wave is equal to the natural frequency of the soil deposit. Figure 2-12 shows the relationship of amplification factor with frequency at different damping condition. It also shows that the damping affects higher frequencies more than the lower ones (Kramer, 1996).

Natural frequency of the soil layer is given by:

$$\omega_n = \frac{Vs}{H}\left(\frac{\pi}{2} + n\pi\right) \tag{2.24}$$

n= 0, 1, 2, 3……

Peak acceleration occurs at n=0, which is fundamental frequency:

$$f_n = V_s/4H \tag{2.25}$$

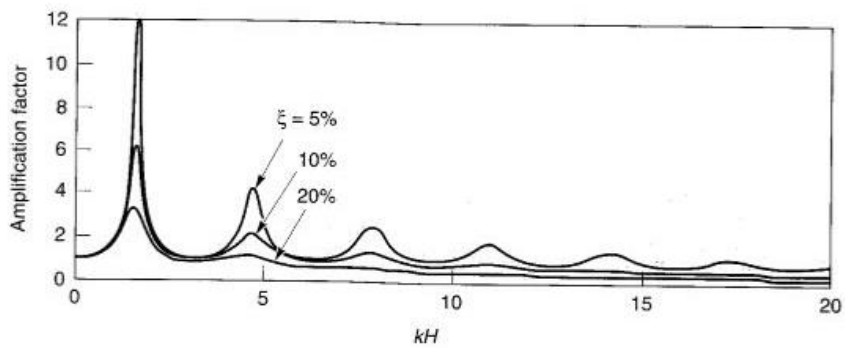

Figure 2-12 Amplification of a damped uniform layer (Kramer, 1996)

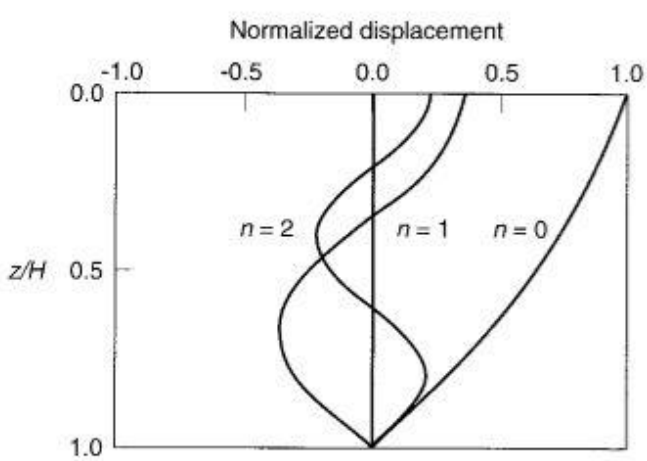

Figure 2-13 Displacement patterns for waves at first (n=0), second (n=1) and third (n=2) natural frequency (Kramer, 1996)

2.1.6.2 Equivalent Linear Approach

Linear approach of site response analysis assumes the soil layer as a uniform mass with constant varying stiffness with depth. The geometry and parameters are idealized to represent by simple mathematical functions. Very simplified assumptions are less likely to incorporate real site condition. In such circumstance, equivalent linear approach or finite element analysis can be performed to get realistic result. Equivalent linear soil properties such as shear modulus, damping ratio can be simulated for seismic loading.

Equivalent shear modulus is represented by the secant shear modulus and the equivalents damping ratio which is represented by the energy dissipation in a single cycle of the hysteresis loop. Modulus reduction and damping curves are obtained by laboratory testing with the concept stated in section 2.1.5. However, actual earthquake motion is not harmonic, rather irregular time history. To simulate this irregular behavior, the loading is provided with a reduction factor of 65% compensate the overestimation of shear strain (Kramer, 1996).

Equivalent linear analysis performed by iteration which is given as a basic concept in the numerical analysis program, SHAKE (Schnabel et al., 1972). The similar concept is applied to other dedicated programs for one dimensional ground response analysis such as EERA (Bardet et al., 2000) and DEEPSOIL (Hashash, 2012). The iteration is performed until the shear modulus and dumping ratio is consistent with the strain induced in each layer (Schnabel et al., 1972).

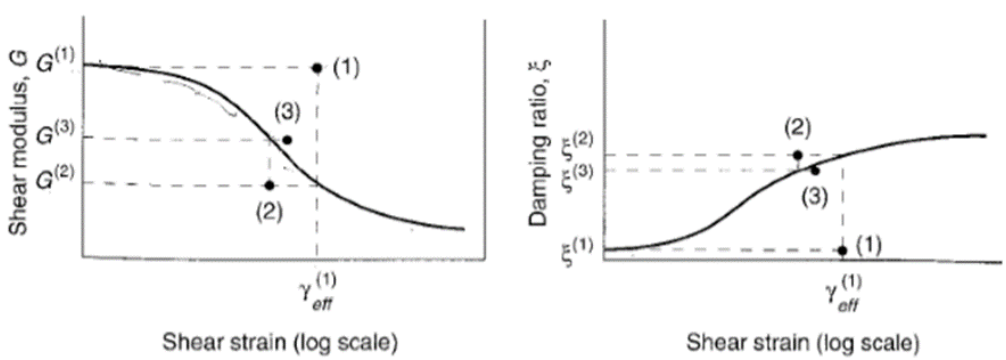

Figure 2-14 Iteration toward strain compatible shear modulus and damping ratio (Kramer, 1996)

2.1.6.3 Non-linear Approach

In non-linear analysis, complex calculations are involved to simulate actual nonlinear behavior of a soil. The calculation is performed within time domain by taking direct numerical integration of equation of motion. The analysis is performed by using discrete models like finite element or lumped mass model. High performance programs such as PLAXIS provides nonlinear analysis (Govindaraju et al., 2004).

Non-linear analysis generally performed by two approaches. It can be done by either explicit method that is followed by rapid calculation and large number of time steps or by implicit method which involves fewer steps but time consuming procedure. Most high functioning programs performs explicit approach (Saha, 2014).

2.1.7 Response Spectrum Analysis

Earthquake response spectrum, is a practical concept of characterizing ground motions and response of structures to them and a very useful tool for seismic design at present. Response spectrum is defined by Chopra (2007) as "a summary of peak response (acceleration, velocity, displacement) of all possible linear elastic *single-degree-of-freedom* (SDOF) system to a particular component of ground motion for a given damping ratio." For different values of damping ratio, there will be different shapes of response spectra. Figure 2-15 shows construction of response spectrum for structures of six different natural period.

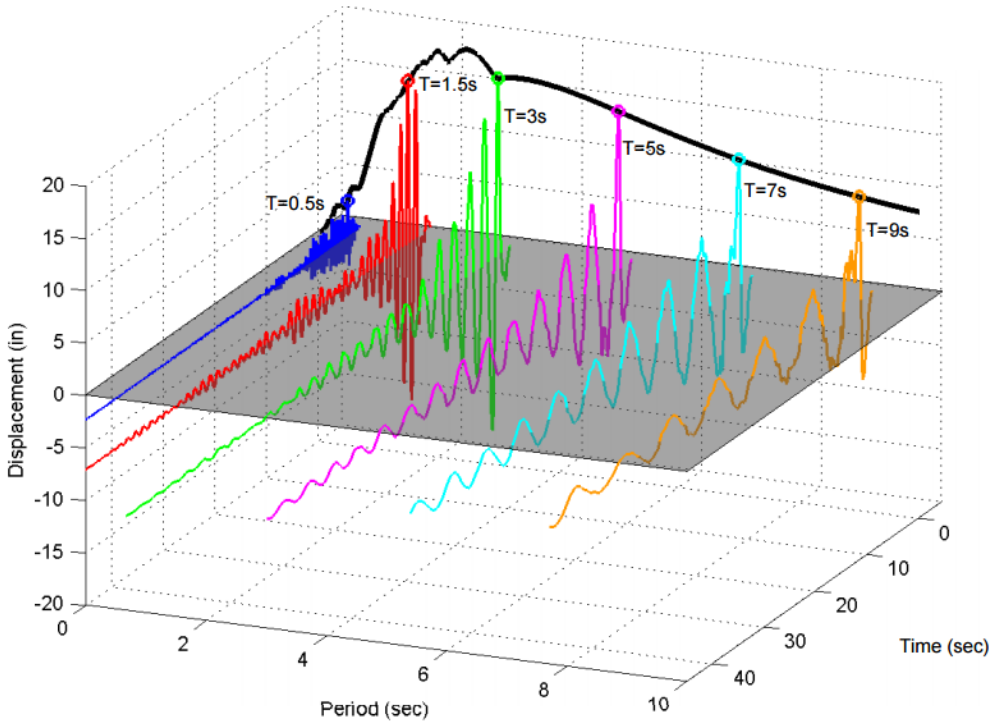

Figure 2-15 Construction of the response spectrum from ("QuakeManager Wiki," 2015) after Stensløkken (2016)

Most commonly applied response spectra are:

1) Deformation response spectrum, $S_D(T, \xi) = \max |S_D(t, T, \xi)|$

Deformation response spectrum provides information to calculate possible maximum deformation $S_D(T, \xi) \equiv u_0$ and inertial forces. The product of maximum displacement and stiffness gives maximum static force (Chopra, 2007).

2) Pseudo-velocity response spectra, $S_v(T, \xi) = \max |S_v(t, T, \xi)|$

V is a quantity corresponding to peak deformation of linear elastic SDOF system with natural frequency ω_n which is expressed as:

$$V = S_v(T, \xi) = \omega_n S_D(T, \xi) = \frac{2\pi}{Tn} S_D(T, \xi) \tag{2.26}$$

Here, V is peak *pseudo-velocity* and gives the maximum kinematic energy stored in a system with mass m during earthquake movement, E_{so}.

$$E_{so} = \frac{1}{2} mV^2 = \frac{1}{2} m [S_v(T, \xi)]^2 \tag{2.27}$$

Pseudo-velocity response spectrum is obtained by plotting V as a function of natural period of motion T_n. It is called "pseudo-velocity" because the magnitude of V is not equal to actual peak velocity $\dot{u}_0$ (Chopra, 2007).

3) Pseudo-velocity response spectra, $S_A(T, \xi) = \max |S_v(t, T, \xi)|$

A is a quantity corresponding to peak deformation of linear elastic SDOF system with natural frequency ω_n which is expressed as:

$$A = S_A(T, \xi) = \omega_n^2 S_D(T, \xi) = \left(\frac{2\pi}{Tn}\right)^2 S_D(T, \xi) \tag{2.28}$$

Here, A is peak *pseudo-acceleration* and gives the maximum base shear V_{bo} of a system with mass m during earthquake movement.

$$V_{bo} = m\,A = m\,S_A(T, \xi) \tag{2.29}$$

Pseudo-acceleration response spectrum is obtained by plotting A as a function of natural period of motion T_n. It is called "pseudo-acceleration" because the magnitude of A is not equal to actual peak acceleration $\ddot{u}$ (Chopra, 2007).

Equation (2.26) and (2.28) shows that all the spectral quantities are interrelated and it is possible to create an integrated presentation. This is useful because combined spectrum can be then readily used for the design purpose. This combined representation of three response spectra is called "triplet plot".

2.1.8 Typical Pile Foundation Damage During Earthquake

Pile foundations are usually necessary to increase bearing capacity and decrease differential settlement in softer or more compressible soil. In case of an earthquake, the forces on pile foundation change due to ground deformation from lateral seismic load. Pile foundation failures over the past years are mostly due to soil liquefaction and thus, studies regarding damage in non-liquefiable soil are very rare (Martin & Lam, 1995). However, several authors studied damage patterns and mechanism of pile foundations under seismic loading. Variety of approaches has been introduced to incorporate the calculation the changed forces due to earthquake. A summary of pile foundation damage during earthquake from findings by M. Hamada (1991) and Mizuno (1987) is presented by Teguh (2006) in figure 2-16. Failure during earthquake can be induced by excessive ground deformation, high shear force and bending moment along pile or excessive shear force at the interface of pile and pile cap among other phenomena (Teguh, 2006).

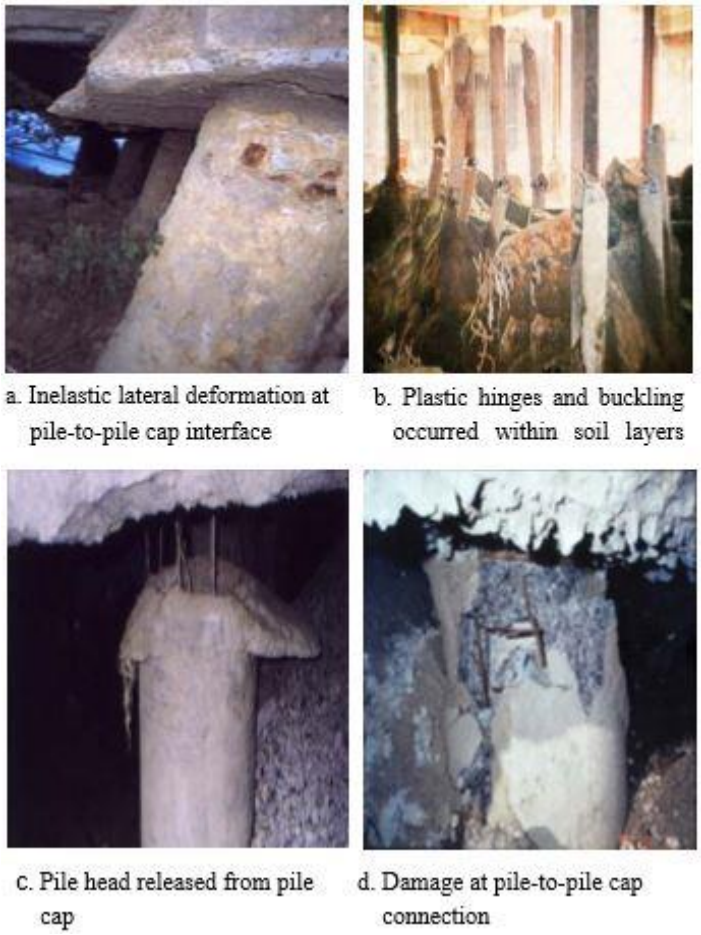

Figure 2-16 Pile foundation damage due to strong earthquakes (Hamada 1991; Mizuno 1987) figure from (Teguh, 2006)

Several studies had been carried out to estimate the sectional forces of pile during earthquake. J. Hamada (2015) conducted a series of shake table and lateral load test on pile in a centrifuge and estimated the influence of ground deformation on bending moment of pile. This study suggested the procedure of estimating bending moment at dynamic condition by subtracting

the bending moment estimated from static loading from bending moment measured from shaking table test. The bending moment in that case is measured from the shear force at pile head using the relationship between bending moment and shear force α= M/Q, where α is a constant factor. Therefore, similar method is used for estimating shear force at dynamic condition.

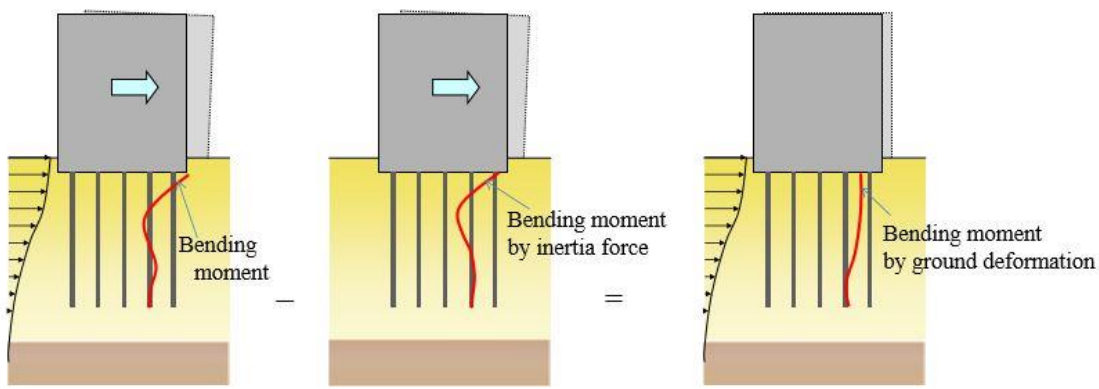

Figure 2-17 Estimation of bending moment in piles caused by ground deformation (J. Hamada, 2015)

2.2 FEM ANALYSIS IN PLAXIS

Finite Element Method (FEM) is an approximate numerical method for solving engineering and mathematical problems. In this method, a large problem element (structure or soil volume) is subdivided into smaller parts. These smaller parts are referred as “finite element”, can be triangular, square or curved boundaries and consist approximate description of behavior of the large element. The elements are then joined by numerical integration and simulates the behavior of the whole element. Deformation of the elements are described by deformations in a set of nodal points (Nordal, 2016).

“PLAXIS 2D is a two-dimensional finite element program, developed for the analysis of deformation, stability and groundwater flow in geotechnical engineering” (Brinkgreve et al., 2016). PLAXIS 2D models can be constructed either plane strain or axisymmetric. It uses 6 or 15 nodal point triangular elements to describe deformation. There are several material models to define the property of the soil. Structural element such as plates, anchors, embedded beams and geogrid can be constructed ("PLAXIS 2D Reference Manual," 2016).

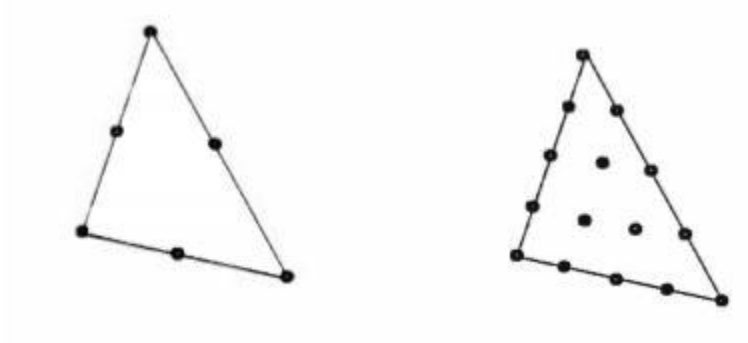

Figure 2-18 Triangular element with 6 and 15 nodes (Nordal, 2016)

2.2.1 Material Models

There different material models can be used to simulate mechanical behavior of soil at different degree of accuracy in PLAXIS. The simplest model is *Linear Elastic model* which is bases on Hooke's law of elasticity and involves only Young's modulus, E and Poisson's ratio, ν to describe soil behavior. Thus, the application of LE model is not appropriate for soil, rather used for concrete material or intact rock. A better approximation of soil behavior can be simulated by linear elastic perfectly plastic Mohr-Coulomb model (MC) which also involves plasticity parameter (c and ϕ) and dilatancy angle, ψ ("PLAXIS 2D Material Models Manual," 2016).

However, soil behavior can be simulated with greater accuracy by advanced models such as Hardening Soil model (HS) or Hardening Soil model with small-strain stiffness (HSsmall). For this thesis, HSsmall model is used to define soil behavior for dynamic analysis. Therefore, basic concepts of HS and HSsmall model are described in this section.

2.2.1.1 Hardening Soil Model

Hardening Soil (HS) model initially proposed for sand and later developed for other types of soil, both soft and stiff soils. In this model, soil stiffness is defined by incorporating several stiffness parameters and has a built in formulation to simulate stiffness that is dependent on effective stress level (Nordal, 2016). The stress dependency of the stiffness moduli (Triaxial stiffness, unloading-reloading stiffness and oedometer stiffness) can be expressed as the following equations:

$$E_{50} = E_{50}^{ref} \left(\frac{c.cos\phi - \sigma_3' sin\phi}{c.cos\phi + P_{ref} sin\phi}\right)^m \tag{2.30}$$

$$E_{ur} = E_{ur}^{ref} \left(\frac{c.cos\phi - \sigma_3' sin\phi}{c.cos\phi + P_{ref} sin\phi}\right)^m \tag{2.31}$$

$$E_{oed} = E_{oed}^{ref} \left(\frac{c.cos\phi - \sigma_1' sin\phi}{c.cos\phi + P_{ref} sin\phi}\right)^m \tag{2.32}$$

In these equations, *m* is the power of stress-level dependency of stiffness which is normally varies between 0.5 to 1.0. P_{ref} = 100 kPa is the atmospheric pressure. Suggested range for E_{50}^{ref}= 15MPa (for loose sand) to 50 MPa (for dense sand) (Nordal, 2016).

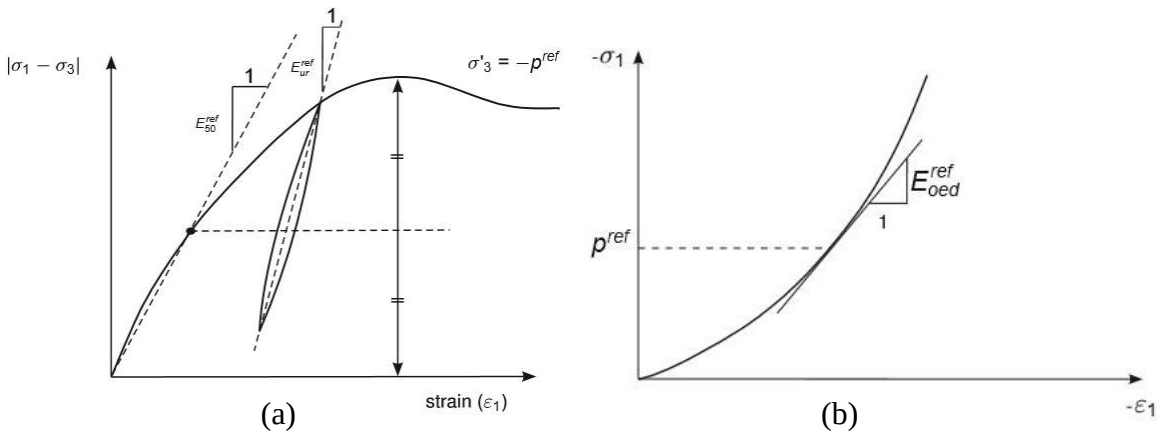

Figure 2-19 Definition of stiffness parameters (a) for drained triaxial test result (b) oedometer test result ("PLAXIS 2D Material Models Manual," 2016)

The isotropic hardening of HS model is connected to two plastic yield surfaces. The Mohr-Coulomb criterion (with mobilized friction) is presented by a “cone” which can expand gradually while loading towards failure. Thus, unlike Mohr-Coulomb model, the yield surface is not fixed in a principle stress rather it can expand because of plastic strain. The position of preconsolidation stress gives a spherical surface or “cap”. The cap expands with increasing preconsolidation stress and results in plastic volumetric strain (Nordal, 2016)

Although this model provides greater accuracy than Mohr-Coulomb model, it does not incorporate anisotropic strength-stiffness behavior, “creep” or time dependent behavior of soil and cyclic loading effect.

2.2.1.2 Hardening Soil Model with Small Strain Stiffness (HSsmall)

HSsmall model is the modification of HS model which incorporates increased stiffness of soil for at small strain. Soil stiffness become very high at very low stiffness compared to engineering stiffness. In such case, strain-stiffness relationship becomes non-linear. To address this behavior, HSsmall model introduces two additional parameters along with other input parameters in HS model i.e.

- small strain shear modulus (strain in the range of 1. 10^{-6}), G_0^{ref}
- strain level at which small-strain shear modulus becomes about 70% of its initial value, $\gamma_{0.7}$

The stress dependency of small strain stiffness is given by:

$$G_0 = G_0^{ref} \left(\frac{c.cos\phi - \sigma_3' sin\phi}{c.cos\phi + P_{ref} sin\phi}\right)^m \tag{2.33}$$

Stress-strain curve for small strain can be described with a hyperbolic low proposed by Hardin and Drnevich (1972):

$$\frac{G_S}{G_0} = \frac{1}{1+\left|\frac{\gamma}{\gamma 0.7}\right|} \tag{2.34}$$

Later simplified by Dos Santos and Correia (2001):

$$\frac{G_S}{G_0} = \frac{1}{1+0.385\frac{\gamma}{\gamma 0.7}} \tag{2.35}$$

This relation is used in PLAXIS to describe stress-strain curve.

Again, according to Vucetic and Dobry (1991) G_s/G_0 vs γ curves depends on plasticity index, PI (usually taken for 50%).

The lower cut-off of tangent shear modulus is given by, $G_t \geq G_{ur}$

Here, unloading-reloading stiffness, $G_{ur} = E_{ur} / 2(1+\nu_{ur})$; E_{ur} is the unloading-reloading modulus and ν_{ur} is the poisson's ratio for loading/unloading.

HSsmall model demonstrates more reliable displacements than HS model and more suitable for dynamic analysis since it captures cyclic behavior ("PLAXIS 2D Material Models Manual," 2016).

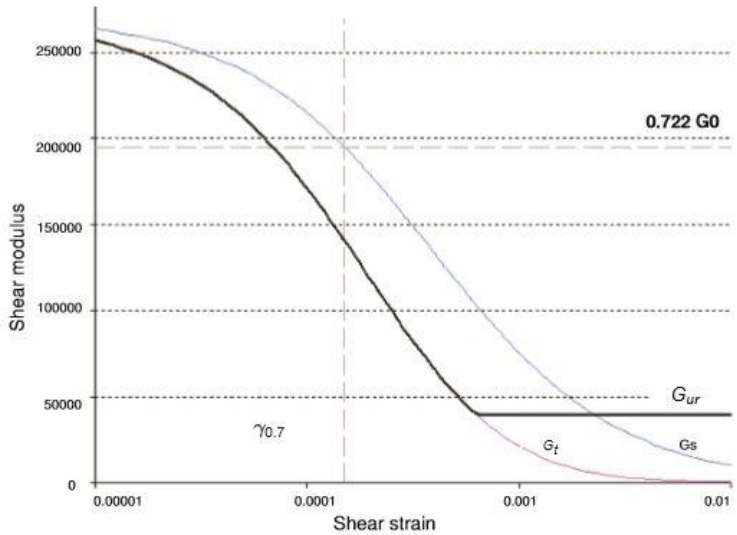

Figure 2-20 Secant and tangent shear modulus reduction curve ("PLAXIS 2D Material Models Manual," 2016)

2.2.2 Dynamic Analysis

Dynamic analysis in PLAXIS can be done for both single source vibration and earthquake problems. Earthquake loads are usually applied at the bottom boundary and the resulting shear waves propagate in upward direction. The soil is simulated in *plain strain model* which does not have geometric damping. Therefore, it is recommended to provide Rayleigh damping to get realistic result ("PLAXIS 2D Dynamic Manual,").

Although the analysis procedure for dynamic load is almost similar to that for static condition, there are few factors that should be taken care of, such as:

- ***Boundary Condition***

In finite element analysis, soil volumes are simulated as a volumetric element, laterally constrained by boundaries although it expands infinitely in reality. This kind of simulation performs well for static analysis and smaller volume costs less time and calculation effort. However, in dynamic analysis, the propagating wave hits the vertical boundaries and reflects into the system, thus causes trapped energy in the model (Stensløkken, 2016). This problem can be solved by incorporating special dynamic boundary condition. Appropriate boundary condition can be chosen from following options ("Plaxis Bv," 2014):

I. *Viscus boundary*, includes viscus damper and absorbs the incoming energy, normally applied when the source of vibration is inside the mesh.

II. *Compliant base boundary*, available only on the base of the mesh, a combination of a line prescribed displacement and a viscous boundary, generally applied for earthquake problems.

III. *Free field boundary*, only available for the lateral boundaries, a combination of a line prescribed displacement and a viscous boundary like *compliant base*, also preferred for earthquakes.

IV. *Tied degree of freedom*, only available for the lateral boundaries and PLAXIS 2D (not available in 3D). The nodes of the left and right boundaries are tied in a way so that they undergo exact same displacement. Normally applied to earthquake problems.

- ***Element Size and Time stepping***

Mesh is generated automatically in PLAXIS based on a robust triangulation procedure. The dimension of triangular elements can be controlled by selecting appropriate element distribution (Laera & Brinkgreve 2015). There are five kinds of element distributions which gives five different relative element size factors (r_e) and corresponding average element size or target element size ("PLAXIS 2D Reference Manual," 2016)

Target element dimension can be approximated based on the equation suggested by (Kuhlemeyer & Lysmer, 1973)

$$\text{Average element size} \leq V_{s,min} / (8 * f_{max}) \qquad (2.36)$$

Here, $Vs_{,min}$ is the lowest shear wave velocity of the layer and f_{max} is the maximum frequency content of the input wave.

PLAXIS automatically ensures that the wave crosses one element per time step. For this, critical time step is calculated according to element size and material stiffness. The time step is then adjusted according to input data points (Laera & Brinkgreve 2015).

$$\delta_t = \frac{\Delta t}{m.n} \qquad (2.37)$$

Here, δ_t is the time step calculated from dynamic time interval Δt, maximum number of steps, m and number of sub steps, n.

- ***Other factors***

Newmark time integration damping under dynamic condition is usually given a default value in PLAXIS analysis:

- α_N= 0.25 and β_N=0.5, for average acceleration
- α_N= 0.3025 and β_N=0.6 for damped Newmark scheme

Relaxation coefficient C_1 and C_2 are applied to improve the absorption quality at the boundaries. It is not necessary when the soil is only subjected to normal pressure wave and can be kept default (C_1=C_2=1). In case of earthquakes, there are normally shear wave and in that case C_2= 0.25, C_1=1 can be applied ("PLAXIS 2D Dynamic Manual,").

2.2.3 Modelling Pile in PLAXIS 2D

Piles are 3D elements and it is difficult yet sometimes necessary to model them in 2D plain strain. There are few alternatives in current practice of FEM modelling in PLAXIS 2D. Previously, modelling used to be done in 2D by either plates elements or node to node anchors. These methods have some benefits as well as limitations. Embedded beam row element is a relatively new feature introduced by PLAXIS to model pile in the out-of-plane direction which results in better realistic results and helps to overcome the limitations of other methods in 2D (Sluis et al., 2014).

Table 2-1 Different available options for modeling pile in PLAXIS 2D

Plate element	**Node to node anchor**	**Embedded beam row**
Allows axial stiffness.	Allows axial stiffness.	Allows axial stiffness.
Interaction with soil by implementing interface.	No interaction with soil.	Interaction with soil due to line to line interface.
No soil flow through plate-discontinuous mesh.	Soil flow through anchors-continuous mesh.	Soil can flow through embedded pile row.
Possibility to enter bending stiffness to obtain structural forces.	No possibility to enter bending stiffness to obtain structural forces.	Possibility to enter bending stiffness to obtain structural forces.
Unrealistic shear plane is introduced.	No unrealistic shear plane is introduced.	No unrealistic shear plane is introduced.

Validation of this feature has been done by authors such as (Dao, 2011) (Sluis, 2012) and (Kwaak, 2015).

Table 2-2 Input parameters for an embedded beam row element

Parameter	Symbol	Unit
Material model	Elastic/elastoplastic/elastoplastic (M-K)	
Young's modulus	E	kN/m^2
Unit weight	γ	kN/m^3
Pile type	Predefined/ user defined	-
Predefined pile type	Massive circular pile/ circular tube/ massive square pile	-
Diameter	D	m
Area	A	m^2
Moment of Inertia	I	m^4
Out of plane center to center distance of piles	$L_{spacing}$	m
Axial skin resistance	T_{skin}	kN/m
Lateral skin resistance	T_{lat}	kN/m
Base Resistance	F_{max}	kN
Interface stiffness factors (axial, lateral and base)	ISF_{Rs}, ISF_{Rn}, ISF_{Kf}	-

2.2.3.1 Principle of Embedded Beam Row in 2D

Embedded beam row is a function which allows the modelling of pile in 2D with a certain spacing in the perpendicular direction to the plane. A volume less beam is created in 2D plane when the feature is applied and after specifying diameter, it creates an equivalent elastic zone around the beam to simulate the pile behavior as a volume element (Dao, 2011).

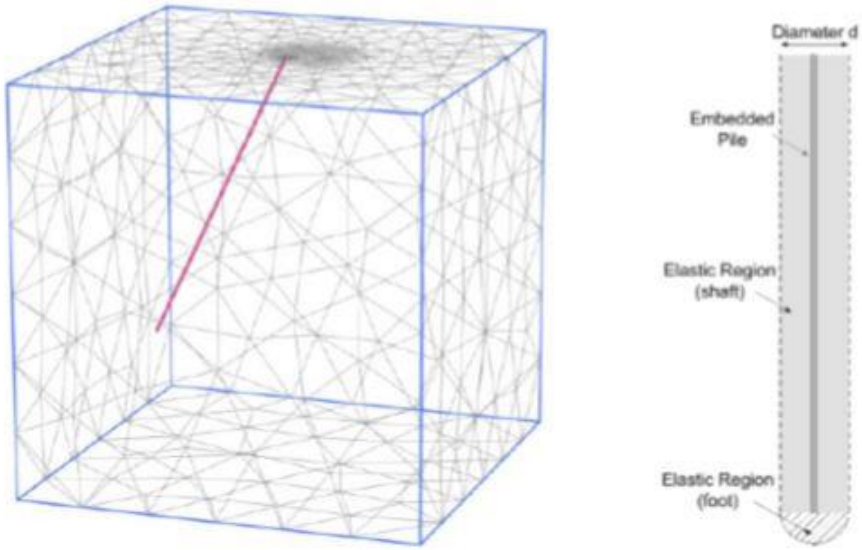

Figure 2-21 Embedded beam in 3D mesh and elastic zone around the beam (Kwaak, 2015)

The features of embedded beam row are described based in "PLAXIS 2D Reference Manual" 2016). The interaction with surrounding soil is defined by special interface. Soil and pile shaft interaction is model by line to volume interface while soil and tip interface is modelled as point to volume interface elements. Pile bearing capacity is an input not a result in embedded beam element. Both skin and tip resistance in axial and lateral direction must be provided as an input while designing embedded beam row element. Figure 2-22 shows the design idea of embedded beam row in 2D plain strain model. 2D plain strain model represents a slice of 1m element which is supposed to be continued out-of-plain direction. Now embedded beam is separated in out-of-plain direction by “pile spacing”. This makes the soil flow around the pile and keep a continuous mesh. Thus, a pile row repeating itself with given spacing is created out-of-plane direction.

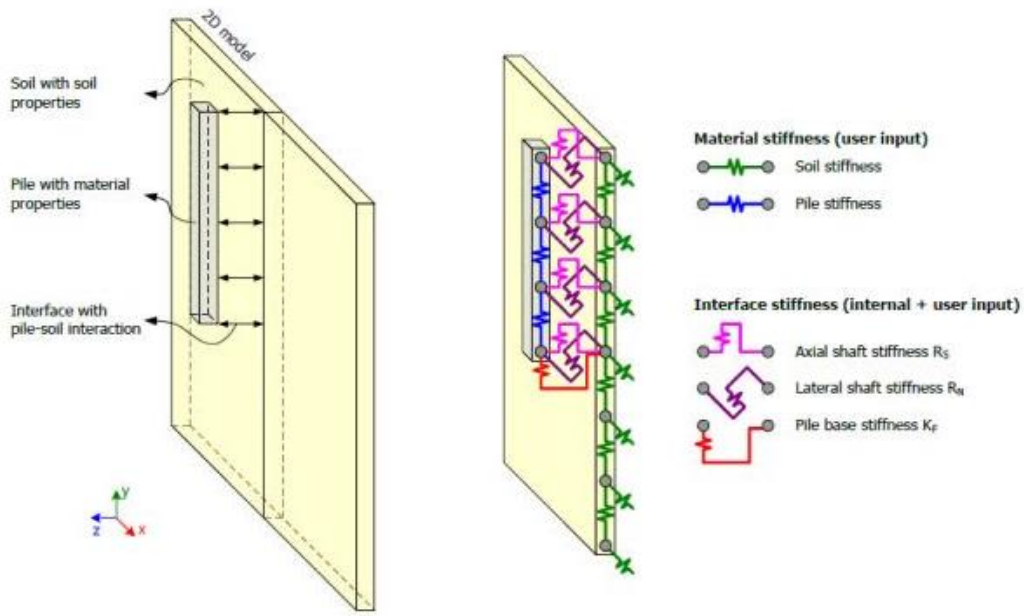

Figure 2-22 Soil structure interaction by special interface elements, concept of embedded beam (row), after Sluis (2012)

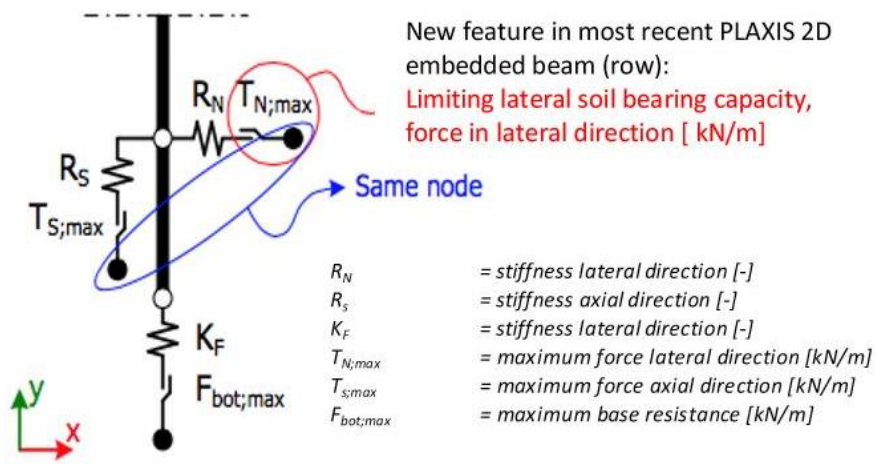

Figure 2-23 Principle of interface by (Sluis et al., 2014)

Sluis (2012) describes the soil structure interaction by special interface elements which connects pile to soil elements (showed in figure 2-22 and 2-23). The interaction along the pile shaft is defines by line-to-area interface and represented by springs with axial stiffness and lateral stiffness. In both directions, the force in the spring is limited by a maximum force. This force is the maximum axial and lateral skin capacity ($T_{s;max}$ and $T_{N;max}$) and which is an input parameter and must be pre-calculated. The interface at the base is a point-to area interface

which is represented by a spring with numerical stiffness (K_F) and a slide. This force is the maximum base resistant (F_{max}) calculated as an input parameter. The values of interface stiffness (R_S, R_N and K_F) can be obtained by using the following formulae derived by Sluis (2012) .The equations are based on soil shear modulus G_{soil}, out-of-plane spacing $L_{scacing}$, and corresponding interface stiffness factors.

$$R_s = ISF_{RS}\ (G_{soil}/L_{spacing})$$

$$R_N = ISF_{RN}\ (G_{soil}/L_{spacing})$$

$$K_F = ISF_{KF}\ (G_{soil} \times R_{eq}/L_{spacing})$$

The interface stiffness factors are calculated automatically by PLAXIS. Based on the study of Kwaak (2015), this automatically generated ISF provides reasonable result for kinematic bending moment compared to D-sheet piling calculation. Sluis (2012) also gave the equations for the interface stiffness factors:

$$ISF_{RS} = 2.5\times\ (L_{spacing}/D_{eq})^{-0.75}$$

$$ISF_{RN} = 2.5\times\ (L_{spacing}/D_{eq})^{-0.75}$$

$$ISF_{KF} = 25\times\ (L_{spacing}/D_{eq})^{-0.75}$$

This feature is validation by Sluis (2012) by using four types of loading conditions:

– Axial compression loading

– Axial tension loading

– Lateral loading by external force

– Lateral loading by soil movement

The results from PLAXIS 2D, 3D and Eurocode displacement curves were compared by Sluis (2012) and it is found that the embedded beam pile provides very reasonable results in case of 3D. It is also concluded that when the usability of embedded beam row depends the center to center lateral spacing to diameter ratio ($L_{spacing}/D$) in 2D. The embedded element gives unrealistic results like plate elements when $L_{spacing}/D$ is less than 2. When $L_{spacing}/D$ becomes higher than 8, it no longer captures the group behavior, rather behaves as a single pile in 2D. Therefore, based on this research, it is inferred that embedded beam row element gives realistic result when $2 < L_{spacing}/D < 8$.

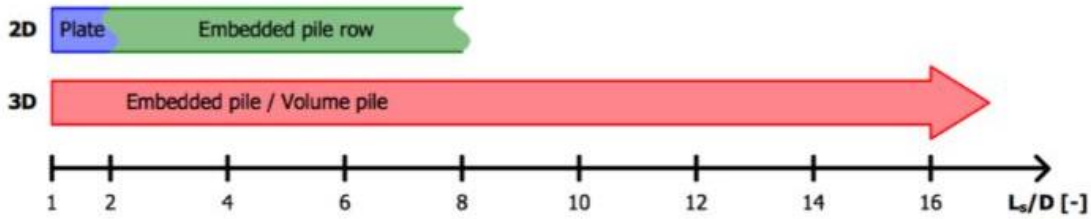

Figure 2-24 Application areas of PLAXIS 2D and 3D modelling a pile row with various structural elements (Sluis, 2012)

2.2.3.2 Calculating Limiting Axial, Lateral and Base Resistance

It is stated in earlier section that the performance of embedded beam row element is sensitive to the input axial, lateral and base resistances. For this reason, it is important to calculate them properly before applying to embedded beams. There are several methods which are widely used by engineers to calculate axial, lateral and base resistance.

Lateral Resistance

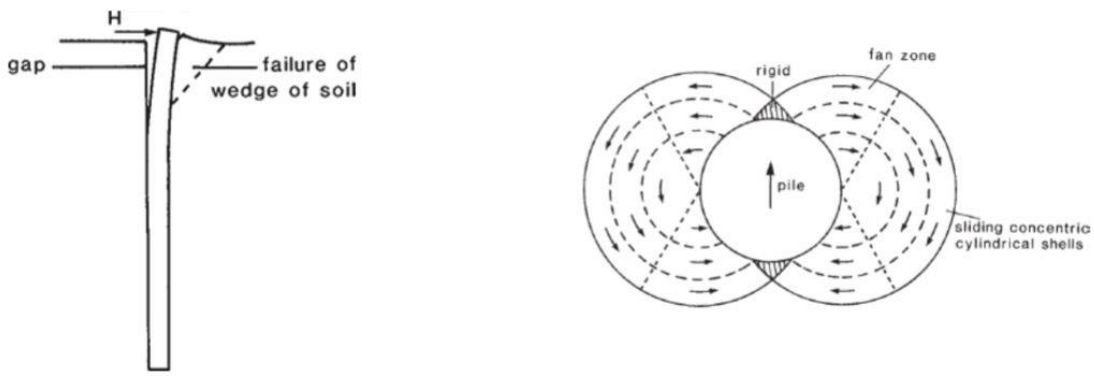

Figure 2-25 Deformation of pile (left) and soil around a pile (right) under active lateral load (Fleming et al., 2008)

Lateral resistance can be calculated using the equations suggested by Brooms (1964). Equation (2.38) given for cohesion less soil.

$$P_u = 3 \times k_p \times \sigma_v' \times D \qquad (2.38)$$

In this equation,

$k_p = \frac{1+\sin\varphi'}{1-\sin\varphi'}$

P_u = Lateral resistance of pile

D = Diameter of pile

σ_v' = Effective vertical stress

For cohesive soil the equations are given as a function of undrained shear strength c_u. It varies with depth for non-uniform clay.

$$P_u = (2+7\times\frac{Z}{3D})\times c_u\times D;\ \text{for } z < 3D \tag{2.39}$$

$$P_u = 9\times c_u\times D;\ \text{for } z \geq 3D \tag{2.40}$$

<u>Axial Resistance</u>

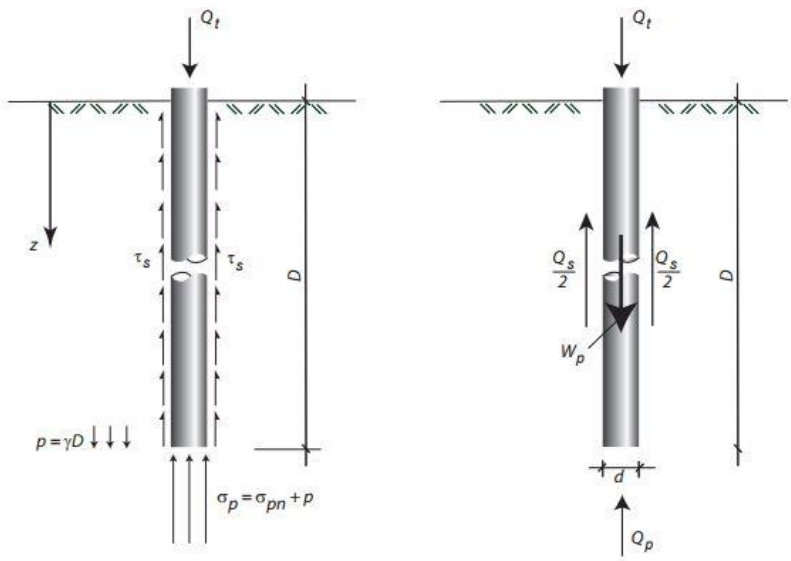

Figure 2-26 Bearing resistance of pile (Eiksund, 2016)

Skin friction for axial loading in clay (Eiksund, 2016):

$$\tau_s = r.\ \tan\varphi'.\ K_A\ (\sigma_v' + a) = S_v.\ (\sigma_v' + a) \tag{2.41}$$

Where,

r = mobilized roughness ratio along the pile (negative for piles in compression)

$\tan\phi'$ = friction in the soil (negative for active earth pressure)

K_A = classical active earth pressure coefficient

S_v = shear ratio can be derived from figure C-1(a) in Appendix C

a = attraction

Skin friction for axial loading in clay is given by,

$$Q_s = \int_0^z \tau_s\ A_s\ dz \tag{2.42}$$

Where,

τ_s = shear stress along the pile (shaft resistance) at depth $z = \alpha\ c_u$

A_s = circumference of the pile cross section

α= normalized side friction of clay can be determined from figure C-2 (b) in Appendix C

<u>Tip resistance</u>

Tip resistance formula in general, $Q_p = A_p . \sigma_{pn}$

Tip resistance of a floating pile in clay:

$$\sigma_{pn} = N_c . \tau_c \tag{2.43}$$

N_c= bearing capacity coefficient for deep quadratic foundations

$= (1+ f_A)\cdot(1+ f_D)\cdot(\pi+2) \approx 9$

Tip resistance of a floating pile in sand:

$\sigma_{pn} = (N_q-1). (\sigma_v' +a)$

Nq = Bearing capacity coefficient, can be found from figure C-1 in Appendix C

2.3 EUROCODE 8

European Standard EN 1998, Eurocode 8 provides the guidance for design of structure for earthquake resistance. It has total 6 parts for design of different structures (EN 1998-1 to EN 1998-6), among which EN-1998-1:2004 (*Eurocode 8: Design of structures for earthquake resistance – Part 1: General rules, seismic actions and rules for buildings)* is applicable to the design of. This is the most relevant parts for this study. While EN 1998-1:2004 provides alternative procedure and values, a national annex is required because of the wide range of seismic characteristics of the member nations (CEN, 2004). Therefore, Norwegian Annex is used as a reference for seismic characterization in this study.

In this study, relevant information is taken from "Nasjonalt tilleg NA" NS-EN 1998-1:2004+A1:2013+NA:2014 (Standard, 2014). The ground type and corresponding design spectrum is calculated according to the guidance provided in section 3. Calculation of shear force at the base of the structure is calculated using lateral force method of analysis described in section 4 (NA. 4.3.3.2). Some important factors, definitions and useful equations are summarized in this section. For better understanding, some definitions are read from English version of European Standard, EN 1998-1:2004.

2.3.1 Identification of Ground Types

According to Eurocode 8, there are seven (A, B, C, D, E, S_1 and S_2) soil types and there should be proper investigation to determine soil type of the site for calculation. These soil types and their corresponding parameters for identification is given in the national annex (Table NA3.1, Appendix A1). It is also suggested that the classification should be done according to average shear wave velocity for first 30m layer if the data is available. The average shear wave velocity at small strain level ($V_{s,\,30}$) is calculated for the top 30m soil layer using following equation (CEN, 2004).

$$V_{s,\,30} = \frac{30}{\Sigma \frac{hi}{vi}} \tag{2.44}$$

In this equation, h_i is the thickness of each layer and v_i is the corresponding shear wave velocity. For each country, the territory is divided into several seismic zones determined by the national authority according the national hazard level. The reference peak ground acceleration for different areas corresponds to a reference return period T_{NCR} of the seismic action or the reference probability of exceedance in 50 years, $P_{NCR.}$ An importance factor γ_I equal to 1,0 is assigned to this reference return period. For return periods, other than the reference the design ground acceleration on type A ground a_g is equal to a_{gR} times the importance factor γ_I (CEN, 2004).

$$a_g = \gamma_I . a_{gR} \tag{2.45}$$

The importance factor for structures are different depending on its usage. The importance classes and their corresponding γ_I values are given in the following table. For the return period mentioned above, the value of γ_I will be 1.

Table 2-3 Seismic Importance Classes according to NS-EN 1998-1, NA.4 (901)

Seismic Importance Class	γ_I values
I	0.7
II	1.0
III	1.4
IV	2.0

Appendix A2 gives seismic zones of Norway (NS-EN 1998-1:2004+NA:2008). The map shows the horizontal spectral acceleration at the bed rock for undamped natural frequency equal to 40 Hz for 5% damping ratio and a return period of 475 years (Rønnquist et al., 2012). Reference ground acceleration of A type soil,

$$a_{gR} = 0.8\ a_{g40HZ} \tag{2.46}$$

Design ground acceleration is found by combining it with impotence factor.

$$a_g = \gamma_I . a_{gR} = \gamma_I .\ 0.8\ a_{g40HZ} \tag{2.47}$$

2.3.2 Basic Representation of Seismic Action

In EN 1998-1: 2004, the earthquake motion at a given point on the surface is represented by elastic response spectrum (figure 2-27). The general version of EC-8 provides elastic response spectrum of similar shape for two levels of earthquake magnitudes. While in Norwegian Annex, there is only one elastic response spectrum to describe earthquake motion at different soil types. More than one shape of spectra should be considered for design seismic action if the site is affected by earthquakes from differing sources. The value of input seismic action a_g will be different for each type of spectrum and earthquake.

There are total four types of elastic response spectrum described in EC-8.

- ***<u>Horizontal elastic response spectrum</u>***

For the horizontal components, $S_e\ (T)$ of the seismic action. Shape is defined by the following equations (CEN, 2004):

$0 \leq T \leq T_B$: $$S_e\ (T) = a_g S\ [1 + \frac{T}{T_B}(2.5\eta - 1)] \tag{2.48}$$

$T_B \leq T \leq T_C$: $$S_e\ (T) = a_g S\ 2.5\eta \tag{2.49}$$

$T_C \leq T \leq T_D$: $$S_e\ (T) = a_g S\ 2.5\eta\ [\frac{T_C}{T}] \tag{2.50}$$

$T_D \leq T \leq 4s$: $$S_e\ (T) = a_g S\ 2.5\eta\ [\frac{T_C T_D}{T^2}] \tag{2.51}$$

In these equations:

- $S_e(T)$ = The horizontal component elastic response spectrum;
- T = Natural vibration period of a linear SDOF system;
- a_g= Design ground acceleration on type A ground ($ag = \gamma_I . a_{gR}$);

- T_B = Lower limit of the period of the constant spectral acceleration branch;
- T_C = Upper limit of the period of the constant spectral acceleration branch;
- T_D =the value defining the beginning of the constant displacement response range of the spectrum;
- S =Soil factor;
- η = Damping correction factor with a reference value of η = 1 for 5% viscous damping.

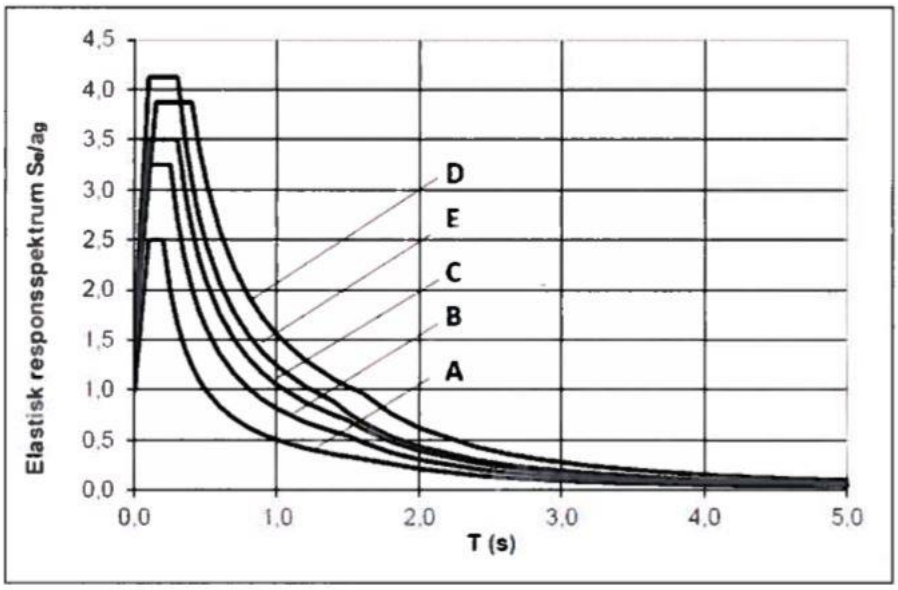

Figure 2-27 Recommended horizontal elastic response spectra in Norway for ground type A to E (Figure NA.3(903) in NS-EN 1998-1:2004+A1:2013+NA:2014)

Table 2-4 Recommended parameters for elastic response spectrum (Table NA.3.3 in NS-EN 1998-1:2004+A1:2013+NA:2014)

Soil Type	S	T_B (s)	T_C (s)	T_D (s)
A	1.00	0.10	0.25	1.7
B	1.30	0.10	0.30	1.5
C	1.40	0.15	0.30	1.5
D	1.55	0.15	0.40	1.6
E	1.65	0.10	0.30	1.4

- ***Vertical elastic response spectrum***

The response spectrum that describes the vertical component of the seismic action, $S_{ve}(T)$. Here, a_{vg} is the vertical component of ground acceleration. Shape of the spectrum is defined by the following equations:

$0 \leq T \leq T_B$: $$S_{ve}(T) = a_{vg}\left[1+\frac{T}{T_B}(3.0\,\eta - 1)\right] \quad (2.52)$$

$T_B \leq T \leq T_C$: $$S_{ve}(T) = a_{vg}\,3.0\eta \quad (2.53)$$

$T_C \leq T \leq T_D$: $$S_{ve}(T) = a_{vg}\,3.0\eta\left[\frac{T_C}{T}\right] \quad (2.54)$$

$T_D \leq T \leq 4s$: $$S_{ve}(T) = a_{vg}\,3.0\eta\left[\frac{T_C T_D}{T^2}\right] \quad (2.55)$$

- ***Elastic displacement response spectrum***

The elastic displacement spectrum is obtained by direct transformation of the elastic response spectra for acceleration $S_e(T)$ by using following expression (CEN, 2004):

$$S_{De}(T) = S_e(T)\left[\frac{T}{2\pi}\right]^2$$

To determine the design ground displacement, d_g, corresponding to the design ground acceleration, when available studies do not indicate otherwise:

$$d_g = 0.025.\ a_g.\ S.\ T_C.\ T_D$$

Further explanation is possible for elastic displacement response spectrum which is not elaborated since it is beyond the scope of this study.

- ***Design spectrum for elastic analysis***

Values of design spectrum for elastic analysis are dependent on the local ground condition, type of structure and seismic Input. Shape of the spectrum can be obtained by following equations (CEN, 2004):

$0 \leq T \leq T_B$: $$S_d(T) = a_g S\left[\frac{2}{3}+\frac{T}{T_B}\left(\frac{2.5}{q}-\frac{2}{3}\right)\right] \quad (2.56)$$

$T_B \leq T \leq T_C$: $$S_d(T) = a_g S\,\frac{2.5}{q} \quad (2.57)$$

$T_C \leq T \leq T_D$: $$S_d(T) = \begin{cases} a_g S\,\frac{2.5}{q}\left[\frac{T_C}{T}\right] \\ \geq \beta a_g \end{cases} \quad (2.58)$$

$T_D \leq T$:

$$S_d\,(T) = \begin{cases} a_g S\ \frac{2.5}{q}\ [\ \frac{T_C T_D}{T^2}] \\ \geq \beta a_g \end{cases} \tag{2.59}$$

Here, q is behavior factor of the structure and β is the lower bound factor for the horizontal design spectrum, can be found in national annex.

The design elastic response spectra described in Eurocode 8 are largely controlled a parameter called "behavior factor, q". This factor defines the ductility of a structure or in other words, the capacity of the structure to dissipate energy. This parameter has different range of values suggested in different parts of Eurocode 8 depending on the ductility classes (low/medium/high) of the structure (Appendix A3).

The capacity of structural systems to resist seismic actions or absorb energy in a non-linear range is higher than a system in elastic range. The behavior factor is introduced to approximate the reduction of the imposed seismic actions on the structure by an elastic analysis to avoid complicated inelastic analysis. In Norway, it is permitted to use low or medium ductility levels and in common practice most of the structures are designed by introducing $q \leq 1.5$, according to Ductility Class Low, DCL. This implies that the structures are analyzed as non-dissipative in Norway (Rønnquist et al., 2012).

It is important to choose the most reasonable value for behavior factor since it has a great influence on the shape of design response spectrum. The choice of behavior factor can be justified by guidance provided in different parts of Eurocode 8. According to NS-EN 1998-1, concrete or steel construction in a relatively low seismic area where a_g S<0.25g = 2.45m / s^2 can be designed as to DCL with $q \leq 1.5$ if the construction is checked for different load effects. This condition portrays the most common cases in Norway (Rønnquist et al., 2012).

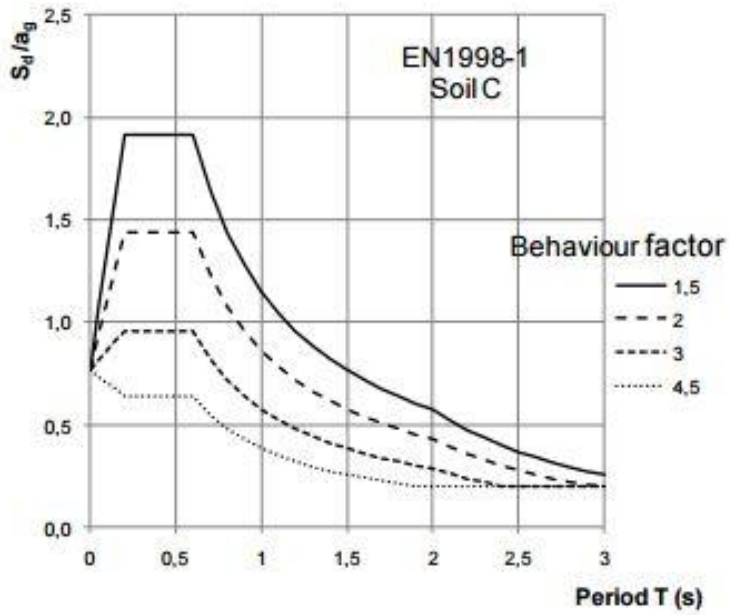

Figure 2-28 Effect of behavior factor on the shape of design response spectrum (Bisch et al., 2012)

2.3.3 Base Shear Force Calculation

The base shear is calculated according to lateral force method of analysis. Method of analysis is given in section 4.3.3.2 in EN 1998-1:2004 (see CEN (2004)).

To be able to use this method, the structure must satisfy the following condition:

$$T_1 \leq \begin{cases} 4Tc \\ 2.0 \end{cases} \tag{2.60}$$

Then shear force generated at the base can be obtained from following equation:

$$F_b = S_d\,(T_1).\ m.\ \lambda \tag{2.61}$$

Where,

- T_1 = is the natural period of vibration of the building for the given motion in the considered direction.
- S_d (T_1) = Component of design spectrum for T_1.
- m= The total mass of the building, above the foundation or above the top of a rigid basement
- λ= the correction factor, the value of which is equal to: λ = 0,85 if $T_1 < 2\ T_C$ and the building has more than two stories, or λ = 1,0 otherwise.

The factor λ accounts for the fact that in buildings with at least three stories and translational degrees of freedom in each horizontal direction, the effective modal mass of the 1st (fundamental) mode is smaller, on average by 15%, than the total building mass.

According to section 4.3.3.2.2 and (3), EN 1998-1:2004 (CEN, 2004), for the determination of the fundamental period of vibration period T_1 of the building, expressions based on methods of structural dynamics (for example the Rayleigh method) may be used. For buildings with heights of up to 40 m the value of T_1 (in second) may be approximated by the following expression:

$$T_1 = C_t . H^{3/4} \tag{2.62}$$

Where,

- C_t is 0,085 for moment resistant space steel frames, 0,075 for moment resistant space concrete frames and for eccentrically braced steel frames and 0,050 for all other structures;
- H is the height of the building, in m, from the foundation or from the top of a rigid basement.

3 CONSTRUCTION OF FEM MODELS AND PARAMETERS

In this section the model geometry, parameter selection and method of dynamic analysis in PLAXIS 2D will be discussed. There are total five models for analysis:

Model 1: Soil profile without structure

Model 2: Single-story structure with shallow foundation

Model 3: Single-story structure with piled raft

Model 4: Four-story structure with shallow foundation

Model 5: Four-story structure with piled raft

3.1 CONCEPT AND GEOMETRY

Two layered soil system is chosen to simulate the problem. A wide boundary is chosen for the soil profile to minimize the boundary condition effect. Soil profile is a rectangle with a dimension 150m×25m. Total soil depth is 25m down to the bedrock. Upper 10m layer is soft clay and next 15m layer is relatively stiff sand. The structure is constructed on the top of the clay layer, first with a shallow foundation at 1m depth. First structure is a single-story building with dimension 5m × 6m. Second structure is a four-story building with 12m× 10m dimension and 3m floor to floor distance, also having a shallow foundation of 1m depth. For this building, columns are provided in the mid-span with node-to-node anchor. Then the structures are modelled with piles bellow the shallow foundation which goes into the sand layer. For the single-story structure, the pile length is 12m and for the four-story structure it is 15m. Since the piles are connected to embedded shallow foundation which contributes load bearing, the foundation system acts as a piled-raft foundation rather than pile group. Model geometry for all five models are given in figure 3-1 to 3-6.

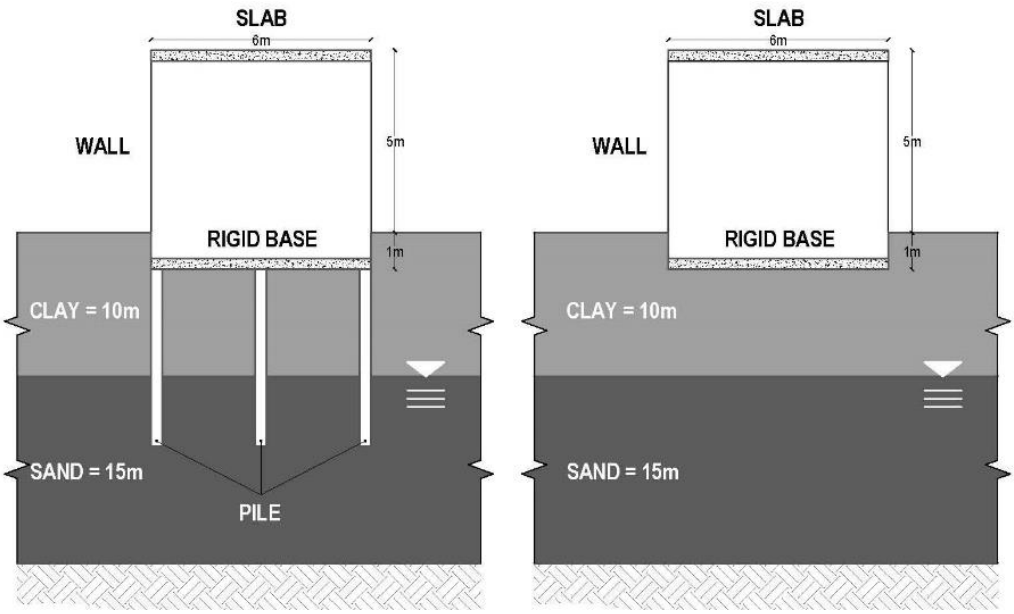

Figure 3-1 Schematic presentation of the model concept with single story structure.

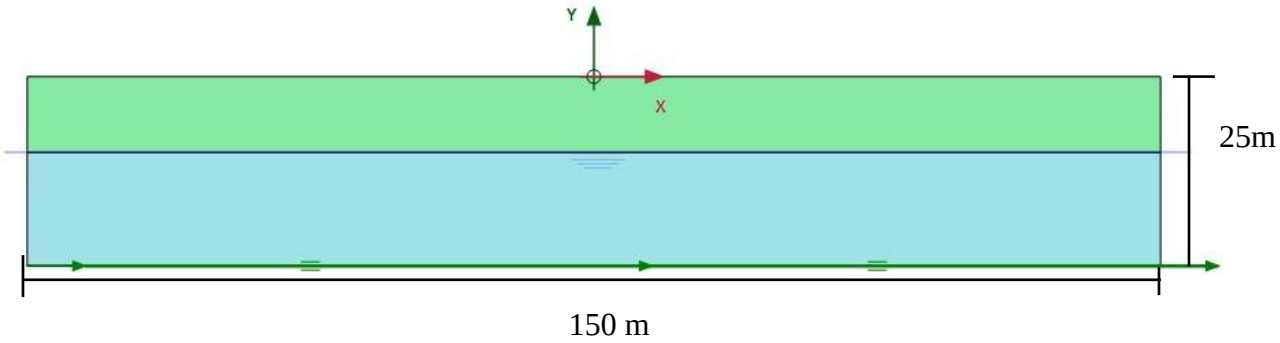

Figure 3-2 Model 1: Soil profile without structure

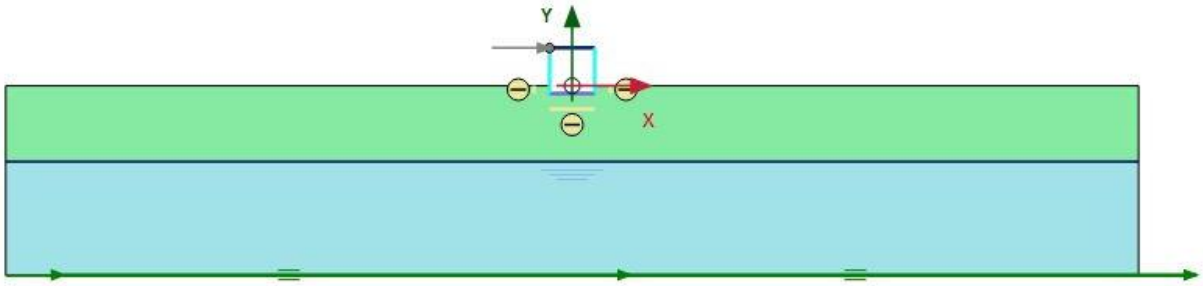

Figure 3-3 Model 2: Single-story structure with shallow foundation

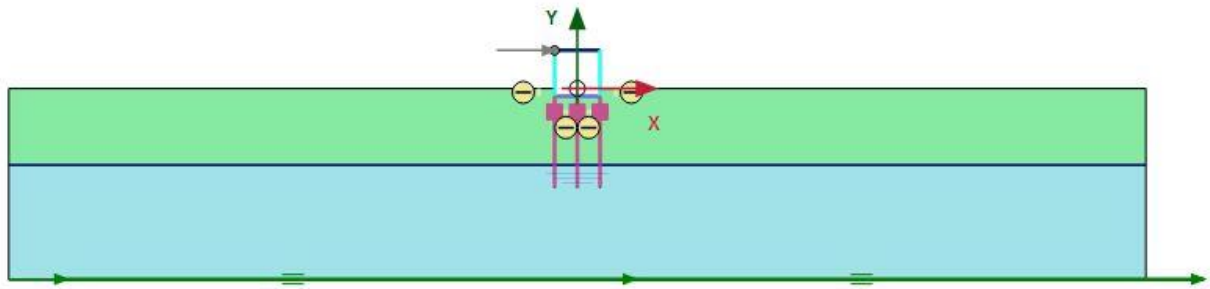

Figure 3-4 Model 3: Single-story structure with piled raft

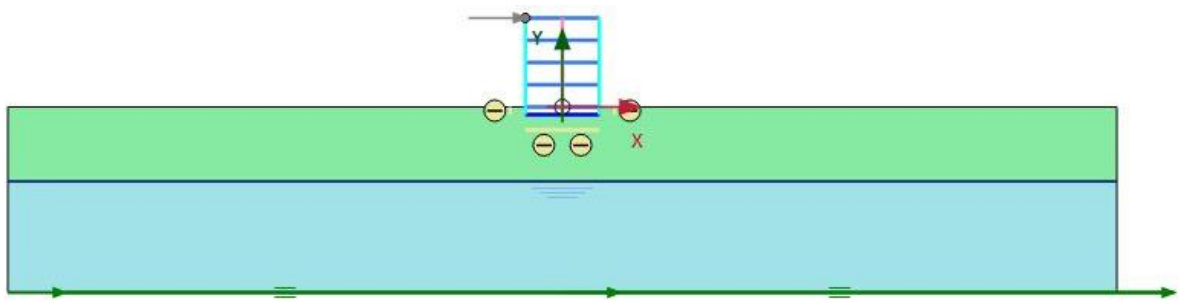

Figure 3-5 Model 4: Four-story structure with shallow foundation

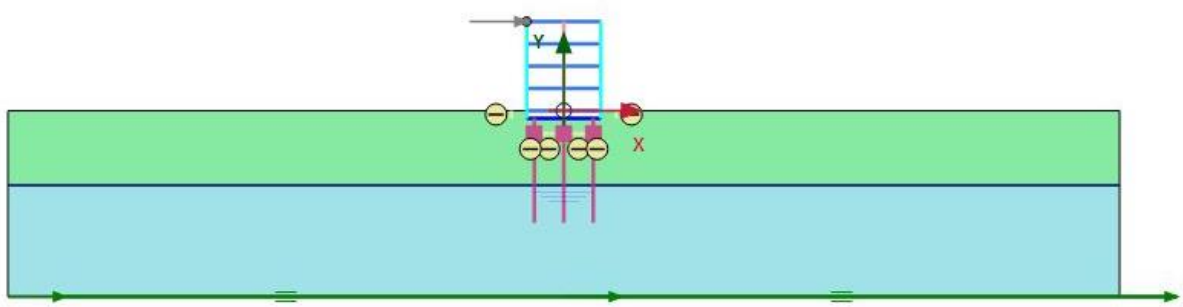

Figure 3-6 Model 5: Four-story structure with piled raft

3.2 MATERIAL PROPERTIES

The material properties are selected based on the discussion in section 2.2 to delineate a representative scenario. Stiffness parameters are chosen in such a way so that the sand is in medium dense range (15MPa < E_{50}^{ref} < 50MPa). As stated earlier, Hardening soil model with small strain stiffness (HSsmall) captures the far field seismic effect better than any other existing model in PLAXIS. Therefore, HSsmall model is chosen in this study to define the soil properties. Usually in case of an earthquake, the loading condition is undrained. Undrained condition can be modelled in PLAXIS in three different ways. In this study the drainage condition is modelled will undrained (A) because of its better performance in numerical simulation compared to undrained (B). In undrained (A), the soil properties are given by effective strength parameters while undrained (B) and (C) uses total stress parameters and in these cases c_u is an input parameter. The soil model can be checked for undrained shear strength by back calculating c_u from PLAXIS and comparing the value with c_u obtained by Mohr-coulomb formula. Undrained shear strength c_u can be calculated as a function of effective stress parameters, cohesion and friction angle. PLAXIS SoilTest option is used to back calculate the depth dependent c_u. It is understandable that the value obtained from HSsmall model by using programmed soil test will be different than that from Mohr-coulomb formula ($C_u = \sigma_p' \sin\varphi + c\cos\varphi$), yet they resemble reasonable similarity in figure 3-7. The calculation procedure is elaborated in Appendix B1 This calibration of undrained behavior is important to obtain a representative material property during earthquake simulation. As stated earlier, the modulus reduction and damping ratio curves of HSsmall model are defined Hardin and Drnevich (1972) and Vucetic and Dobry (1991) for plasticity index 50% (figure 3-8).

Table 3-1 Soil parameters for HSsmall model

Parameter	Symbol	Unit	Clay layer	Sand Layer
Material model			HS small	HS small
Drainage Type			Undrained (A)	Undrained (A)
Soil unit weight, saturated	γ_{sat}	kN/m^3	20	20
Soil unit weight, unsaturated	γ_{unsat}	kN/m^3	16	20
Secant stiffness in standard drained triaxial test	E_{50}^{ref}	MPa	20	20

Tangent stiffness for primary oedometer loading	E_{oed}^{ref}	MPa	25	35
Unloading/reloading stiffness	E_{ur}^{ref}	MPa	80	110
Stress-level dependency power	m		1.0	1.0
Cohesion (effective)	C’	KPa	10	5
Dilatancy angle	ψ	^{0}	0	0
Shear strain at G_s= 0,722G_0	$\gamma_{0.7}$		0.12E-3	0.15E-3
Shear Modulus at very small strain	G_0^{ref}	MPa	180	240
Poisson’s Ratio	ν_{ur}		0.2	0.2
Reference pre-consolidation pressure	P_{ref}	KPa	100	100
K_0- for normally consolidated soil	K_0		0.691	0.5305

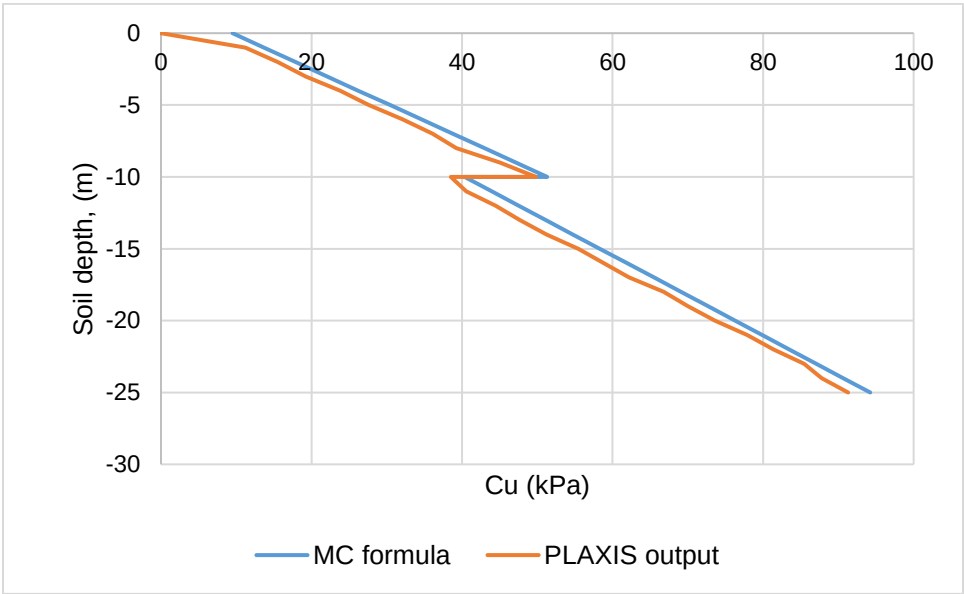

Figure 3-7 Cu parameter compared to MC formula

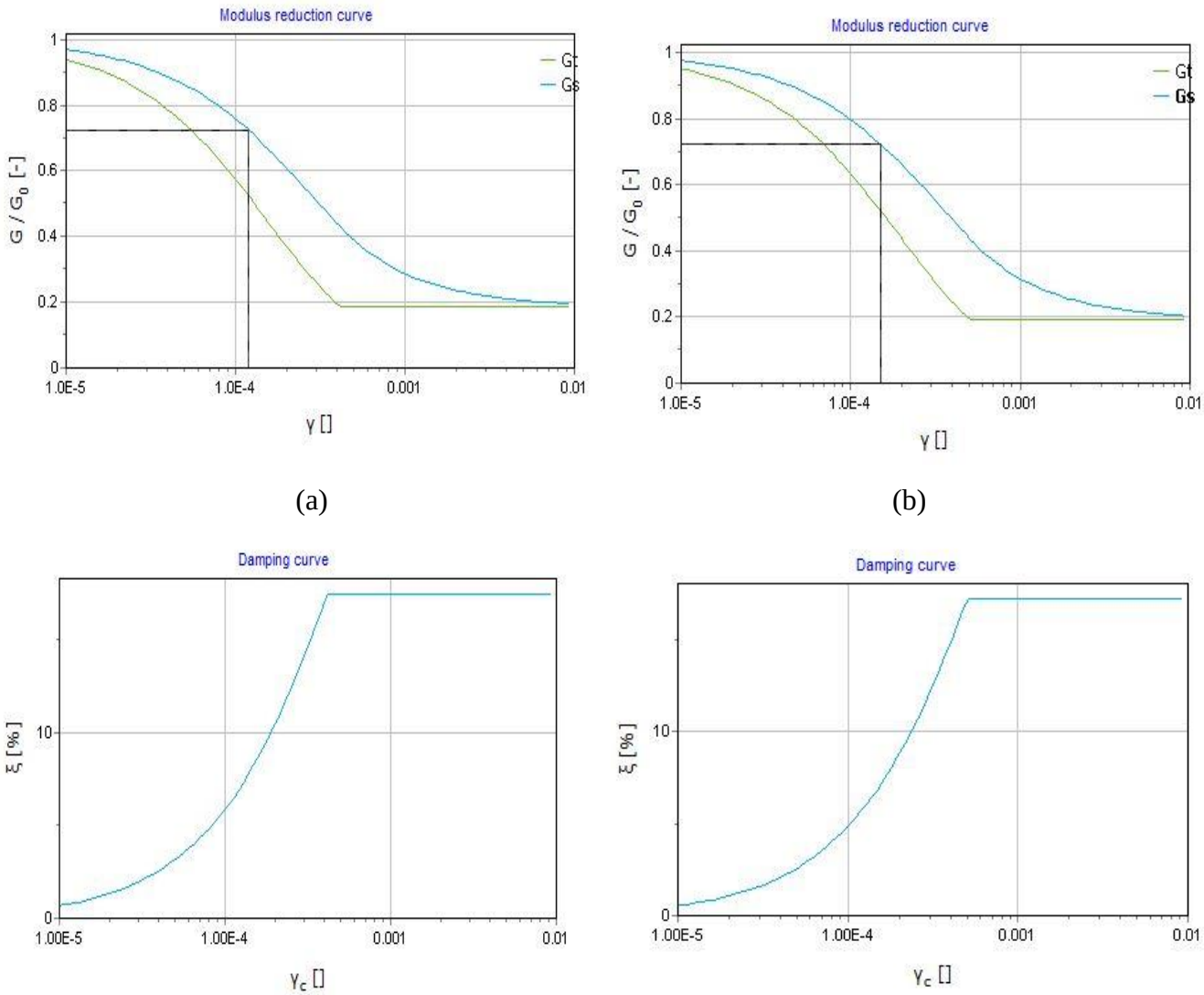

Figure 3-8 Modulus reduction curve for (a) clay and (b) sand, damping cure for (c) clay and (d) sand

Since the interface of soil-structure is weaker and more flexible than the surrounding soil, it is suggested by PLAXIS reference manual to use an interface factor less than 1 to depict the scenario. Therefore, interface between structure and clay is provided with same material property as clay except a manual interface factor R_{inter} 0.7.

Material properties of structural elements are given below. All the material properties are same for the structures accept unit weight. Unit weights are given in different charts.

Table 3-2 Material Properties of basement, slab and wall of the structures (set type: Plate)

Parameter	**Symbol**	**Unit**	**Basement, floors, slab and walls of both structures**
Material Type			Elastic Isotropic
Axial Stiffness	EA	kN/m	12×10^6
Inertial Stiffness	EI	kNm^2/m	160×10^3
Raleigh Damping	α		0.2320
Raleigh Damping	β		8.000E-3

Table 3-3 Weights of different parts of the structure in kN/m/m

Parts of the structures	**Single story**	**Four story**
Basement	10	20
Slab and floors	20	10
Walls	5	5

Table 3-4 Material Properties of columns (set type: Node to node anchor)

Parameters	**Symbol**	**Unit**	**Column**
Material Type			Elastic
Axial Stiffness	EA	kN	2.500E6
Spacing	$L_{spacing}$	m	3.0

3.2.1 Shear Wave Velocity and Soil Type

The shear wave velocity for each layer are determined using equation 2.1.

Detailed calculation is presented in Appendix B, table-B. G_0 is calculated for both layers using equation (2.33)

$$G_0 = G_0^{ref}\left(\frac{c.cos\phi - \sigma_3{}'sin\phi}{c.cos\phi + P_{ref}sin\phi}\right)^m$$

The formula for shear wave velocity is given by equation (2.1):

$$Vs=\sqrt{\frac{G}{\rho}}$$

Depth dependent shear wave velocity is calculated with these equations and presented in figure 3-10 and 3-12. An average shear wave velocity for each layer is approximated from these curves. For clay layer, the average shear wave velocity is 100 m/s and for sand layer it is 148 m/s.

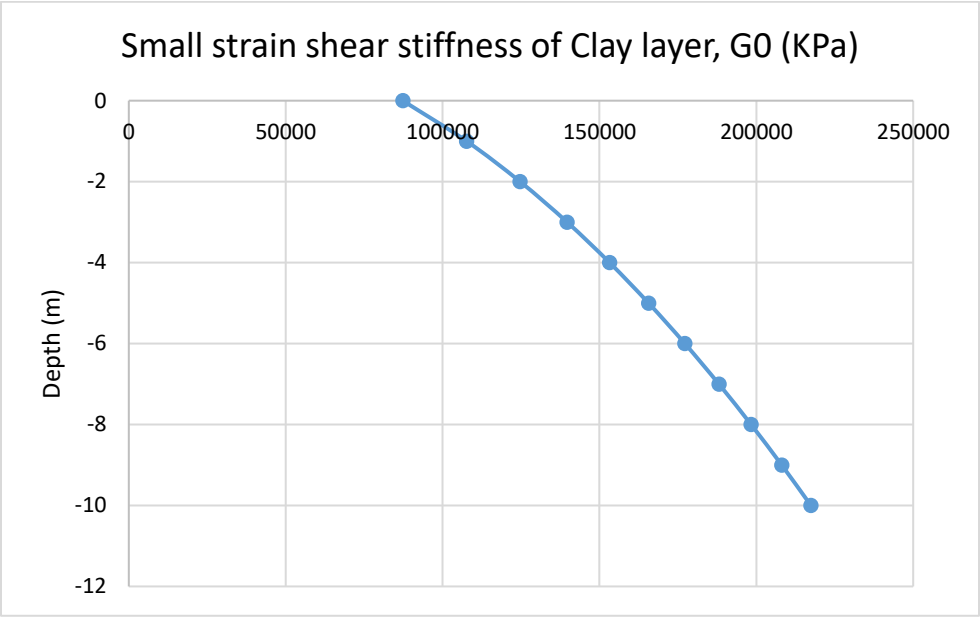

Figure 3-9 Small strain stiffness of clay layer

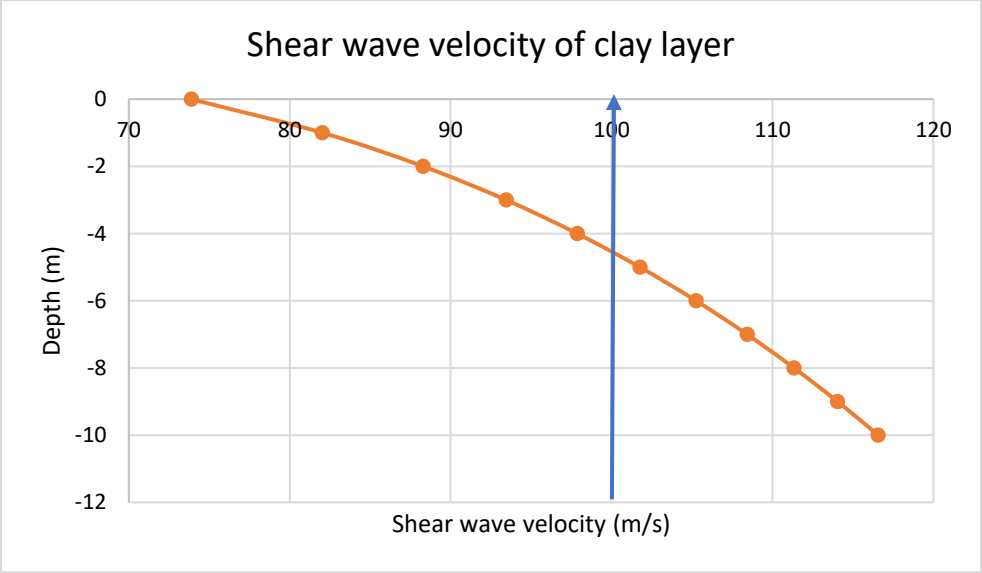

Figure 3-10 Shear wave velocity of clay layer

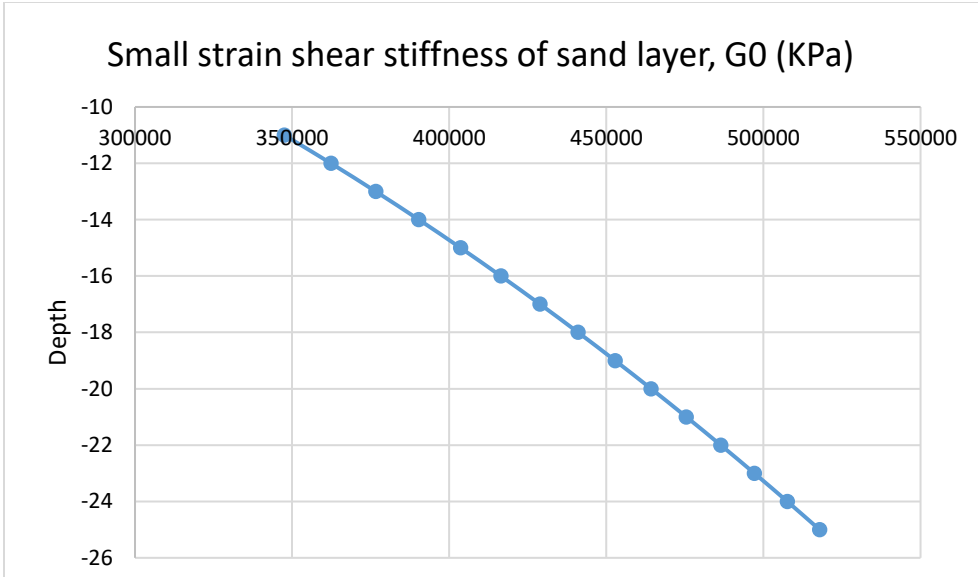

Figure 3-11 Small strain stiffness of sand layer

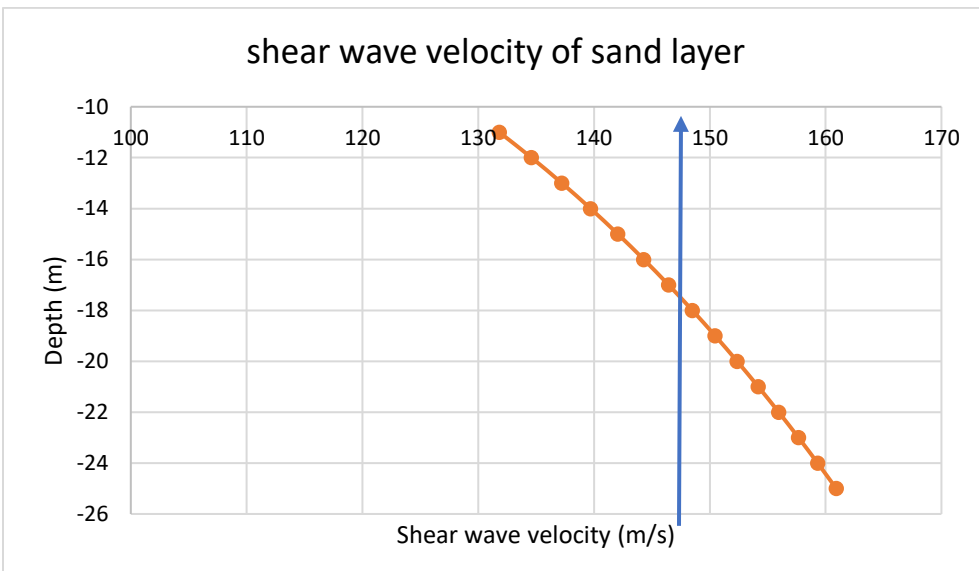

Figure 3-12 Shear wave velocity of sand layer

To identify soil type from Eurocode 8, the average shear wave velocity of the top 30m layer is required. Now the model gives shear wave velocity of 25m and after that it is assumed that the soil type is bed rock or A type soil. It can be assumed that the soil beneath 25m has a shear velocity as high as 1000 m/s. Therefore, the average shear wave velocity of top 30 m is given by

$$V_{s,\,30} = \frac{30}{\Sigma\frac{hi}{vi}} = \frac{30}{\left(\frac{10}{100}\right)+\left(\frac{15}{148}\right)+\left(\frac{5}{1000}\right)} = 146.78 \text{ m/s}$$

From Appendix A1, the soil type for this corresponding shear wave velocity is “D”. Type D soil represents an envelope of a deep deposit having shear wave velocity in the range of 130-180 m/s.

3.2.2 Damping Parameters

Rayleigh parameters for the model are determined based on the discussion in section 2.1.3. The first target frequency is the average natural frequency of the soil deposit and the second one is the ratio of fundamental frequency of the input motion to the natural frequency of the soil.

Average shear wave velocity of 25m deposit is computed by:

$$V_{s,\,25} = \frac{25}{\Sigma\frac{hi}{vi}} = \frac{25}{\left(\frac{10}{100}\right)+\left(\frac{15}{148}\right)} = 125.85 \text{ m/s}$$

Now natural frequency of the soil deposit from:

$$f_1 = \frac{vs}{4H} = \frac{125.81}{4\times 25} = 1.25 \text{ Hz}$$

Fundamental frequency of the input motion, f_2= 2 Hz

f_2/f_1= 2/1.25= 1.6, Next odd number of this ratio is 3

Target damping ratio for both cases is 1%.

Resulting Rayleigh parameters: $\alpha = 0.1109$ and $\beta = 0.7490E\text{-}3$

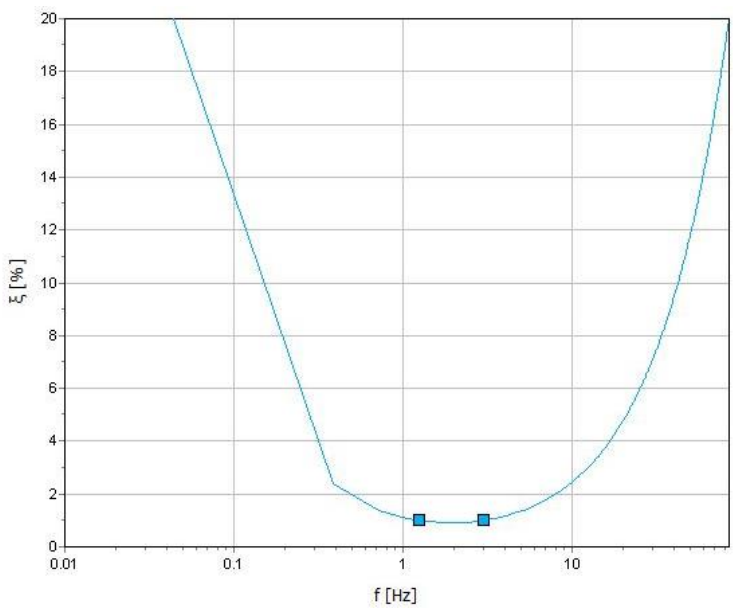

Figure 3-13 Rayleigh damping curve obtained from PLAXIS

3.3 CONSTRUCTION OF PILE USING EMBEDDED BEAM ROW

The construction of pile as an embedded beam row element is done based on the theory discussed in section 2.2.3. It is stated that the performance of embedded beam is sensitive to the input resistance. For this reason, the axial lateral and base resistances are calculated first. Axial resistance is calculated using equations given in section 2.2.3.2. for upper 10m for cohesion less soil and next 15m for cohesive soil. Lateral resistance is calculated in a same manner using given equations. Although it was enough to calculate base resistance at the end point of pile, it is calculated for 25 meters so that the values could just be picked from the table even if the pile length is changed. Detailed calculation in excel is given in Appendix C. Pile center to center spacing in the plane is 3m for single story structure and 4m for four story structure.

Table 3-5 Input parameters of embedded beam row

Parameter	**Symbol**	**Unit**	**Pile**
Material model			Elastic
Young's modulus	E	kN/m^2	30.00E6
Unit weight	γ	kN/m^3	25
Pile type	-	-	Predefined massive circular pile
Diameter	D	m	0.5
Area	A	m^2	0.1963
Moment of Inertia	I	m^4	3.068E-3
Out of plane center to center distance of piles	$L_{spacing}$	m	3 (for 1-story) & 4 (for 3-story)
Axial resistance	T_{skin}	kN/m	Figure 3-14 and Appendix C
Lateral resistance	T_{lat}	kN/m	Figure 3-15 and Appendix C
Base Resistance	F_{max}	kN	Appendix C (based on depth)
Interface stiffness factors			Default values, generated by PLAXIS
Axial stiffness factor	ISF_{Rs}	-	0.6521
Lateral stiffness factor	ISF_{Rn}	-	0.6521
Base stiffness factor	ISF_{Kf}	-	6.521

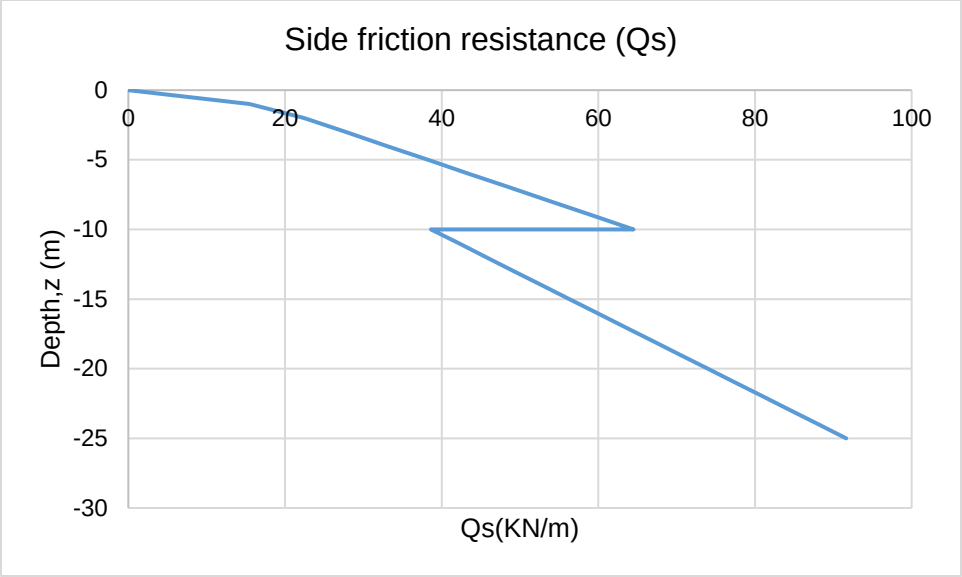

Figure 3-14 side friction resistance along pile length (sharp change indicates change in soil layer)

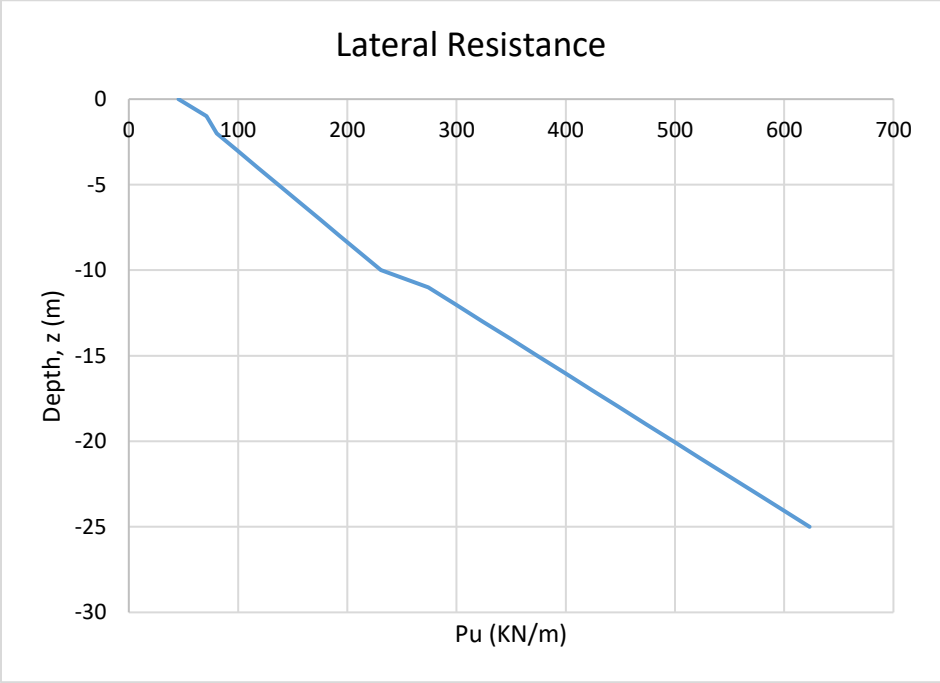

Figure 3-15 Lateral resistance along pile length

3.4 DYNAMIC ANALYSIS IN PLAXIS 2D

The PLAXIS 2D model is constructed with 15-node triangular element in plain strain condition which means that the out-of-plane strain is fixed hence zero. After modelling soil and structural geometry and applying material property, the models need to be provided with loading and proper boundary conditions before starting analysis. Steps of dynamic analysis are listed below.

3.4.1 Mesh generation

Minimum average shear wave velocity of the soil profile ($V_{s,min}$) can be read from figure 3-10 that is 100 m/s. The maximum frequency of the input motion is 2 Hz from table 3-6. This gives an average element size 6.25 m for equation 2-36 in section 2.2.2.

$$\text{Average element size} \leq V_{s,min} / (8 * f_{max})$$

Table 3-6 Average element sizes for different distributions

Element Distribution	relative element size factors (r_e)	average element size, m
Very coarse	2	18.356
Coarse	1.33	12.235
Medium	1	9.178
Fine	0.67	6.122
Very fine	0.33	4.589

Table 3-6 shows different average element sizes for different element distributions and element size corresponding to *fine* mesh meets the target element size obtained from equation 2-36. Therefore, element distribution is set to *fine* for analysis.

3.4.2 Stage Construction

Table 3-7 and 3-8 shows that the model without structure is constructed with two phases while rest of the models are constructed with total five phases.

Table 3-7 Stage construction for Model 1

Phase	**Calculation type**	**Description**
Initial Phase	K0- Procedure	
Phase-1	Dynamic	20 second dynamic time interval

Table 3-8 Stage construction for Model 2 to 4

Phase	Calculation type	Description
Initial Phase	K0- Procedure	Structures deactivated
Phase 1	Plastic	Activated Structure, excavation to -1m
Phase II	Plastic	Horizontal load activated, displacement reset to zero
Phase III	Dynamic	Dynamic time interval 3 second
Phase IV	Dynamic	Starts from Phase I, dynamic time interval 20s, displacement reset to zero

3.4.3 Loading and Boundary Condition

The input ground motion used in this study is an artificially generated time history in SIMQKE (Appendix D). SIMQKE is a program for artificial time history generation, written by Dario Gasparini and Erik Vanmarke in 1976 (Chadha, 2015). The advantage of using artificial time history is that the properties can be known without going through time consuming analysis. The properties of the input motion are given in the table 3-9. The ground motion is applied at the bottom of the boundary as dynamic line displacement. The x-component of the line displacement of the bottom boundary is *prescribed* with a uniform value of 1.0m and the y-component is *fixed*. The duration of the input motion is 20 second with 0.01 second time interval. Therefore, the maximum number of step is provided 20/0.01 or 2000 by manual time step determination. The number of sub step is calculated for the maximum number of step by clicking *Retrieve.* As stated earlier, the vertical boundaries at the both sides are provided with sufficient distance to minimize the effect of boundary condition. Common practice is providing three times of the depth of the soil profile (3H) in each sides (Magar, 2016). In this study, all the models are provided with 75m width each side (total 150m) for 25m depth. The most feasible boundary condition for dynamic analysis is selected based on previous studies by different authors such as Brandt (2014); Chadha (2015); Magar (2016). Based on boundary condition test by Magar (2016), *fixed base*, *tied degree of freedom* and *free lateral boundarie*s gives good results compared to analytical solution for dynamic analysis in a plane symmetric model. Therefore, *tied degree of freedom* is provided to lateral direction of the boundaries at

the both sides and vertical direction is kept with standard fixities (*none*). Boundary relaxation coefficient C_2 is adjusted to 0.25 to improve absorption in the presence of shear wave. C_1 is kept with the default value (1.0).

Table 3-9 Properties of input motion

Parameters	**value**
Peak acceleration, a_{gR}	0.1g
Damping Co-efficient, ξ	5%
Period, T	0.5s
Frequency, f	2 Hz

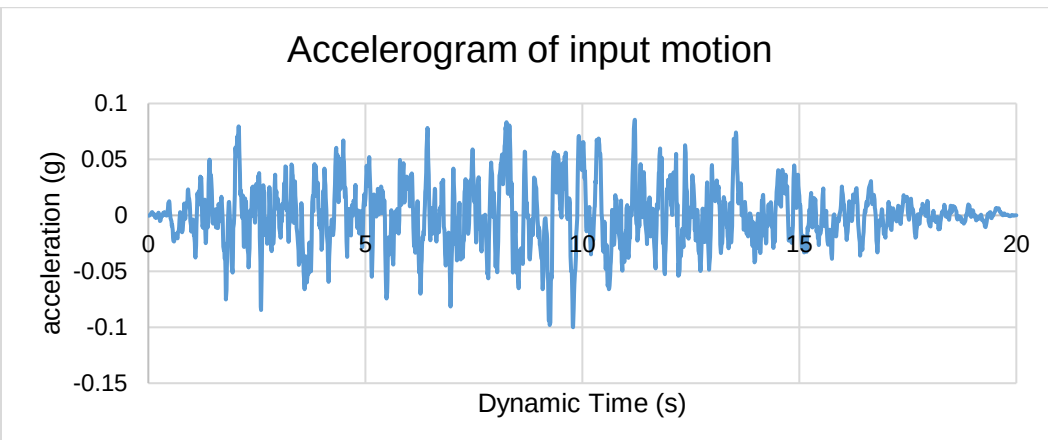

Figure 3-16 Time history of input motion from SIMQKE

Thus, the FEM models are created in PLAXIS 2D and analyzed for the input motion. The steps of analysis and corresponding results are presented in the next chapter.

3.4.4 Test on Boundary Condition

Boundary condition are chosen based on previous works and recommendations. It is important to check the performance boundary condition with analytical solution and evaluate the applicability. This is done using a simple homogeneous linear elastic material to save computation and avoid complicated parameter selection. Soil model is built with *Linear Elastic: Undrained (c)* with thickness 25m and shear wave velocity 300m/s. This gives soil natural frequency 3 Hz. Mesh coarseness is selected *medium*. Boundary conditions are selected same as the previous section. The profile is shaken with five harmonic motions with different

frequencies. Amplification factor is determined using equation (2.4) in section 2.1.2. Amplification factor from PLAXIS is determined as the ratio of output to input motion. The outcome shows good agreement with theoretical value. That means the selected boundary condition provides good performance and can be used for further analysis. Theoretical calculation and first three modal shapes are given in Appendix E.

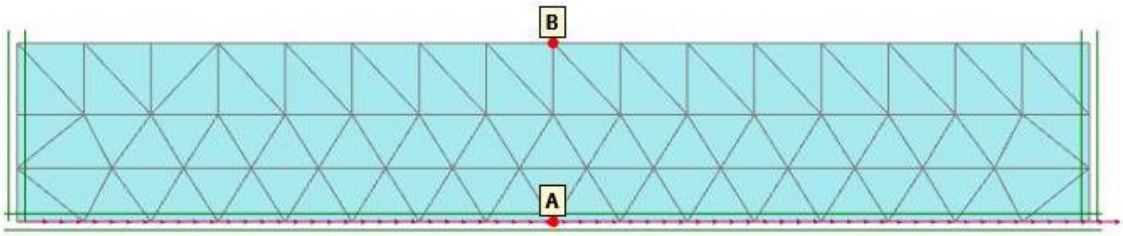

Figure 3-17 Deformed mesh and selected nodes of the test model

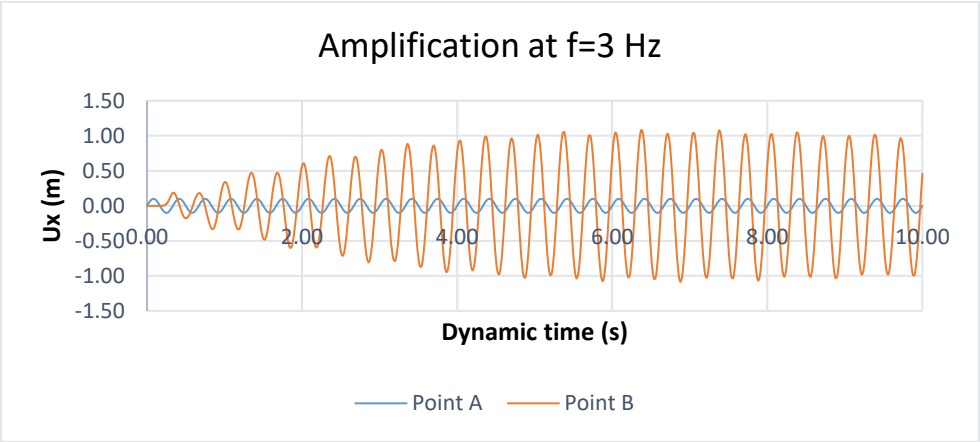

Figure 3-18 Acceleration at point A and Point B for f=3 Hz

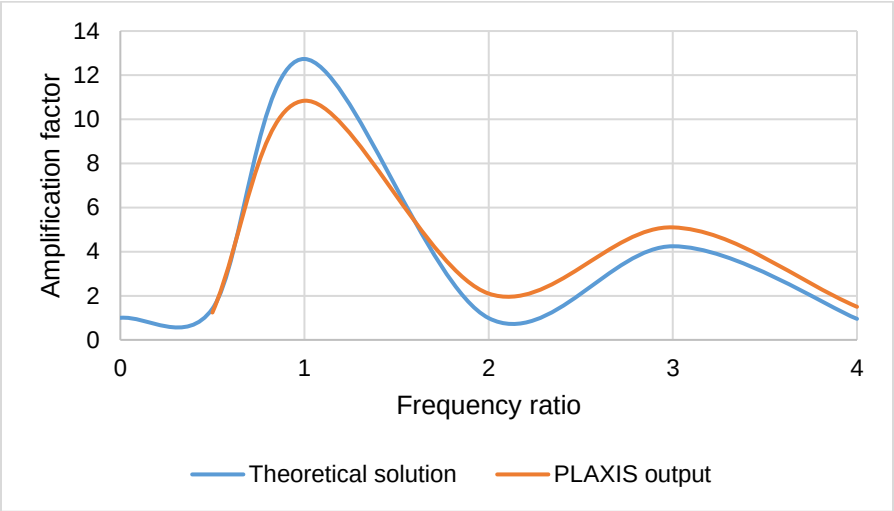

Figure 3-19 Amplification factor over frequency ratio

4 ANALYSIS AND RESULTS

In the previous chapter the construction of FEM model in PLAXIS 2D is described. The constructed models are analyzed for the given input motion. Analyses are done in following order:

- At first, a free field analysis is conducted to get the behavior of soil material without any structure on it. The response of the soil is then compared to a one-dimensional analysis in DEEPSOIL to verify the result.
- Then the structures are constructed and free vibration analysis of all the models with the structures are carried out to get the natural frequencies of the structures.
- Finally, a full dynamic analysis is performed with structures on all four models. The shear force at the base is calculated from PLAXIS 2D analysis.
- Natural period of the structure and shear force at the base is calculated according to Eurocode 8. The obtained results are then compared.

4.1 FREE FIELD ANALYSIS

Free field analysis is performed to get the response of a soil deposit to an input earthquake motion. It describes the distribution of shear wave motion from bedrock to the surface of the soil layer. It also provides the site amplification of the input acceleration through the soil layer. Site amplification is important to understand the intensity of the seismic wave that is going to be encountered by the structure and predict critical natural frequency of a structure for that seismic motion. For this study, free field analysis is important to calibrate the PLAXIS 2D soil model with one dimensional analysis in DEEPSOIL. The results should display a reasonable level of similarity if the models are correctly constructed. Although it is expected to get some discrepancies between the outcome of these two analyses because of the difference of analysis method and assumptions. The results of these two analyses are presented in terms of:

- Acceleration (g) vs Time (sec)
- Response Spectra: PSA (g) vs Period (sec)

4.1.1 Two-Dimensional Analysis in PLAXIS

A non-linear dissipative model is created in PLAXIS 2D with HS small model which incorporates the hysteresis behavior of soil during earthquake. Soil parameters are used as provided in section 3.2. Two nodes are selected from the generated mesh to observe the result, one at the bedrock level and another at the surface.

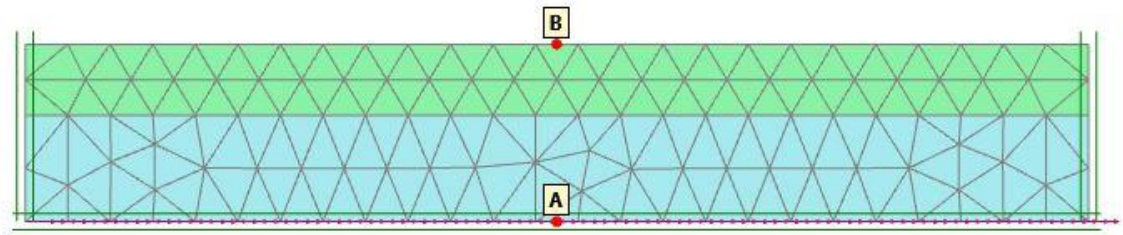

Figure 4-1 Generated mesh with selected nodes

Table 4-1 Co-ordinates of selected nodes

Nodes	Co-ordinate	Location
A	(0, -25)	At the bottom of the soil layer
B	(0, 0)	Surface level

Accelerogram obtained at bedrock level (input motion) and at a point on the surface (B). It is visible from figure 4.2 that the input acceleration got amplified as it hits surface of the layer. While the maximum acceleration of the input motion is 0.1g at the bedrock, it gets amplified to 0.2g at the surface. This means the signal get 2.0 times higher than the input signal. This peak acceleration will have direct contact with the overlaying structure. Site amplification factor can be calculated as:

$$\textit{Amplification factor} = \frac{Peak\ surface\ acceleration}{Peak\ ground\ acceleration} = \frac{a,\max(0,t)}{a,\max(H,t)} = \frac{0.2}{0.1} = 2.0$$

Peak spectral acceleration response spectrum shows that the maximum acceleration occurs at a period of 0.34s. This peak acceleration response spectrum is for a default 5% of damping which is common for reinforced concrete structures.

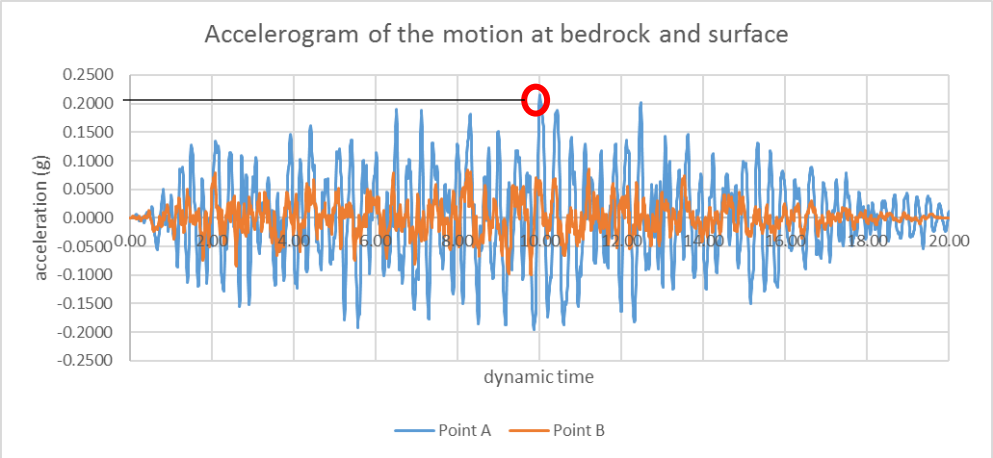

Figure 4-2 Free field response in terms of acceleration

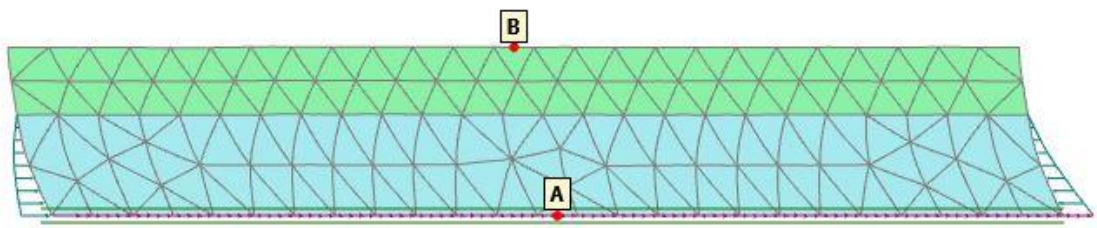

Figure 4-3 Deformation pattern of free field motion at dynamic time 10.01s (when maximum acceleration occurs at the surface). Scaled up 500 times.

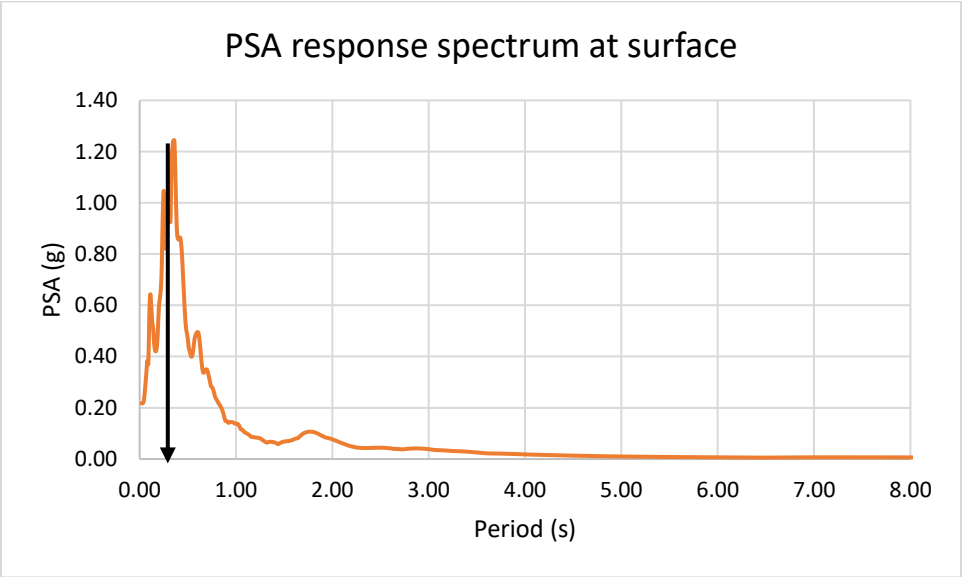

Figure 4-4 : PSA response spectrum at point B on the surface

4.1.2 One Dimensional Analysis in DEEPSOIL

One dimensional equivalent linear ground response analysis has been carried out using a dedicated software DEEPSOIL. The analysis is carried out with a total stress approach in frequency domain. Soil layers are defined with same unit weight and average shear wave velocity as applied in PLAXIS 2D. The material model used in this program can be chosen from the predefined data set, for example Vucetic and Dobry (1991) model for clay. In this study, user defined modulus reduction curve is selected according to equation given by Hardin and Drnevich (1972) and damping ratio curve based on Vucetic and Dobry (1991) at plasticity index 50% to match it with HSsmall model (Appendix F). Calculations are done using equations described in section 2.2.1.2. After providing material data the software generates profile summary. It is possible to choose bedrock properties in elastic half space. Shear wave velocity of the bedrock is assumed to be 1000 m/s. Unit weight 35 KN/m^3 and default damping ratio 2%. Number of iterations are chosen to be 15 and effective shear strain ratio is 0.65. Complex shear modulus is chosen to be frequency independent where,

$$G^* = G\,(1+2i\xi)$$

Input motion described in section 3.4.3 is used in DEEPSOIL as well. After completing all the steps with input parameters, the model is analyzed to get ground response at the top layer. The profile summary is given in Appendix F (figure F-1)

Obtained accelerogram shows that the peak acceleration increases from 0.1g to 0.23g. This gives site amplification factor 2.3 and the peak acceleration occurs at period of 0.39s (figure 4-6 (b)). Peak acceleration response spectra are for 5% damping.

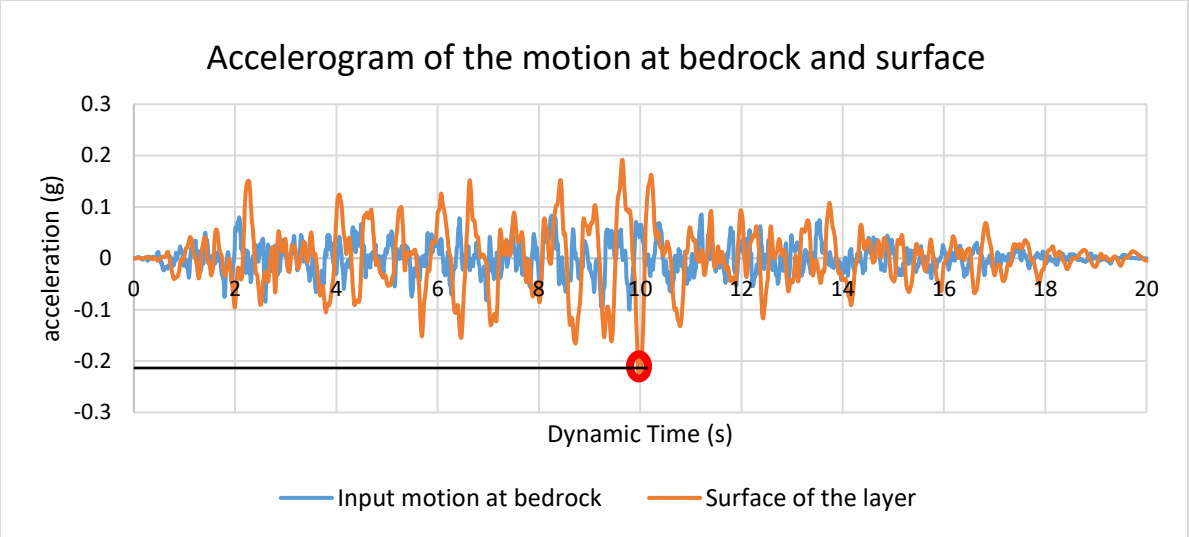

Figure 4-5 One dimensional site response in terms of acceleration

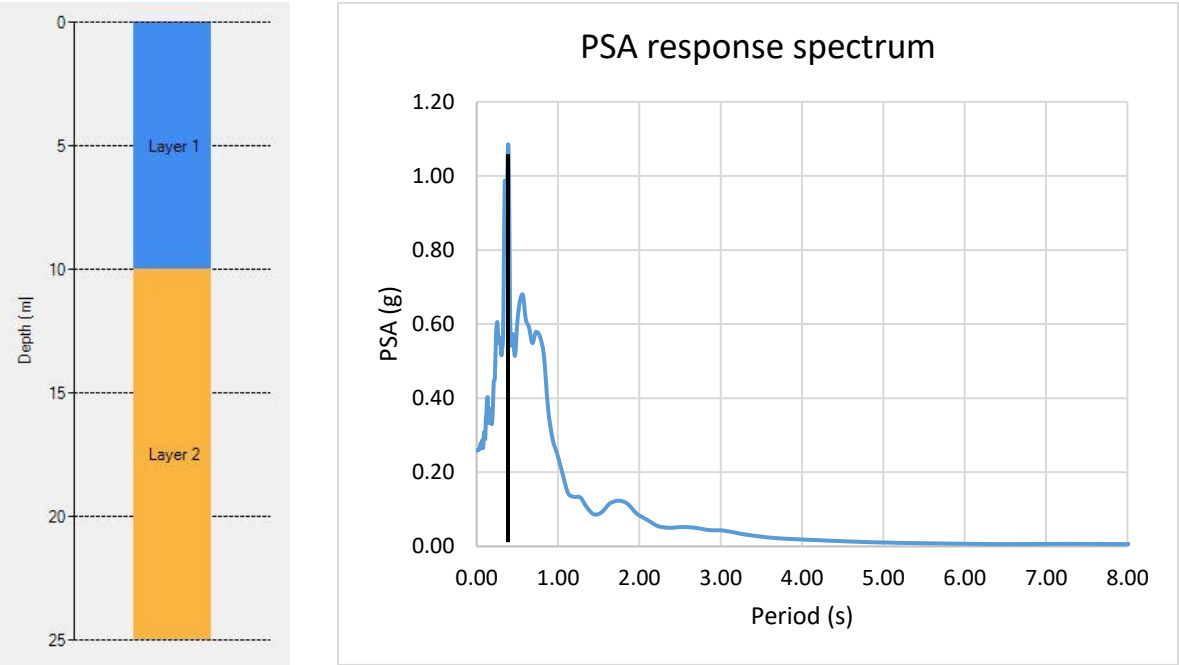

(a) (b)

Figure 4-6 : (a) Input profile in DEEPSOIL (b) PSA response spectrum at point B on the surface

4.1.3 Summary and Discussion

Obtained results from PLAXIS and DEEPSOIL are presented in figure 4-7 and 4-8 in terms of accelerogram at surface and PSA response spectra. Outcome shows satisfactory similarities (table 4.2). Peak acceleration is in the range between 0.2g to 0.23g which means the base of the structure will encounter a peak acceleration of 0.2g to 0.23g under an earthquake of 0.1g. In both cases, the peak occurs at a dynamic time close to 10s.

The period at which the peak acceleration occurs is 0.34s and 0.39s. This provides the natural period of structure (ideally characterized for a SDOF system) at which it will be in resonance with the earthquake and will oscillate with very high amplitude. If there is a structure of similar natural frequency, then heavy damage can happen due to resonance. The SODF systems are characterized by different stiffness (k) with same damping percentage (ξ) which are excited by an identical motion. Stiffness of the system can be obtained from natural period. Natural period of a structure can be calculated in many ways. Analytically it is calculated with stiffness and damping ratio. Later in this paper, natural frequency of structures is calculated from PLAXIS, logarithmic decrement and Eurocode 8. The x-axis of the response spectra provides the period at which maximum acceleration may occur for SDOF system.

Table 4-2 Result summary of free field analysis

	PLAXIS 2D	DEEPSOIL
Site amplification	2.0	2.3
Period of peak acceleration	0.34s	0.39s

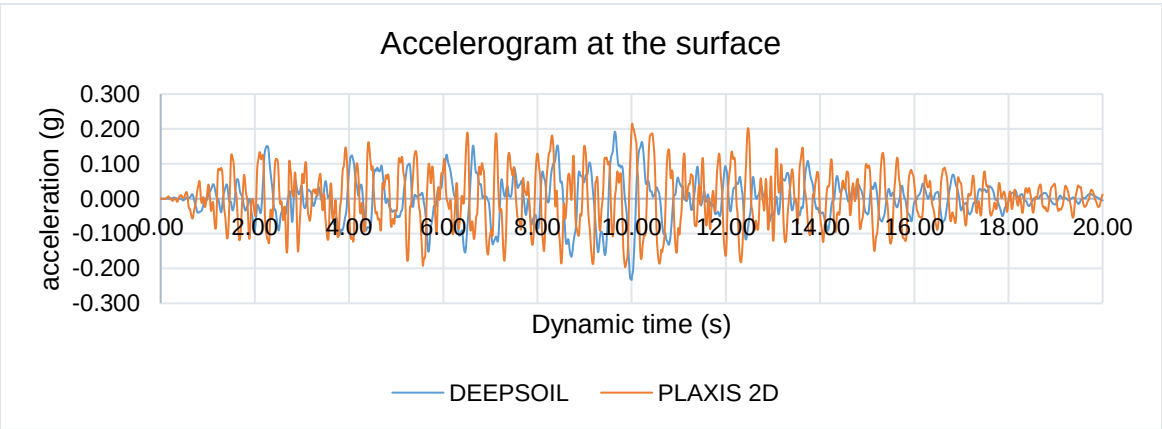

Figure 4-7 Acceleration from DEEPSOIL and PLAXIS at the surface

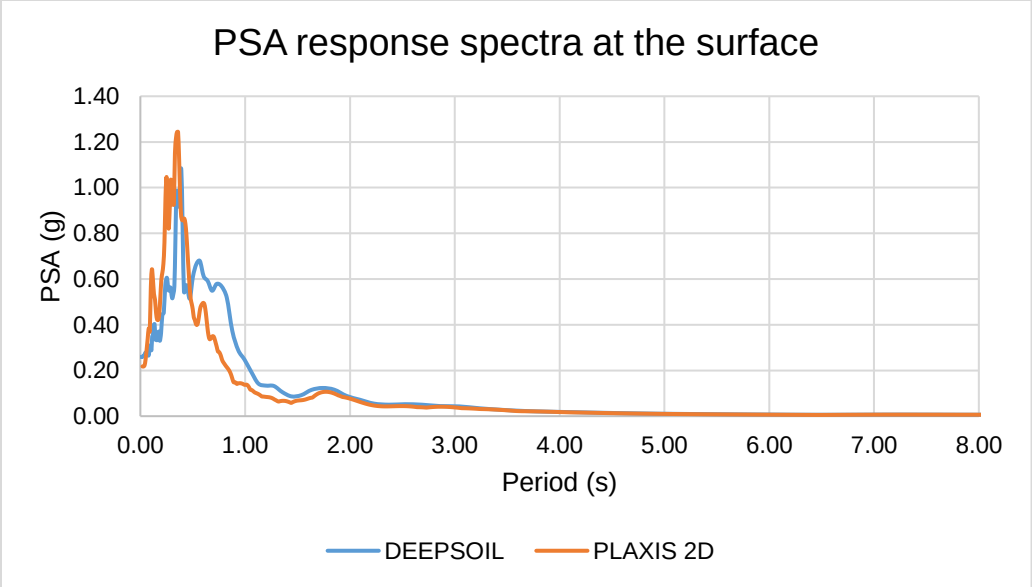

Figure 4-8 PSA response spectra from DEEPSOIL and PLAXIS at the surface

Although there is distinct dissimilarity in the shape of output curve hence damping of the wave between PLAXIS and DEEPSOIL output. The soil model in PLAXIS 2D is characterized by HSsmall model which incorporates the non-linear dissipative behavior and proper stiffness properties according to input value while DEEPSOIL is characterized by manually defined material properties and input shear wave velocity and unit weight. It is difficult to match the stiffness properties of these two programs and the manual calculation is not calibrated for each other. Boundary conditions may also have impact on the outcome. The bedrock characteristics were defined in DEEPSOIL with specific shear wave velocity and unit weight. While in PLAXIS, it was only defined with fixed boundary in the y direction and prescribed displacement in the x direction. Therefore, a large amplitude periodic vibration generated in PLAXIS because the boundary in the bottom of the deposit is set as a fully reflective one. Furthermore, the assumptions of one dimensional linear equivalent analysis is based on the concept of updating secant shear modulus and dumping ratio by iteration until it becomes consistent with the level of strain in each layer. While analysis in PLAXIS is based on non-linear hysteresis behavior of soil. However, the end results give the actual behavior of the soil model and since the results are in a good agreement, it is logical to proceed with this soil model for further analysis.

4.1.4 Additional Information

Usually earthquake response is shown in terms of acceleration, but it is also necessary to observe other parameters to describe earthquake characteristics properly. For example, the frequency content gives the distribution of ground motion amplitude over frequencies. This is important to know the frequency range within which the concentration of seismic input energy is high. It is possible to get the accelerogram in frequency domain i.e. Fast Fourier Transform (FFT) or power spectrum from PLAXIS output (Laera & Brinkgreve 2015). Obtained FFT at the base level and at the bedrock are provided in Figure 4.9. In addition to that, the maximum relative displacement of all the SDOF systems which are characterized in the same way as for the PSA response spectra, can also be observed by relative displacement response spectra given in Figure 4.10.

Figure 4.9 shows that the corresponding frequency to the maximum acceleration at foundation level is 3.40 Hz. Most dominant energy content is distributed between 2.85 Hz to 3.9 Hz. On the other hand, the energy content of input acceleration is almost uniformly distributed between 0.6 Hz to 4.85 Hz. This means that the filter effect of soil deposit modified the energy content and concentrated it in smaller range.

Relative displacement response spectrum gives the maximum displacement of structure that can occur for this given condition. From this maximum displacement, maximum static force can be calculated by taking the product of displacement and stiffness of the structure ("PLAXIS 2D Reference Manual," 2016). It can be seen from the figure that the displacement for structures of low natural periods are very low and it increases as the natural period increases. When T=0, which means an undamped fully rigid structure, the maximum displacement is 0. For a highly flexible structure where T> 9, the maximum displacement as high as the maximum displacement of the soil.

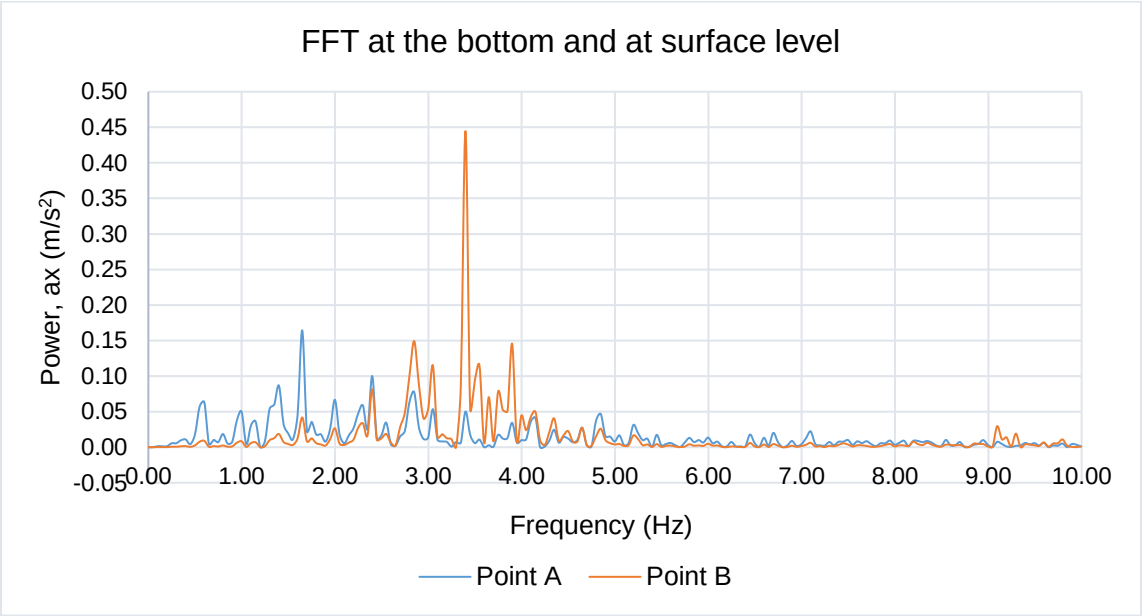

Figure 4-9 FFT at the top and bottom of the mesh

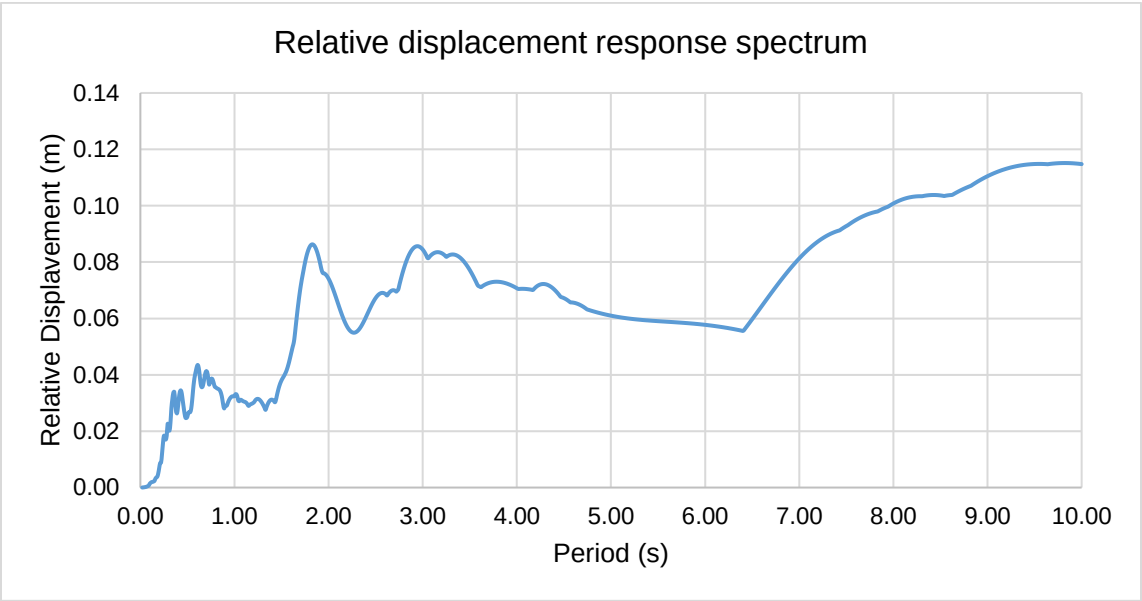

Figure 4-10 Relative displacement response spectrum

4.2 FREE VIBRATION ANALYSIS

Once the free field analysis gives reasonable results in comparison to one dimensional ground response analysis, the structure is constructed in the model to proceed with further analysis.

At first a free vibration analysis is carried out to determine the natural frequency of the structure. For this unit load (1 KN/m) is applied to the upper left corner of the building. The earthquake motion is applied for 3 dynamic seconds and the structure is allowed to vibrate freely. Thus, the natural frequency of the structure is obtained.

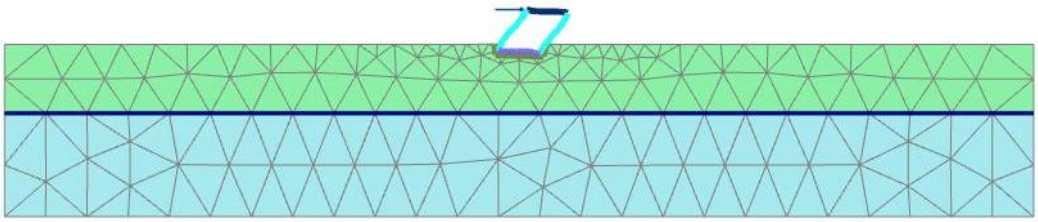

Figure 4-11 Free vibration of single story structure

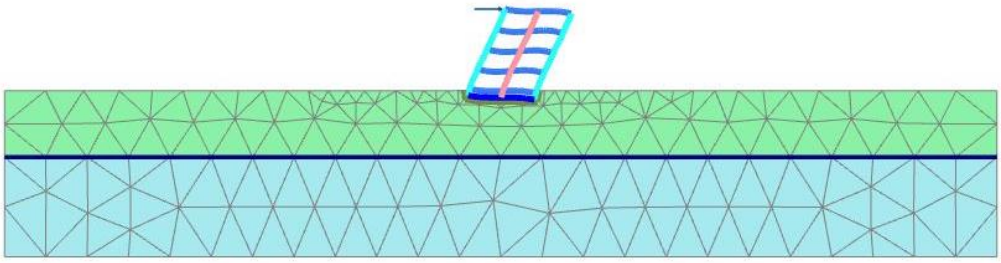

Figure 4-12 Free vibration of four story structure

4.2.1 Summary and Discussion

The natural frequency of two sets of structures are determined from PLAXIS output. The natural frequency of single story structure is 3Hz for both foundation cases, although the displacement curve is slightly altered. For four-story structure, the application of 14m pile does not affect the natural frequency. The natural frequency of the structure in both condition is 1.667 Hz. The added stiffness of pile on these simple structure does not change the frequency characteristics.

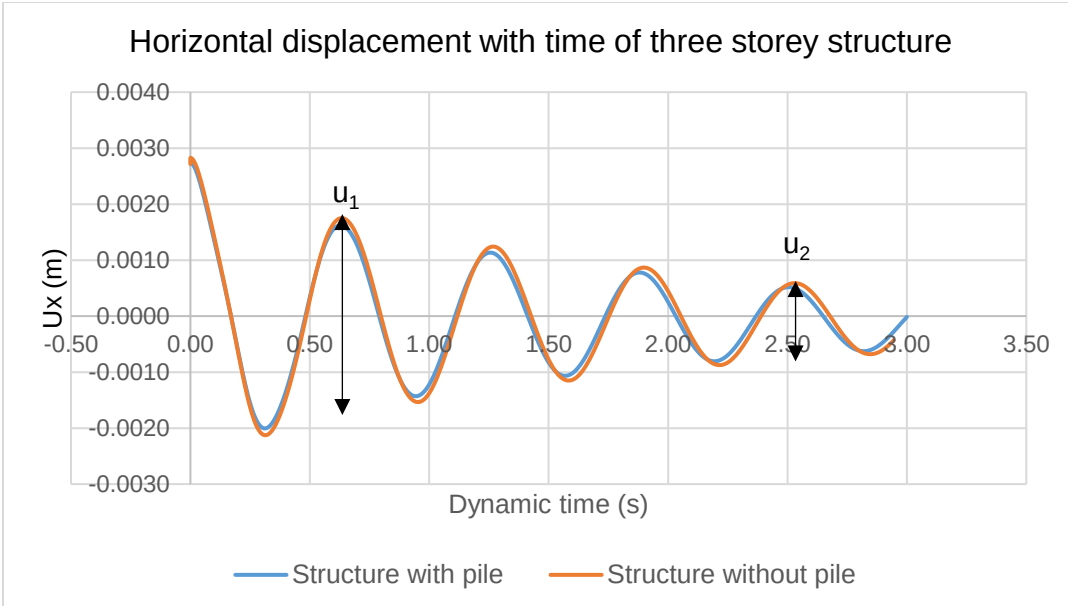

Figure 4-13 Natural period of vibration of four story structure

The natural frequency obtained from PLAXIS can be compared with frequency calculated by logarithmic decrement method described in section 2.1.4. From figure 4-13, logarithmic decrement δ is calculated for the four-story structure first. using equation (2.16) for four story structure:

$$\delta = \frac{1}{n} \ln \frac{u_1}{u_{n+1}} \cong \frac{1}{3} \ln \frac{3.2}{1.3} = 0.3$$

Rewriting equation (2.15) gives:

$$\zeta = \frac{1}{\sqrt{1+(\frac{2\pi}{\delta})^2}} = 0.0477$$

From figure 4-14, $T_D = \frac{1}{3}(2.51-0.65) = 0.62s$

From equation (2.14), natural period of vibration $T_n = T_D\sqrt{1-\zeta^2} = 0.62 \times 0.9988 = 0.62s$

Similar calculation from figure 4.14 gives natural period of vibration for a single-story structure, $T_n = 0.336s$

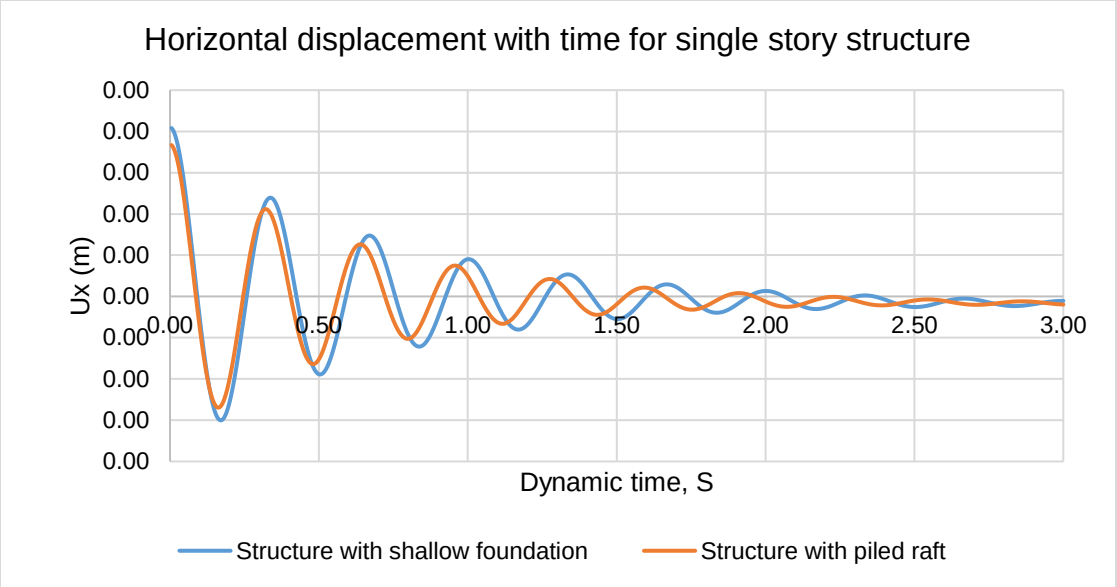

Figure 4-14 Natural period of vibration of single story structure with shallow foundation

The summary of the calculations for both structures show good agreement with PLAXIS:

Table 4-3 Summary of obtained natural frequency

Natural period	**Four story structure**	**Single story structure**
PLAXIS	0.60	0.33
Logarithmic decrement	0.62	0.33

4.3 SEISMIC RESPONSE ANALYSIS IN PLAXIS

After computing natural frequency, the input motion is provided for full dynamic time (20 seconds). Both models undergo deformation due to earthquake motion. The response of the structure is determined from result charts. Acceleration and horizontal displacement over dynamic time is presented from PLAXIS output.

To get the response of the structure at base and slab level, three nodes have been selected.

Table 4-4 Co-ordinates of selected nodes

Nodes	Co-ordinate	Location
A	(0, -25)	At the bottom of the soil layer
B	(0, -1)	Mid-point of the base
C	(0, 5) & (0, 12)	Mid-point of the slab for 1-story and 4-story structure

4.3.1 Single Story Structure with shallow foundation

The deformed mesh at maximum acceleration at the slab at dynamic time 10.03s is given in figure 4-15. The output is scaled up 200 times. Accelerogram in figure 4-16 shows that the amplitude of acceleration at the top of the structure is amplified considerably from the ground acceleration. The peak value at point C is 0.626g from an input maximum amplitude 0.1g at point A. The response amplitude is amplified 6.26 times from the input acceleration in case of a shallow foundation. The slab of the structure will shake with a force as high as 6.14 ms^{-2}. From time displacement curve in figure 4-17, the maximum horizontal displacement of the roof of the structure is found 50mm that occurs at t= 4.43s.

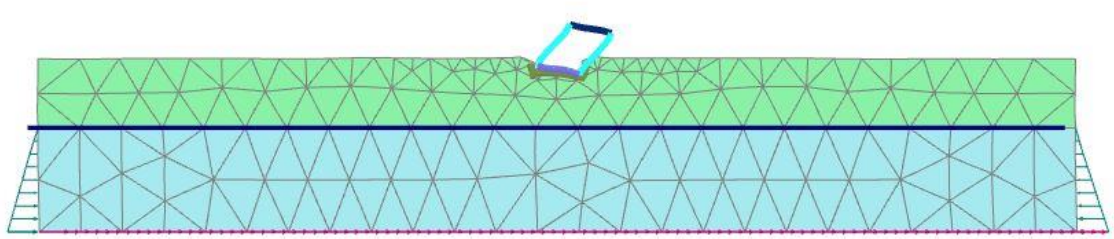

Figure 4-15 deformed mesh at maximum acceleration at t =10.03s.

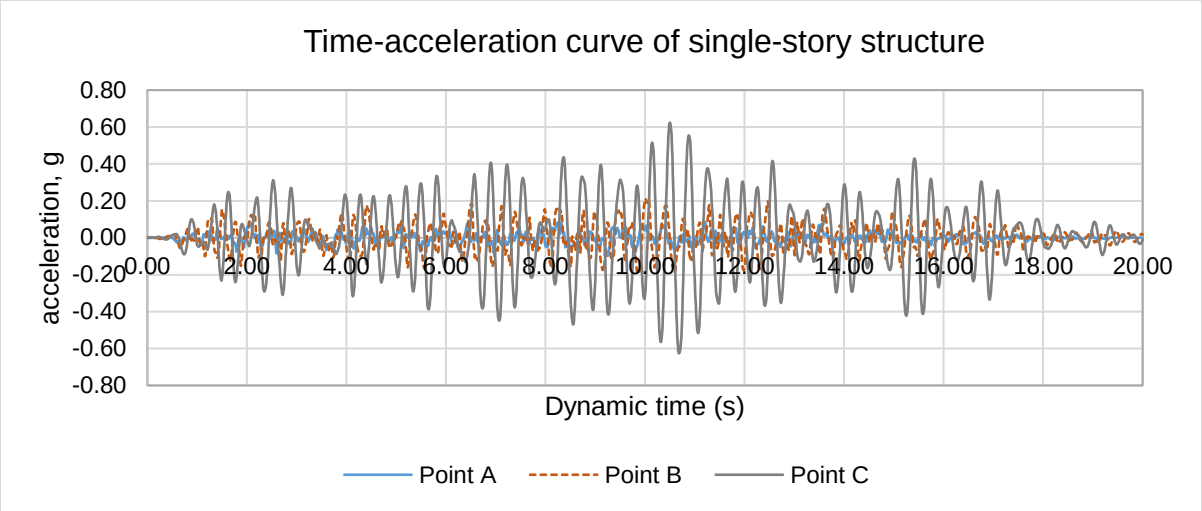

Figure 4-16 Time-acceleration curve of single-story structure

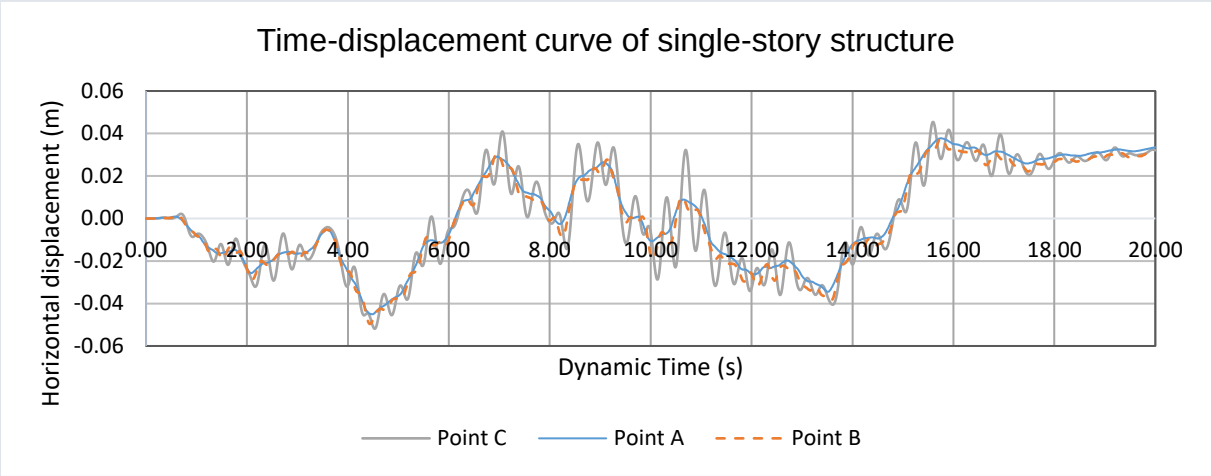

Figure 4-17 Time-displacement curve of single-story structure

4.3.2 Single Story Structure with Piled raft

After introducing the 12m long pile, the response acceleration of the structure is modified and it gets increased. Therefore, the structure with oscillate with even higher acceleration with a pile support than a rigid shallow base. The peak acceleration occurs at the top of the structure at dynamic time 10.65s with a magnitude of 8.32 ms^{-2} which is 8.49 times higher than the input acceleration and 4.25 times higher than the base acceleration (figure 4-19). The maximum displacement is 50mm that occurs at t= 4.53s (figure 4-20). Displacement remains same as expected. Deformed mesh is shown in figure 4-18.

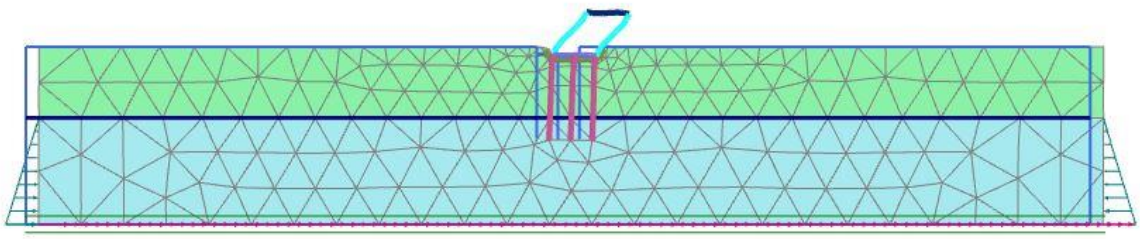

Figure 4-18 deformed mesh at maximum acceleration at t =10.65s.

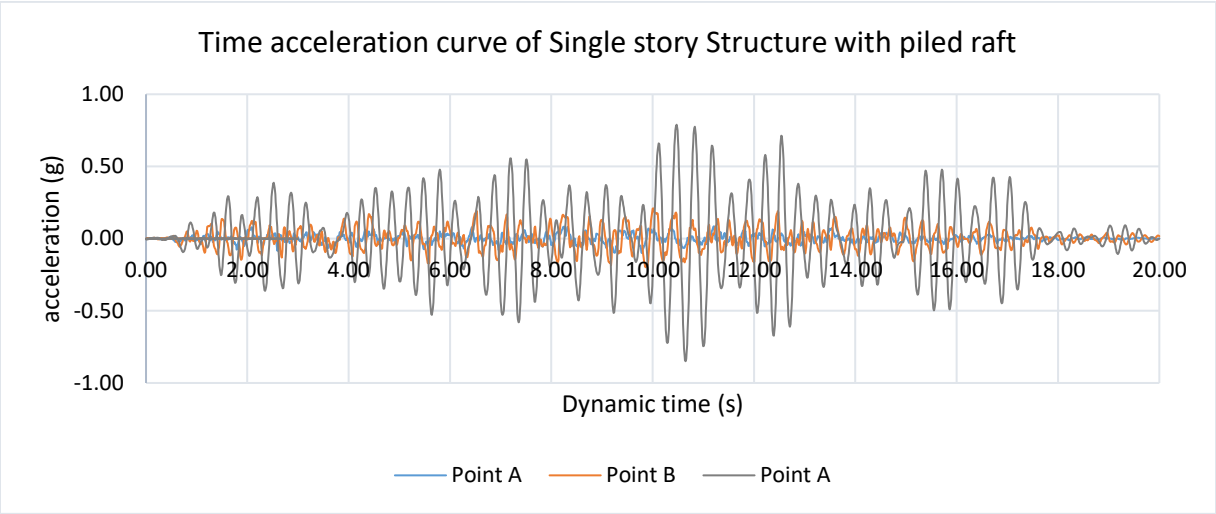

Figure 4-19 Time acceleration curve of Single-story Structure with Piled raft

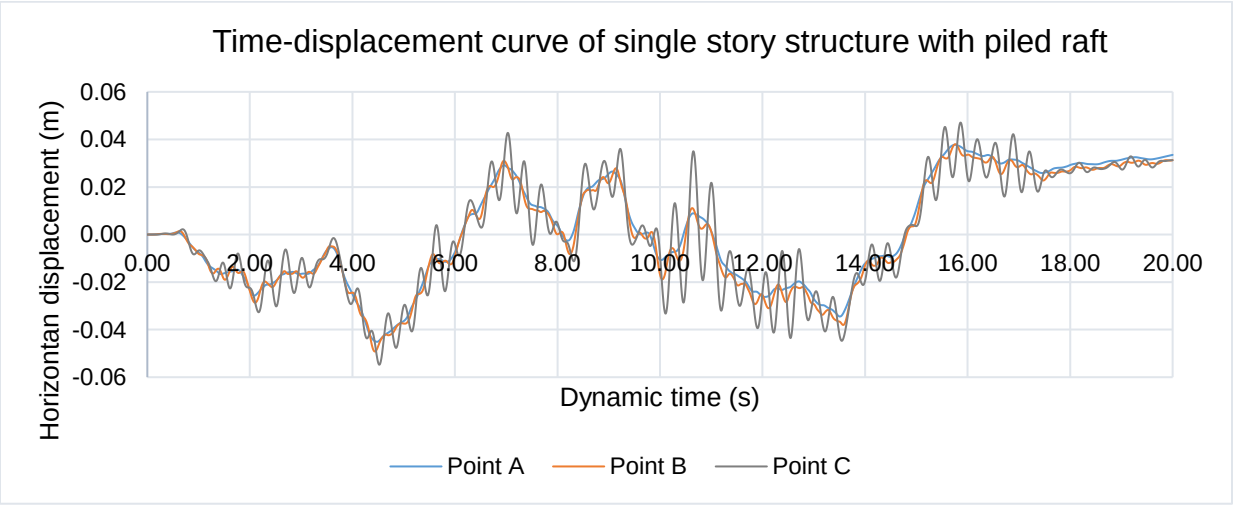

Figure 4-20 Time-displacement curve of single story structure with piled raft

4.3.3 Four Story Structure with shallow foundation

Four story structure with shallow base on the same soil profile is shaken with same input motion. The resulting deformed mesh and deformation patterns for acceleration and horizontal displacement are shown in figure 4-21, 4-22 and 4-23. Maximum acceleration at the top of the structure is 0.33g which occurs at t= 10.04s. The acceleration is amplified 3.3 times than the input acceleration and 1.65 times higher than the acceleration at base level. Maximum horizontal displacement is 60mm that occurs at t=4.65.

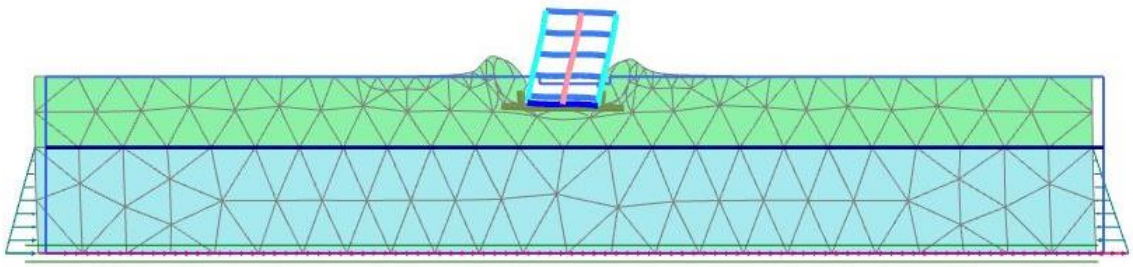

Figure 4-21 deformed mesh at maximum acceleration on the top at t= 10.03s scaled up 100 times

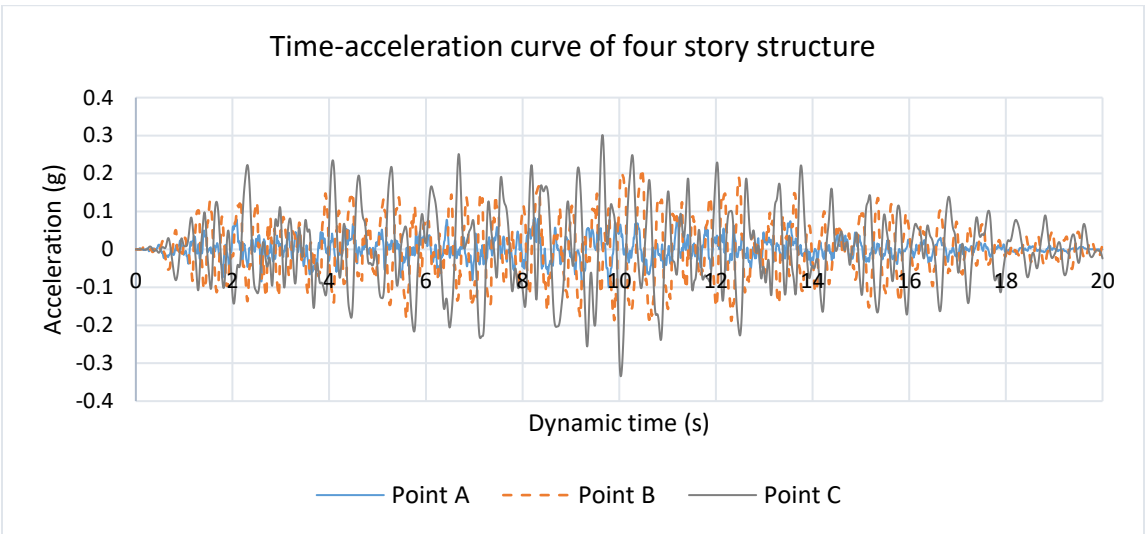

Figure 4-22 Time-acceleration curve of four story structure

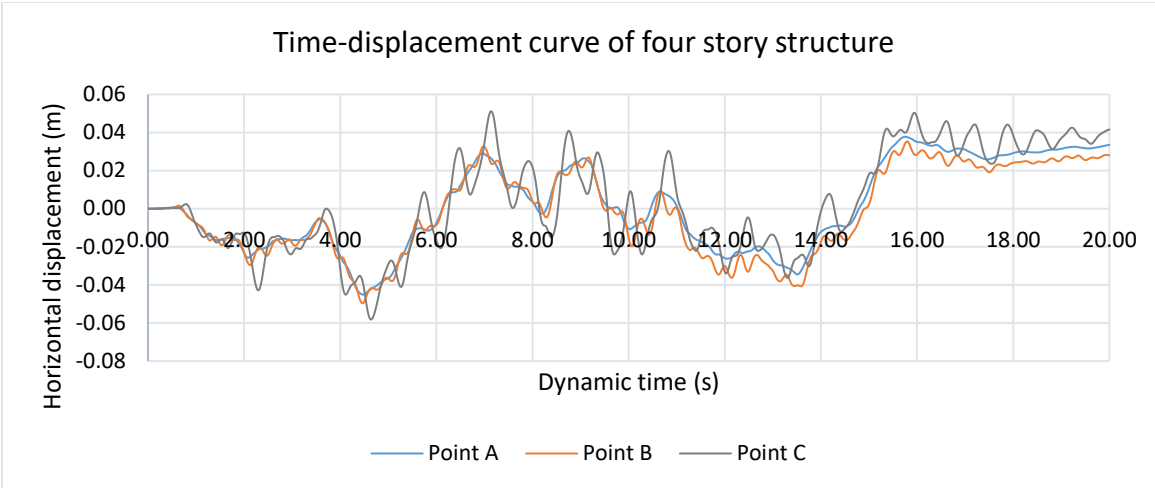

Figure 4-23 Time-displacement curve of four story structure

4.3.4 Four Story Structure with Piled Raft

The four-story structure is provided with 14m long piles and analyzed for the input motion. The presence of pile increases the acceleration of the structure and the deformation pattern of the structure and interfaces change due to it. The deformation of surrounding soil is less than that of shallow foundation (figure 4-24). The maximum acceleration at the top of the structure is 0.477g occurring at t= 10.04s which is 4.77 times amplified than the input motion and 2.39 times amplified than the base acceleration (figure 4-25). The maximum horizontal displacement remains 60mm at t=4.67 (figure 4-26)

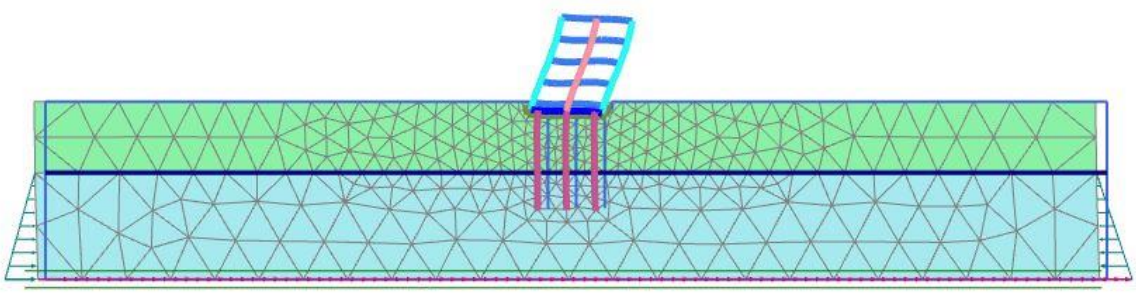

Figure 4-24 Deformed mesh at maximum acceleration

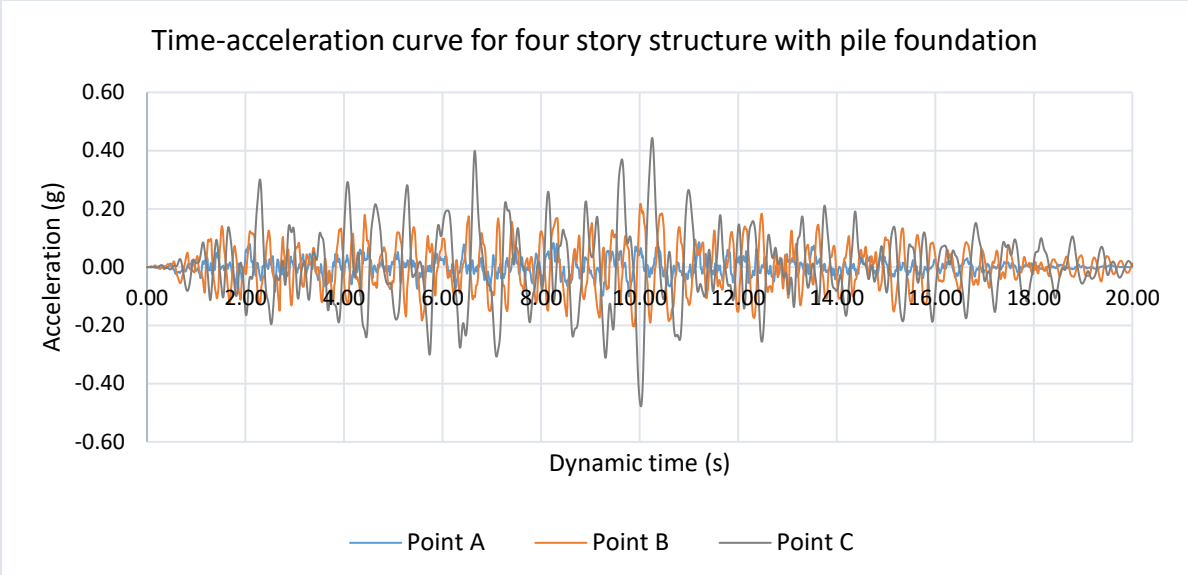

Figure 4-25 Time-acceleration curve for four story structure with piled raft

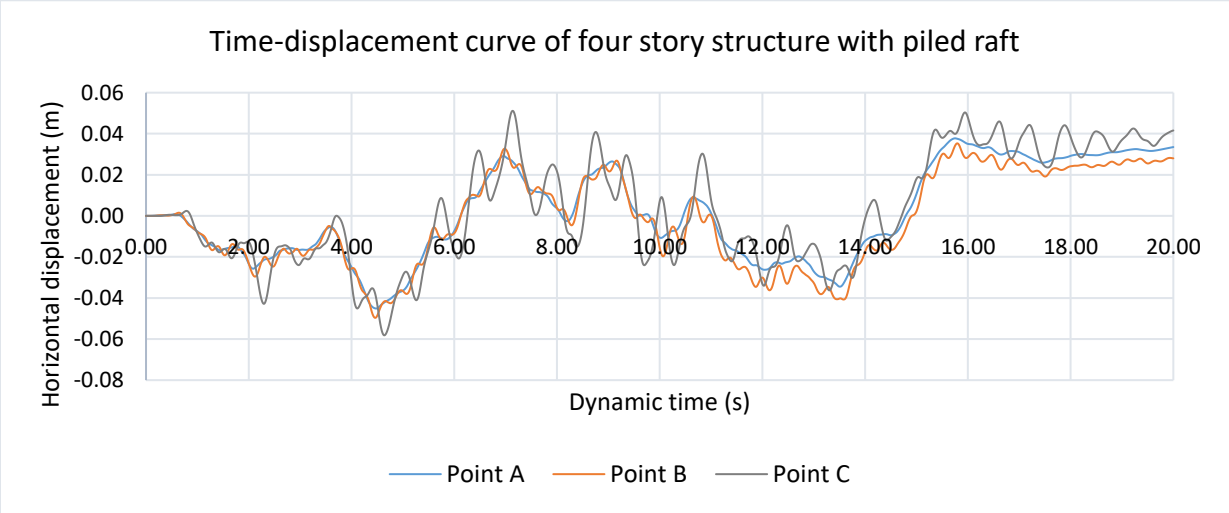

Figure 4-26 Time-displacement curve of four story structure with piled raft

4.3.5 Summary and Discussion

The observation of seismic response of structures with two types of foundation gives idea about the influence of foundation type. The accelerograms show how the response of the structure differs from input and free field motions for different kinds of foundations. Structures oscillate with higher acceleration with piled raft than shallow foundation. It can be expected that there is considerable change in shear force at the base as well since it depends on the intensity of acceleration. For a single-story structure, the acceleration increases over 40% and the for the four-story structure it is over 45%. Based on this observation, shear force developed at the base

of the structures will be calculated in the next section. To calculate base shear force, four deferent steps are selected where accelerations are high.

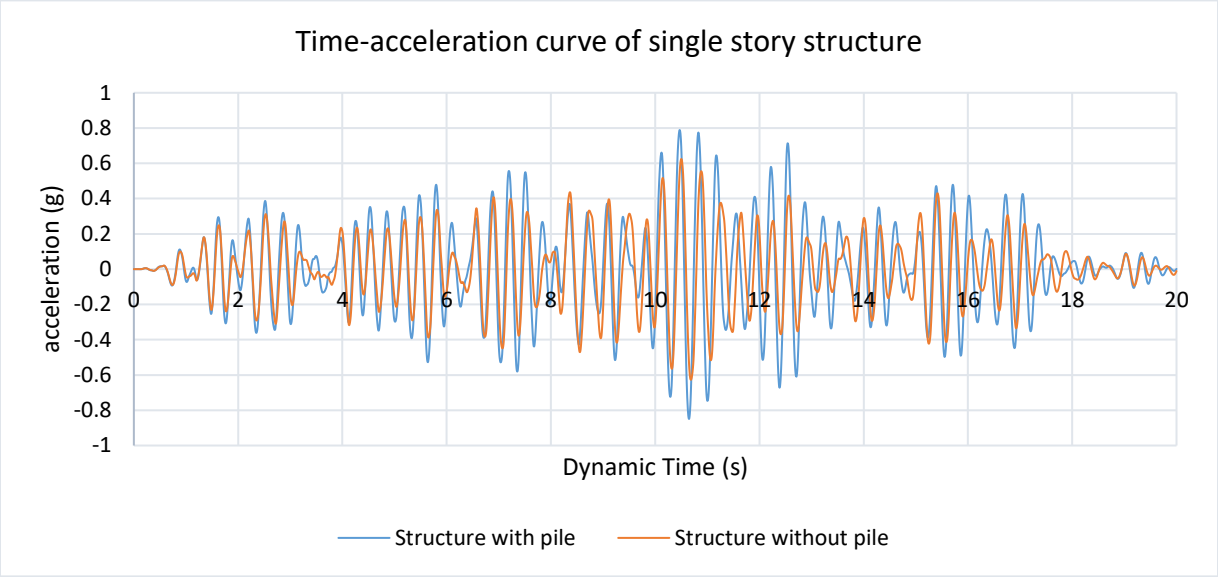

Figure 4-27 Time-acceleration curve of single story structure

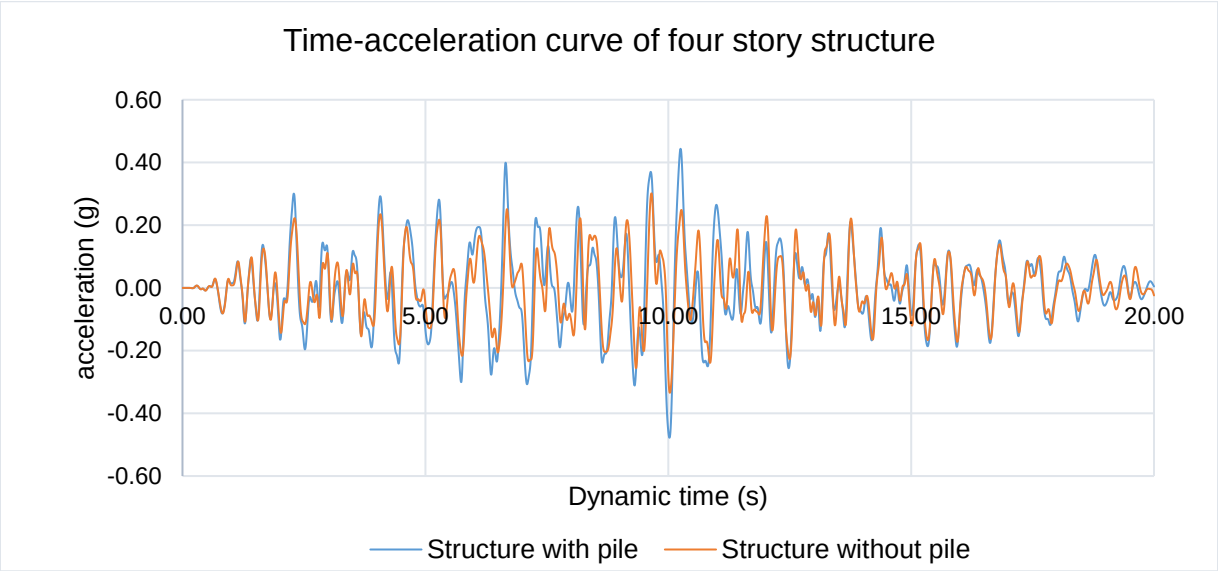

Figure 4-28 Time-acceleration curve of four story structure

4.4 CALCULATION OF SHEAR FORCE AT THE SHALLOW BASE

4.4.1 Eurocode 8

The shear force at the rigid base is calculated based on the lateral force method given by Eurocode 8 which is discussed in section 2.3.3. To calculate these shear forces, the horizontal component of design spectrum S_d (T) is calculated for the given seismic action. The calculation is based on the formulae given in section 2.3.2.

For this it is required to choose reasonable value for behavior factor "q". As described in section 2.3, Eurocode 8 suggests ranges of values for three "Ductility Classes" i.e. DCL/DCM/DCH (low/medium/high) depending on the ground acceleration of the site under consideration and material type of the structure. In case of Norway, the maximum normalized peak ground acceleration of type A ground, a_{g40HZ}=0.9 m/s^2 near Bergen. In this study, the peak acceleration of input motion a_g is 0.1g or 0.98m/s^2. The soil type is determined type "D" in section 3.2.1 based on Norwegian national annex. The soil factor S is 1.55 from table 2.4 for a structure with seismic class II, the ground acceleration will be,

$$a_gS = 1.55 \times 0.98 = 1.52 \text{ m/s}^2$$

From section 2.3, concrete or steel structures where $a_gS < 0.25g = 2.5$ m/s^2 can be considered as DCL (Ductility Class Low) hence the value of behavior factor $q \leq 1.5$ should be taken. Here q= 1.0 refers to a fully elastic structure. In Norway, it is common to use $q \leq 1.5$. And while comparing to PLAXIS results, it is better to use q=1.0 because the model in PLAXIS is modelled as elastic material. Therefore, horizontal components of design spectra are calculated for both q=1.0 and 1.5 to observe the difference between outcome later in the study.

Table 4-5 The summary of input parameters for design spectrum

Parameters	**value**	**Parameters**	**Value**
Peak acceleration of seismic input, a_g	0.1g	Soil factor, S	1.55
Period of input motion, T	0.5s	T_B	0.15s
γ (Seismic class II)	1.0	T_C	0.40s
Behavior factor, q (for DCL)	1.0 & 1.5	T_D	1.6s

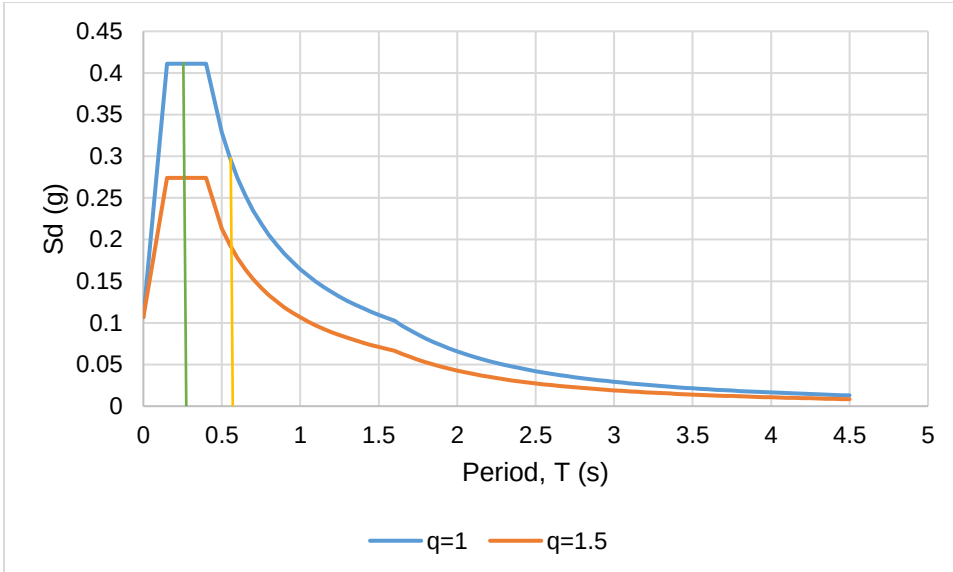

Figure 4-29 Horizontal component of design response spectra for given seismic action and soil type

<u>Base shear of Single Story Structure</u>

To be able to calculate the shear, the natural period of the structure must satisfy the condition

$T_1 \leq \begin{cases} 4Tc \\ 2.0 \end{cases}$; equation (2.60) stated and discussed in section 2.3.3.

Natural period from equation (2.62), $T_1 = C_t . H^{3/4}$

In this case, H= 6m (from the rigid base)

C_t= 0.085 for moment resistant space steel frames

$T_1 = 0.085 \times 6^{3/4}$

$= 0.32$ s

Now, $4\ T_c = 4 \times 0.4$ (T_c= 0.4 from Table: 4-5)

$= 1.6$

That means the criteria in equation (2.60) is met.

From table 4-5, $T_C < T_1 \leq T_D$, so the component of design spectrum of seismic action S_d (T) for T_1 can be calculated from equation (2.56) to (2.59) or read from the graph in 4-29.

The weight of the structure above rigid base is calculated from table 3-3

m = 20×1 + 5×2 = 30 KN/m/m

For $T_1 < 2\ T_C$, Correction factor, λ= 0.85

$S_d (T_1) = S_d (0.32) = 0.42 \times 9.81 = 4.11 ms^{-2}$ for q=1

$= 0.27 \times 9.81 = 2.64\ ms^{-2}$ for q=1.5

Now the shear force at the base of the structure from equation (2.61)

$$F_b = 4.11 \times 30 \times 0.85 = 104.8 \text{ KN/m for } q=1.0$$

$$= 2.64 \times 30 \times 0.85 = 67.46 \text{ KN/m for } q=1.5$$

<u>Base shear of Four Story Structure</u>

Similar calculation procedure is followed for a four-story structure. First, the natural period is verified.

Natural period $T_1 = 0.085 \times 13^{3/4}$

$= 0.58s$

As calculated before, $4\ T_c = 1.2$.

Therefore, $T_1 \leq \begin{cases} 4Tc \\ 2.0 \end{cases}$

Now the mass above the rigid foundation is calculated from material property in table 3-3

$m = 10 \times 5 + 5 \times 2 = 60$ KN/m

For $T_1 < 2\ T_C$ and structure more than two story, correction factor, $\lambda = 0.85$

Horizontal component of designed response spectra can be calculated from (2.56) to (2.59) or read from figure 4-29

$$S_d\ (T_1) = S_d\ (0.58) = 0.3 \times 9.81 = 2.943 \text{ m/s}^2 \text{ for } q=1.0$$

$$= 0.2 \times 9.81 = 1.96 \text{ m/s}^2 \text{ for } q=1.5$$

Now the shear force at the base of the structure from equation (2.61):

$$F_b = 2.93 \times 60 \times 0.85 = 149.3 \text{ KN/m for } q=1.0$$

$$= 1.96 \times 60 \times 0.85 = 99.96 \text{ KN/m for } q=1.5$$

4.4.2 PLAXIS 2D

Maximum shear force at the interface of the shallow base is developed at the peak acceleration. The shear stress at this acceleration can be obtained from PLAXIS output by clicking on the interface. From this shear stress, shear force at the interface is calculated by taking the summation of force at each node. Stress effect from the side wall of the embedded parts in considered by adding the maximum absolute stress in those parts.

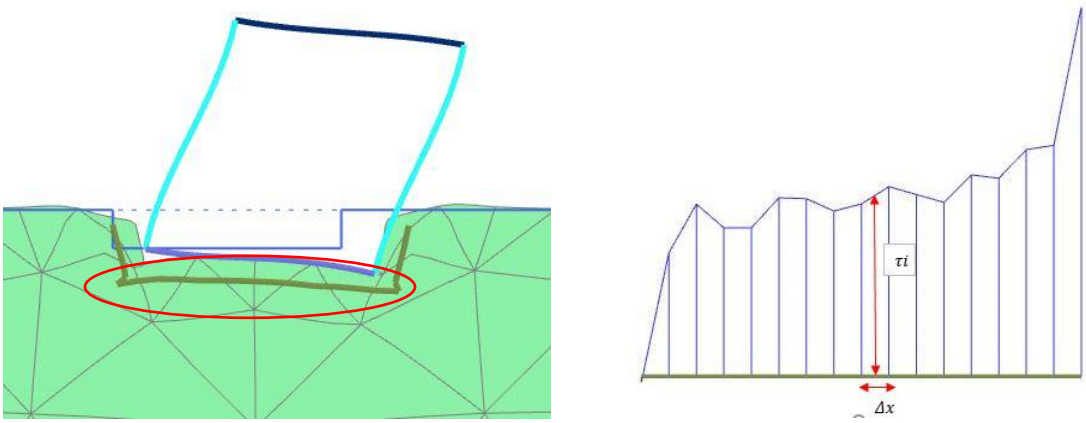

Figure 4-30 Calculation of shear force at the base

Total shear force on the base interface, $F_{base} = \sum \tau i . \Delta x +$ maximum absolute force from 1m side wall

When the pile is added, part of shear for at the base is taken by pile. Therefore, this shear force should be added while calculating base shear force.

Shear force developed due to earthquake movement is assumed based on the concept of J. Hamada (2015):

shear force due to earthquake induced ground deformation = Shear force at peak acceleration – shear force due to inertia

Fig 4-31 shows that at the high acceleration condition, the shear force developed at the pile head is dominant compared to inertial force. Inertial forces get transferred to the soil by raft and lateral forces caused by earthquake is shared by raft and pile. This concept is applied to all the piles in a plane to get the total shear force carried by pile head at peak acceleration ($V_{pile\ head}$).

Base shear force at the interface with pile= F_{base}+ $V_{pile\ head}$

Shear force is calculated at maximum accelerations occurring at different dynamic steps to observe the variation in different modes.

Single-story Structure with Shallow Foundation

An example calculation for base shear is given at calculation step 1675 when the peak acceleration of the top of the structure occurs (0.626g). At this step the total shear force is calculated. The sample calculation is given in Appendix G, table G-1.

$$F_{base} = 29.79+13.13+7= 49.22 \text{ KN/m}$$

The conventional method, F= total mass of the structure× Peak acceleration at the foundation level. From the results obtained from free field analysis, peak acceleration at the base level= 0.2×30× 9.81= 58.86 KN/m. This means that the obtained value from shear force calculation is in a good agreement with the conventional method. Base shears at other acceleration conditions are also calculated to observe the difference at different modes. Accelerations are picked from accelerogram in figure 4-17.

Summary of the calculation at different steps:

Table 4-6 Calculated base shears at different peak accelerations

Peak acceleration with direction (g)	Number of step	Calculated Base Shear (KN/m)
0.626	1675	49.92
0.626	1674	46.11
-0.624	1656	48.68
-0.62	1657	47.0

Single Story Structure with Piled raft

Base shear force at the interface with pile= F_{base}+ $V_{pile\ head}$

Calculation of base is done using the same method as described earlier. Additional force that is transferred to the pile is added. (Appendix G, table G-2)

The shear force at the base with pile foundation is calculated considering the shear force at the interface as described before and adding the force that is taken by the piles (pile 1, pile 2 and pile 3 in the plane). At step number 1068 when maximum acceleration at the top of the structure occurs

F_{base}+ $V_{pile\ head}$= 37.93+(17.58+36.8-0.8) = 90.37 KN/m

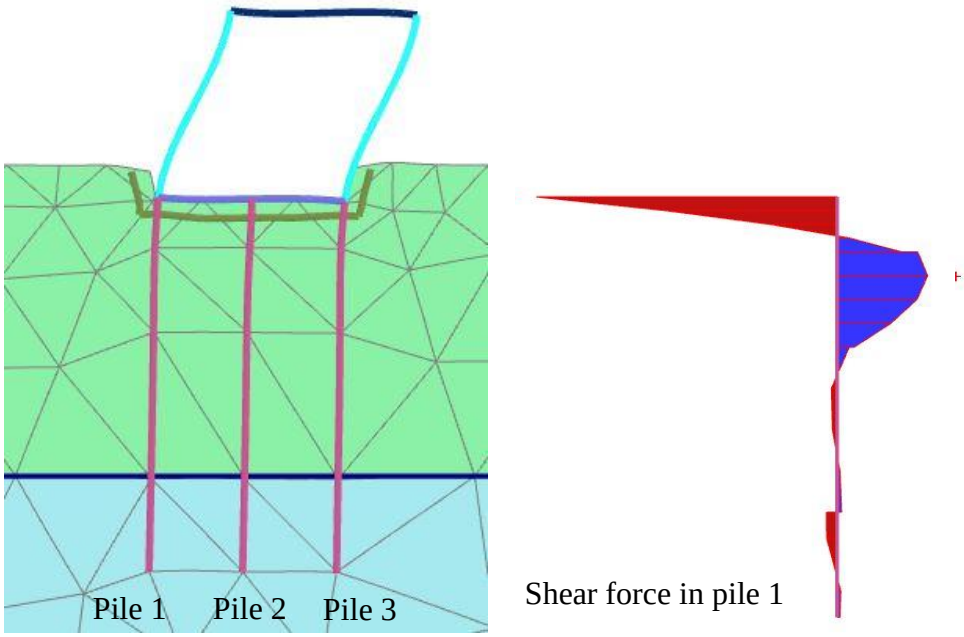

Figure 4-31 Pile arrangement and shear force in the reference pile

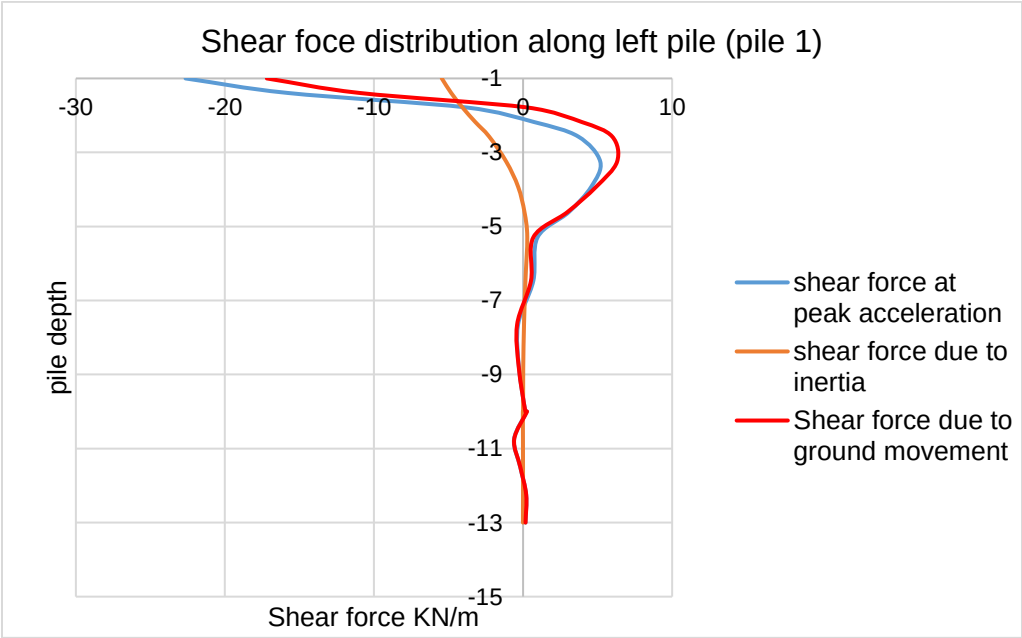

Figure 4-32 Calculation of shear force at the pile head

For different peak accelerations (from figure 4-19) the base shears are calculated using this method and results are summarized in table 4-7

Table 4-7 Calculated base shears at different peak accelerations

Peak acceleration with direction (g)	Number of step	Calculated Base Shear (KN/m)
0.849	1068	90.37
0.842	1067	83.01
-0.789	1050	87.95
-0.775	1086	64.19

Four story Structure with shallow foundation

Similar calculation method as single story structure is applied for four story structure as well. The base shear force is calculated at four different steps where dominant accelerations occur so that shear force at different modes can be calculated (from acceleration diagram in figure 4-22).

Table 4-8 Calculated base shears at different peak accelerations

Peak acceleration with direction (g)	Number of step	Calculated Base Shear (KN/m)
-0.334	1651	73.65
0.301	1835	54.63
-0.256	1852	52.44
0.249	1630	47.85

Four story Structure with piled raft

Calculation with pile foundation for four story structure is performed following the similar procedure as single story structure with pile. Number steps are chosen from figure 4-26 where high accelerations occur.

Table 4-9 Calculated base shears at different peak accelerations

Peak acceleration with direction (g)	Number of step	Calculated Base Shear (KN/m)
-0.477	1608	133.95
0.443	1631	119.7
0.399	1271	95.58
-0.307	1315	92.96

4.4.3 Summary and Discussion

The maximum shear forces from all the calculated values are summarized in the tables below. Although behavior factor q=1.0 is assumed for comparison with PLAXIS, result for both q=1.0 and 1.5 are shown.

Table 4-10 Obtained base shear for single story structure in KN/m

Eurocode 8		PLAXIS 2D	
q= 1.0	q=1.5	Shallow foundation	Piled raft
104.8	67.46	49.92	90.37

Table 4-11 Obtained base shear for four story structure in KN/m

Eurocode 8		PLAXIS 2D	
q= 1.0	q=1.5	Shallow foundation	Piled raft
149.3	99.96	73.65	133.95

It shows that the presence of pile increases the base shear force at a considerable extent. For both structures, the shear force gets almost twice as high with the introduction of piles. It implies that although piles are essential or provide good performance in case of bearing capacity or vertical displacement, it does not help in case of an earthquake. Therefore, adequate consideration should be made while designing the structure with piled raft foundations or pile groups for any expected seismic action. In case of a very high base shear, the structure can be subjected to heavy damage and cracks, i.e., damage in pile-raft interface, crack in walls and the adjacent utility systems. The results also indicate the necessity of specific analysis of design base shear for structures rather than simplified analysis to avoid over estimation.

For a single-story structure with shallow foundation, the shear force calculated from PLAXIS 2D is 48% of the value that is calculated from Eurocode 8. For the same structure with pile, the shear force becomes 86% of Eurocode 8. In case of a four-story structure, it is 49% and 90% respectively. It is expected that the estimated shear force from Eurocode 8 will considerably higher than obtained shear force from numerical analysis. Calculation suggested by Eurocode 8 is based on very simplified assumptions and should be adequate for all kinds of structures on a given envelope of soil. In this case, the soil type was D which is defined by a range of shear wave velocity 120-180 m/s. This range represents a wide range of soil type with

different stiffness. The design spectra for this soil is for different structures on that range of soil. The value calculated from Eurocode should be adequate for all the kinds of soil and structure within that design spectra. The case of this study represents a soil type with medium stiffness in the range (146.78 m/s) and two simple structure. Now the base shear for shallow foundation is less than the simplified method as expected while for piled raft, the value is quite high and very close to the simplified method. For this reason, seismic loads should be calculated for pile foundations and compared with simplified method to ensure safety.

It is to be noted that the basic representation of seismic action of Eurocode 8 is largely influenced by the assumption of behavior q. It is allowable to assume $q \leq 1.5$ for DCL materials. The behavior factor 1.5 reduces the base shear to 64% and 67%. There is several guidance for selection of "q" in different parts of Eurocode 8 which must be carefully followed to get reasonable results. Moreover, the formulae for simplified lateral force method and elastic response spectrum analysis suggested by Eurocode 8 is based on a linear single degree of freedom (SDOF) system on a fixed base. In reality, the structures are MDOF systems which may affect the estimation. In this study, the first simple structure is simulated with an attempt to portray a SDOF system but the rocking effect of the structure adds another degree of freedom. Therefore, none of the structure represents SDOF system in the study even though the results are obtained from Eurocode on that assumption.

The calculation of shear force at the interface of shallow foundation and piled raft is performed by taking summation of nodal shear stress. Since the side walls are embedded to -1m, the shear stress effect of side walls is also added. This rough calculation method is highly time consuming. The effect of inertial stress can result in ambiguity. Thus, it is difficult to represent the exact shear force that is only induced due to earthquake using this method. Moreover, it is difficult to simulate pile as 2D element. The design based on embedded beam row which is dependent on provided resistance and ISF factors which can influence the results in dynamic condition.

5 DISCUSSION AND CONCLUSION

5.1 SUMMARY

Earthquake response of two kinds of foundations (shallow foundation and piled raft) is carried out for a given input motion with peak acceleration 0.1g and a soil profile that have shear wave velocity within the range of soil type "D". Numerical analysis is performed in the finite element program PLAXIS 2D for these two types of foundations and preliminary influence of pile is obtained. The results are compared with calculation of based shear based on Eurocode 8.

Prior to analysis, a representative model of soil and structure is constructed in PLAXIS 2D. Material parameters are chosen based on recommendation of previous studies. Soil type is determined from Eurocode 8 based on average shear wave velocity of the layers. The piles are modelled as an embedded beam row in PLAXIS 2D. The pile bearing resistance for lateral and axial loading is determined to provide as input parameters for the embedded piles. After providing all the necessary material parameters, proper boundary conditions and mesh settings for dynamic analysis are chosen. Tied degree of freedom is provided in the lateral direction. Before proceeding to the actual analysis, dynamic boundary conditions are tested for a simple linear elastic material model with a harmonic motion. The test gives satisfactory result compared to analytical solution which implies that the choice of boundary condition is compatible for dynamic analysis. Finally, the input motion, generated using SIMQKE, is given as displacement boundary condition at the bed rock level and full dynamic analysis is carried out.

5.2 DISCUSSION AND CONCLUSION

This section elaborates the general discussions and conclusions on the results that are drawn throughout the procedure based on the objective mentioned in the beginning.

- Free field site response analysis to evaluate the behavior of soil profile during earthquake and comparing the result with one dimensional analysis in DEEPSOIL.

The free field soil response analysis is carried out to evaluate the soil behavior under seismicity. The reason of comparing the result with one dimensional analysis is to check if the soil response shows a certain degree of similarity for a given earthquake. PLAXIS 2D performs a non-linear dissipative analysis in 2D while DEEPSOIL conducts equivalent linear analysis in frequency domain. The results obtained by these two analyses are in good agreement and provides similar site amplification and peak acceleration response spectra. For an input motion of 0.1g, the maximum acceleration is obtained 0.2g and 0.23g from PLAXIS and DEEPSOIL respectively. Critical natural period of structure for given condition is 0.34s and 0.39s respectively which means that any structure with natural period of oscillation within this range will be in resonance with the underlying soil and heavy damage may occur. Furthermore, frequency content gives the distribution of amplitude over frequencies and relative displacement spectra are also observed and discussed to understand the free field soil behavior.

- Free vibration analysis to determine natural frequency of the structures.

Natural frequency of the structures is obtained by a free vibration analysis. Natural frequency of the single-story structure is 3 Hz and for four story structure it is 1.66 Hz for both kind of foundations. Obtained natural periods of vibration from PLAXIS analysis are compared with theoretical calculated values from logarithmic decrement method. These results are found in good agreement with the natural period calculated based on Eurocode 8.

- Seismic response analysis of the structures with shallow and pile foundations and evaluating the effect of the piles.

Seismic response analysis of the models is carried out for the given earthquake. The response of the top of the structure and the base is presented in terms of acceleration and displacement over dynamic time. It is observed that the presence of pile increases the acceleration of the top of the structure. For a single-story structure, the acceleration increases over 40% and the for the four-story structure it is over 45%.

- Calculation of base shear force based on simplified method recommended by Eurocode 8, NS-EN 1998-1:2004+A1:2013+NA:2014.

The shear force at the rigid base is calculated based on the lateral force method given by Eurocode 8. To calculate these shear forces, the horizontal component of design spectrum S_d (T) is calculated according to basic representation of seismic action suggested by Eurocode 8. At first the horizontal components of design spectrum are calculated for given seismic action assuming the structures to be fully elastic (q=1.0). Base shear is calculated 104.8 KN/m for the single-story structure and 149.3 KN/m for the four-story structure. Components for q=1.5 are also determined to observe the difference. The results show that the behavior factor 1.5 reduces the base shear to 64% and 67%. Natural period of the structure is calculated and compared with previously obtained values from PLAXIS.

- Shear force calculation on the rigid base of the structure from PLAXIS output and evaluating the correspondence with calculation based on Eurocode 8.

Shear force at the interface of the rigid base is calculated from PLAXIS output for both structures and both kinds of foundations. Obtained result shows that the pile increases base shear by almost 100% for both cases. This indicates the importance of special design consideration for base shear when pile foundations are essential. Otherwise, the performance of structures can be vulnerable in case of an earthquake. When the values are compared to Eurocode 8, base shear for piled raft demonstrate good agreement with current practice while for shallow foundation Eurocode 8 gives overestimation of base shear which may not be cost effective.

The results show considerable influence of piles on the seismic response of structures. This thesis studied the influence of piles for a single soil, a single input motion and two simple structures. Although presence of piles increase the base shear, the value remains less than the simplified method obtained from spectral analysis as expected. Therefore, results are compatible with existing assumptions of design spectra for this specific condition.

6 RECOMMENDATION FOR FURTHER WORK

As discussed earlier that to understand the spectral behavior for different foundation systems, analysis is required for a series of earthquakes, structures and soil conditions. This can provide an updated seismic design provision for different types of foundation systems in a more cost effective and less conservative way. This study demonstrates a possibility of further analysis for other common foundation systems using similar approach.

The calculation method in this study is directly from PLAXIS which is time consuming. A recent coupling tool is announced by PLAXIS in April, 2017 which gives facility to combine PLAXIS 3D and SAP 2000 and allows users to perform coupled structural and geotechnical analysis. This tool will also provide facility to perform kinematic interaction of soil and structure which can also be a topic of Interest. Moreover, according to Eurocode 8; div. NS-EN 1998-5: 2004, it is recommended to analyze the pile for inertial and kinematic interaction for certain soil and seismic condition. It will also be possible to observe how piles change the shear at different levels in the structure and compare the value with Eurocode 8 with the help of this new tool. More information is available in the official website of PLAXIS ("Plaxis Bv," 2017).

Further investigations can be done with experimental soil data and three-dimensional numerical models which can simulate 3D behavior of the piles more accurately.

BIBLIOGRAPHY

Bardet, J. P., Ichii, K., & Lin, C. H. (2000). *EERA A Computer Program for Equivalent-linear Earthquake site Response Analyses of Layered Soil Deposits*. Retrieved from

Bisch, P., Carvalho, E., Degee, H., Fajfar, P., Fardis, M., Franchin, P., . . . Plumier, A. (2012). Eurocode 8: seismic design of buildings worked examples. *Luxembourg: Publications Office of the European Union*.

Brandt, M. (2014). *Earthquake Analysis of Subsea Structure on Caisson Foundation using 3D Finite Element Solution.* (Master of Science), NTNU, Trondheim, Norway.

Brinkgreve, R. B. J., Kumerswamy, S., & Swolfs, W. M. (2016). *PLAXIS 2D 2017- General Information* Netherlands

Brooms, B. B. (1964). Lateral resistance of piles in cohesionless soil. *Journal of Soil Mechanics and Foundations, 90*(ASCE).

CEN. (2004). Eurocode 8: Design of structures for earthquake resistance—Part 1: General rules, seismic actions and rules for buildings (EN 1998-1: 2004). *European Committee for Normalization, Brussels*.

Chadha, K. (2015). *Jordskjelvberegning i henhold til Eurokode 8 og PLAXIS 2D.* (Master of Science), NTNU, Trondheim.

Chopra, A. K. (2007). *Dynamics of Structures: Theory and Application to Earthquake Engineering* (Third Edition ed.). New Jersey: Prentice Hall.

Clough, R. W., & Penzien, J. (1993). Dynamics of structures. *Copyright of Applied Mechanics & Materials*.

Dao, T. (2011). Validation of plaxis embedded piles for lateral loading. *Master of Science Thesis, Delft University*.

Dos Santos, J., & Correia, A. (2001). *Reference threshold shear strain of soil. Its application to obtain an unique strain-dependent shear modulus curve for soil.* Paper presented at the Proceedings of The International Conference on Soil Mechanics and Geotechnical Engineering.

Eiksund, G. R. (2016). *Pile Handout*.

Fleming, K., Weltman, A., Randolph, M., & Elson, K. (2008). *Piling engineering*: CRC press.

Govindaraju, G. V., Ramana, C., Hanumantha, R., & Sitharam, T. G. (2004). Site-specific ground response analysis. *CURRENT SCIENCE, VOL. 87, NO. 10*.

Guerreiro, P., Kontoe, S., & Taborda, D. (2012). *Comparative Study Of Stiffness Reduction And Damping Curves*. Paper presented at the 15 WCEE, LISBON.

Hamada, J. (2015). *Bending moment of piles on piled raft foundation subjected to ground deformation during earthquake in centrifuge model test* Paper presented at the The 15th Asian Regional Conference on Soil Mechanics and Geotechnical Engineering.

Hamada, M. (1991). *Damage of Piles by LiquefactionInduced Ground Displacements*. Paper presented at the The Third US Conference Lifeline Earthquake Engineering, Los Angeles, US.

Hardin, B. O., & Drnevich, V. P. (1972). Shear modulus and damping in soils: Design Equations and Curves. *ASCE: Journal of the Soil Mechanics and Foundations*.

Hashash, Y. M. A. (2012). *DEEPSOIL USER MANUAL AND TUTORIAL*. Department of Civil and Environmental Engineering, University of Illinois at Urbana-Champaign.

Hudson, M., Idriss, I. M., & Beikae, M. (1994). *QUAD4M- A computer program to evaluate the seismic response of soil structures using finite element procedures and incorporating a compiant base. Center for Geotechnical Modeling*.

Imtiaz, A. B. A. (2009). *Seismic Microzonation of Cox's Bazar Municipal Area. .* (M.Sc. in Geotechnical Engineering M.Sc. Engg. Thesis), Bangladesh University of Engineering and Technology.

Kramer, S. L. (1996). *Geotechnical Earthquake Engineering*. Prentice Hall.

Kuhlemeyer, R. L., & Lysmer, J. (1973). Finite element method accuracy for wave propagation problems. *Journal of Soil Mechanics & Foundations Div, 99*(Tech Rpt).

Kwaak, B. v. d. (2015). *Modelling of dynamic pile behaviour during an earthquake using PLAXIS 2D: Embedded beam (rows).* (Master of Science), Delft University of Technology, Delft, Netherlands.

Laera, A., & Brinkgreve , R. B. J. (2015). *Ground Response Analysis in PLAXIS*.

Magar, A. T. (2016). *Earthquake Response of Different Types of Retaining Walls.* (Master of Science), NTNU, Trondheim.

Martin, G. R., & Lam, I. P. (1995). *Seismic Design of Pile Foundations: Structural and Geotechnical Issues.* Paper presented at the Third International Conference on Recent Advancement in Geotechnical Earthquake Engineering and Soil Dynamics, St. Louis, Missouri.

Mizuno, H. (1987). *Pile Damage During Earthquake in Japan (1923-1983).* Paper presented at the Geotechnical Engineering Division of the American Society of Civil Engineers in conjunction with the ASCE Convention Atlantic City, New Jersey.

Nordal, S. (2016). *Geotechnical Engineering Advanced Course: Lecture notes and background material*. NTNU, Geotechnical Division, Trondheim

PLAXIS 2D Dynamic Manual. http://www.gemsoft.us/Manuals/Plaxis/Plaxis%202D%20v9.0%20-%207%20Dynamics%20Manual.pdf

PLAXIS 2D Material Models Manual. (2016). from Plaxis Bv https://www.plaxis.com/support/manuals/plaxis-2d-manuals/

PLAXIS 2D Reference Manual. (2016). from Plaxis Bv https://www.plaxis.com/support/manuals/plaxis-2d-manuals/

Plaxis Bv. (2014). *On the use of dynamic boundary conditions.* Retrieved from https://www.plaxis.com/support/tips-and-tricks/on-the-use-of-dynamic-boundary-conditions/

Plaxis Bv. (2017). *Using the PLAXIS Coupling Tool.* Retrieved from https://www.plaxis.com/support/videos/using-plaxis-coupling-tool/

QuakeManager Wiki. (2015). *What is a Response Spectrum?* Retrieved from https://sites.google.com/site/quakemanagerwiki/record-manager/spectra/what-is-a-response-spectrum

Rønnquist, A., Remseth, S., & Lindholm, C. (2012). *Earthquake engineering design practice in Norway: Implementation of Eurocode 8*. Paper presented at the The 15th World Conference on Earthquake Engineering, Lisbon, Portugal.

Saha, A. (2014). *Determination of Amplification Factor Using DEEP SOIL.* (B.Sc in Civil Engineering), Bangladesh University of Engineering and Technolog, Dhaka, Bangladesh.

Schnabel, P. B., Lysmer, J., & Seed, H. B. (1972). *SHAKE: A computer program for earthquake response analysis of horizontally layered sites*. Retrieved from Earthquake Engineering Research Center:

Seed, H. B., Wong, R.,Idriss, I., Tokimatsu, K. (1986). *Moduli and damping factors for dynamic analysis of cohesionless soils*. Retrieved from Journal of Geotechnical Engineering, ASCE:

Sluis, J. (2012). Validation of embedded pile row in PLAXIS 2D. *Delft University of Technology, Delft*.

Sluis, J., Besseling, F., & Stuurwold, P. (2014). Modelling of a pile row in a 2D plane strain FE-analysis.

Standard, N. (2014). Eurokode 8: Prosjektering av konstruksjoner for seismisk påvirkning Del 1: Allmenne regler, seismiske laster og regler for bygninge, *Nasjonalt tilleg NA*: Standard Norge.

Stensløkken, A. (2016). *Study of the Effect of Added Soil Mass on Earthquake Response of Subsea Structures on Closed Caisson Foundations.* (Master of Science), NTNU, Trondheim, Norway.

Teguh, M., Duffield, C.F., Mendis, P.A., Hutchinson, G.L. . (2006). Seismic performance of pile-to-pile cap connections: An investigation of design issues *Electronic Journal of Structural Engineering, 6*.

Toma, M. A. (2016). *One Dimensional Ground Response Analysis Using DEEPSOIL and PLAXIS*. Retrieved from NTNU, Trondheim:

Vucetic, M., & Dobry, R. (1991). Effect of soil plasticity on cyclic response. *Journal of Geotechnical Engineerin*.

ACRONYMS

CEN	European Committee for Standardization
DCL	Ductility Class Low
DCM	Ductility Class Medium
DCH	Ductility Class High
DOF	Degree of Freedom
EC-8	Eurocode 8
EERA	Equivalent-linear Earthquake Response Analysis
EN	European Standards
FEM	Finite Element Method
FFT	Fast Fourier Transformation
HS	Hardening Soil
HSsmall	Hardening Soil with small strain stiffness
ISF	Interface Stiffness Factor
LE	Linear Elastic
MC	Mohr-Coulomb
MDOF	Multiple Degree of Freedom
NS	Norsk Standard
PGA	Peak Ground Acceleration
PSA	Pseudo Spectral Acceleration
SDOF	Single Degree of Freedom

APPENDICES

Appendix A

Relevant parts of Eurocode 8 (NS-EN 1998-1:2004+A1:2013+NA:2014)

A-1 Ground Types

Tabell NA.3.1 – Grunntyper [1)]

Grunn-type	Beskrivelse av stratigrafisk profil	Parametere [2) 3)]		
		$v_{s,30}$ (m/s)	N_{SPT} (slag/30cm)	c_u (kPa)
A	Fjell eller fjell-liknende geologisk formasjon, medregnet høyst 5 m svakere materiale på overflaten.	> 800	–	–
B	Avleiringer av svært fast sand eller grus eller svært stiv leire, med en tykkelse på flere titalls meter, kjennetegnet ved en gradvis økning av mekaniske egenskaper med dybden.	360 – 800	> 50	> 250
C	Dype avleiringer av fast eller middels fast sand eller grus eller stiv leire med en tykkelse fra et titalls meter til flere hundre meter.	180 – 360	15 - 50	70 - 250
D	Avleiringer av løs til middels fast kohesjonsløs jord (med eller uten enkelte myke kohesjonslag) eller av hovedsakelig myk til fast kohesjonsjord.	120 – 180	10 – 15	30 – 70
E	Et grunnprofil som består av et alluviumlag i overflaten med v_s-verdier av type C eller D og en tykkelse som varierer mellom ca. 5 m og 20 m, over et stivere materiale med v_s > 800 m/s.			
S_1	Avleiringer som består av eller inneholder et lag med en tykkelse på minst 10 m av bløt leire/silt med høy plastisitetsindeks (PI > 40) og høyt vanninnhold.	< 100 (antydet)	–	10 - 20
S_2	Avleiringer av jord som kan gå over i flytefase (liquefaction), sensitive leirer eller annen grunnprofil som ikke er med i typene A – E eller S_1.			

[1)] Hvis minst 75 % av konstruksjonen står på fjell og resten på løsmasser, og konstruksjonen står på ett kontinuerlig fundament (platefundament), kan grunntype A benyttes.

[2)] Valget av grunntype kan være basert på enten $v_{s,30}$, N_{SPT} eller c_u. $v_{s,30}$ anses som den mest aktuelle parameteren å benytte.

[3)] Der det er tvil om hvilken jordtype som skal velges, velges den mest ugunstige.

A-2: Seismic Zones

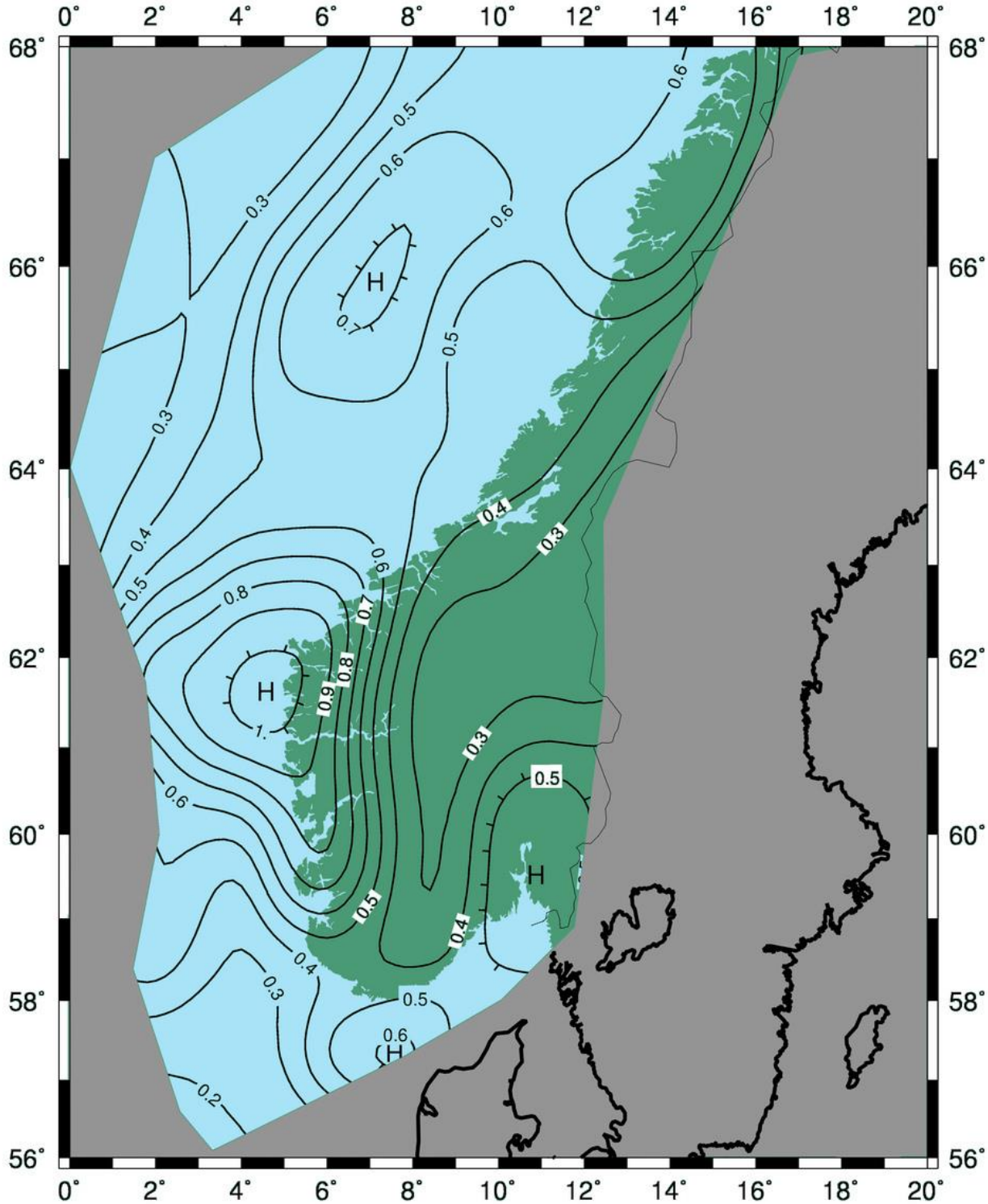

Figure NA.3(901): Seismic zones of south Norway, a_{g40Hz} in m/s^2

A-3: Selection of Seismic Classes and Ductility Classes

Tabell NA.4(902) – Veiledende tabell ved valg av seismisk klasse

Byggverk	I	II	III	IV
Byggverk der konsekvensene av sammenbrudd er særlig store				X[1)]
Viktig infrastruktur: sykehus, brannstasjoner, redningssentraler, kraftforsyning og lignende			(X)	X
Høye bygninger, mer enn 15 etasjer		(X)	X	
Jernbanebruer [2)]			X	(X)
Veg- og gangbruer [2)]		(X)	X	(X)
Byggverk med store ansamlinger av mennesker (tribuner, kinosaler, sportshaller, kjøpesentre, forsamlingslokaler osv.)		(X)	X	
Kaier og havneanlegg		X	(X)	
Landbaserte akvakulturanlegg for fisk		X	(X)	
Tårn, master, skorsteiner, siloer	(X)	X	(X)	
Industrianlegg		X	(X)	
Skoler og institusjonsbygg		(X)	X	
Kontorer, forretningsbygg og boligbygg		X	(X)	
Småhus, rekkehus, bygg i én etasje, mindre lagerhus osv.	X	(X)		
Støttemurer med høyde lavere enn 3 m langs veger i klasse II [3)]	X	(X)		
Kulverter	X	(X)	(X)	
Landbruksbygg	(X)			
Kaier og fortøyningsanlegg for sport og fritid	(X)			

[1)] For byggverk der konsekvensene av sammenbrudd er særlig store, for eksempel ved atomreaktorer og lagringsanlegg for radioaktivt avfall, store dammer og marine konstruksjoner bør jordskjelvrisikoen vurderes spesielt, eventuelt basert på en risikoanalyse.

Lagertanker for flytende gass og store hydrokarbonførende rørledninger over land er behandlet i NA til NS-EN 1998-4.

[2)] Se veiledende tabell for valg av seismisk klasse for bruer i NA til NS-EN 1998-2.

[3)] For støttemurer langs jernbane, støttemurer langs veger med høyde over 3 m og støttemurer langs viktige veier (klasse III) benyttes samme seismiske klasse som for vegen eller jernbanen

Tabell NA.6.1 – Dimensjoneringsprinsipper, duktilitetsklasser og øvre grense for referanseverdier for konstruksjonsfaktorer

Dimensjoneringsprinsipp	Konstruksjonens duktilitetsklasse	Område av referanseverdier for valg av konstruksjonsfaktor q
Prinsipp a) Konstruksjon med lite energiabsorpsjon	DCL (Lav)	$\leq 1{,}5$
Prinsipp b) Energiabsorberende konstruksjon	DCM (Middels)	≤ 4 Også begrenset av verdiene for DCM i tabell 6.2
	DCH (Høy)	Som for DCM

Appendix B

Determination of material properties.

Table B: Calculation chart of material properties

	Depth z	Vertical stress $\sigma_v = Z\gamma$	Pore Pressure $u = Z\gamma_w$	effective vertical $\sigma'_v = \sigma_v - u$	k	$\sigma'_h = K.\ \sigma'v$	vertical preconsolidation pressure	$\sigma'_p = 0.5\ (\sigma'_v + \sigma'_h)$	c'	ϕ'	C_u (MC formula)	Cu from PLAXIS	G_0^{ref}	G_0	shear wave velocity (Vs)
Clay	0	0	0	0	0.691	0	0	0	10	18	9.51	0	180000	87320.99	73.88
	-1	16	0	16	0.691	11.056	16	13.528	10	18	13.69	11.2	180000	107652	82.03
	-2	32	0	32	0.691	22.112	32	27.056	10	18	17.87	15.5	180000	124711.5	88.29
	-3	48	0	48	0.691	33.168	48	40.584	10	18	22.05	19.22	180000	139703.2	93.44
	-4	64	0	64	0.691	44.224	64	54.112	10	18	26.23	23.84	180000	153235.1	97.86
	-5	80	0	80	0.691	55.28	80	67.64	10	18	30.41	27.6	180000	165665.3	101.76
	-6	96	0	96	0.691	66.336	96	81.168	10	18	34.59	32.1	180000	177225.8	105.25
	-7	112	0	112	0.691	77.392	112	94.696	10	18	38.77	36.1	180000	188077.1	108.42
	-8	128	0	128	0.691	88.448	128	108.224	10	18	42.95	39.25	180000	198335.6	111.34
	-9	144	0	144	0.691	99.504	144	121.752	10	18	47.13	45	180000	208089	114.04
	-10	160	0	160	0.691	110.56	160	135.28	10	18	51.31	49.82	180000	217405.2	116.57
sand	-10	200	100	100	0.5305	53.05	200	76.525	5	28	40.34	38.53	240000	332037.8	128.85
	-11	220	110	110	0.5305	58.355	220	84.1775	5	28	43.93	40.55	240000	347532.6	131.82
	-12	240	120	120	0.5305	63.66	240	91.83	5	28	47.53	44.47	240000	362365.5	134.60
	-13	260	130	130	0.5305	68.965	260	99.4825	5	28	51.12	47.7	240000	376614.6	137.23
	-14	280	140	140	0.5305	74.27	280	107.135	5	28	54.71	51.23	240000	390343.9	139.70
	-15	300	150	150	0.5305	79.575	300	114.7875	5	28	58.30	55.47	240000	403606.5	142.06
	-16	320	160	160	0.5305	84.88	320	122.44	5	28	61.90	58.8	240000	416446.9	144.30
	-17	340	170	170	0.5305	90.185	340	130.0925	5	28	65.49	62.2	240000	428903	146.44
	-18	360	180	180	0.5305	95.49	360	137.745	5	28	69.08	66.8	240000	441007.5	148.49
	-19	380	190	190	0.5305	100.795	380	145.3975	5	28	72.67	70.01	240000	452788.5	150.46
	-20	400	200	200	0.5305	106.1	400	153.05	5	28	76.27	73.6	240000	464270.7	152.36
	-21	420	210	210	0.5305	111.405	420	160.7025	5	28	79.86	77.89	240000	475475.6	154.19
	-22	440	220	220	0.5305	116.71	440	168.355	5	28	83.45	81.36	240000	486422.5	155.95
	-23	460	230	230	0.5305	122.015	460	176.0075	5	28	87.05	85.44	240000	497128.5	157.66
	-24	480	240	240	0.5305	127.32	480	183.66	5	28	90.64	87.77	240000	507608.6	159.31
	-25	500	250	250	0.5305	132.625	500	191.3125	5	28	94.23	91.29	240000	517876.8	160.92

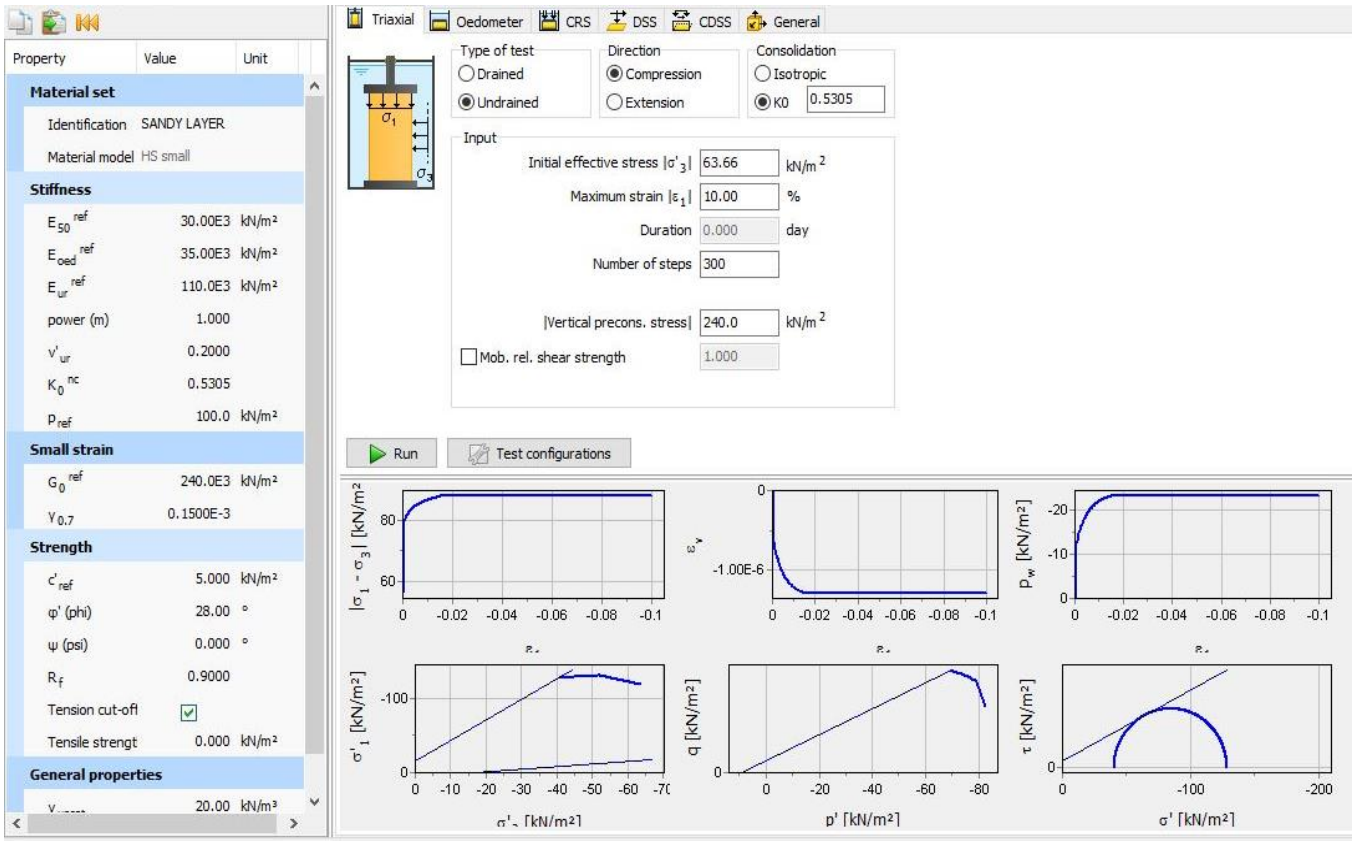

Figure B-1: Output from PLAXIS SoilTest at 12m depth

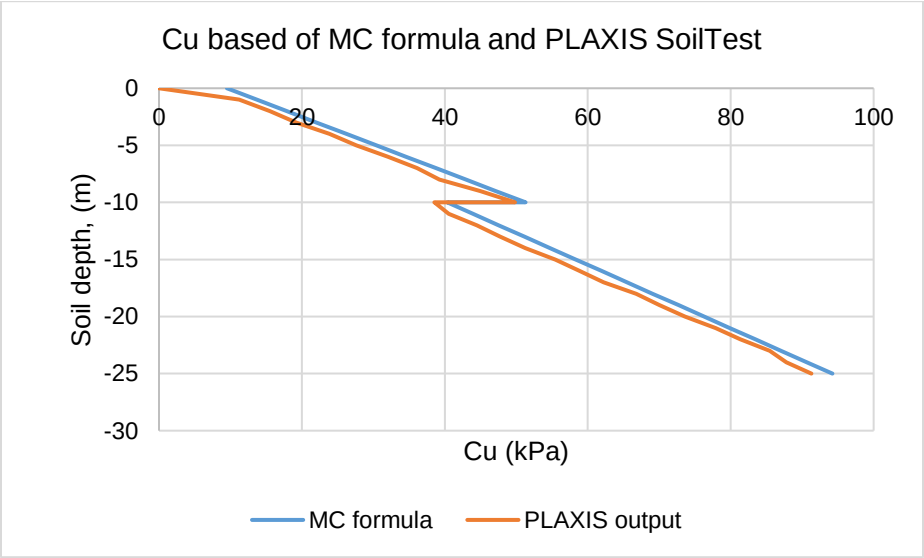

Figure B-2 Cu parameter from SoilTest compared to MC-formula

Appendix C

Determination of limiting resistance of pile for PLAXIS input

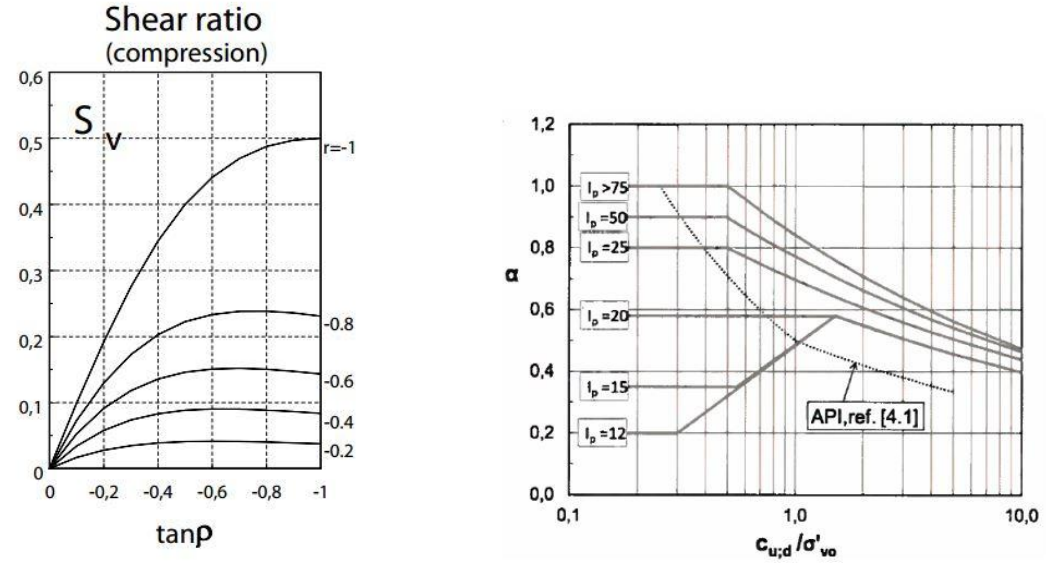

Figure C-1: a) shear ratio for piles in compression for effective stress analysis and b) The recommended procedure for normalized side friction of clay (a-value) (Eiksund, 2016)

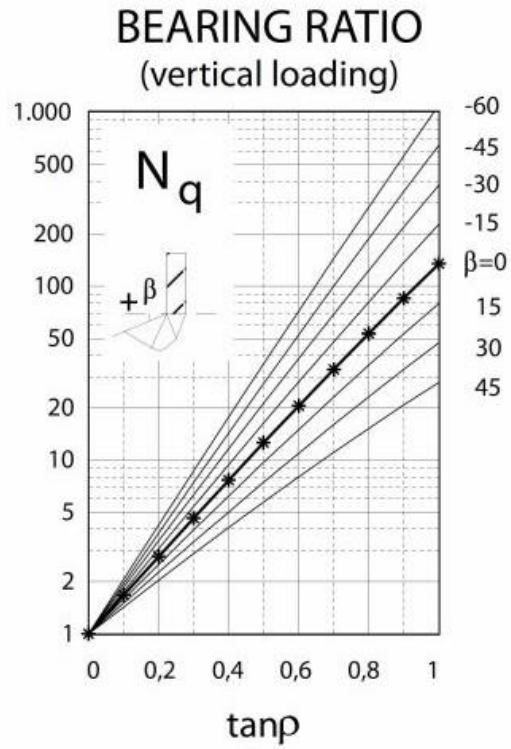

Figure C-2: Bearing capacity factor for the calculation of base resistance based on effective stress analysis (Eiksund, 2016)

Table C: Calculation chart of limiting resistances of pile

	z	$\sigma'_v = \sigma_v - u$	$\sigma'_h = K.\sigma'v$	$\sigma'_p = 0.5(\sigma'_v + \sigma'_h)$	C_u	C_u/σ'_v	α	τ_s	Total side friction Q_s	Lateral Resistance, Pu	End Bearing
Clay	0	0	0.00	0.00	9.51	-	-	-	0.00	-	-
	-1	16	11.06	13.53	13.69	0.86	0.72	9.86	15.48	45.50	96.78
	-2	32	22.11	27.06	17.87	0.56	0.80	14.30	22.46	71.01	126.33
	-3	48	33.17	40.58	22.05	0.46	0.80	17.64	27.71	80.42	155.87
	-4	64	44.22	54.11	26.23	0.41	0.80	20.99	32.96	99.23	185.42
	-5	80	55.28	67.64	30.41	0.38	0.80	24.33	38.21	118.04	214.97
	-6	96	66.34	81.17	34.59	0.36	0.80	27.67	43.47	136.86	244.52
	-7	112	77.39	94.70	38.77	0.35	0.80	31.02	48.72	155.67	274.07
	-8	128	88.45	108.22	42.95	0.34	0.80	34.36	53.97	174.48	303.62
	-9	144	99.50	121.75	47.13	0.33	0.80	37.71	59.22	193.29	333.17
	-10	160	110.56	135.28	51.31	0.32	0.80	41.05	64.48	212.10	362.72
sand	-10	100	53.05	76.53	40.34	-	-	21.25	33.38	230.92	4296.14
	-11	110	58.36	84.18	43.93	-	-	23.20	36.44	274.23	4688.84
	-12	120	63.66	91.83	47.53	-	-	25.14	39.49	299.16	5081.54
	-13	130	68.97	99.48	51.12	-	-	27.08	42.54	324.09	5474.24
	-14	140	74.27	107.14	54.71	-	-	29.03	45.59	349.02	5866.94
	-15	150	79.58	114.79	58.30	-	-	30.97	48.64	373.95	6259.64
	-16	160	84.88	122.44	61.90	-	-	32.91	51.69	398.88	6652.34
	-17	170	90.19	130.09	65.49	-	-	34.85	54.74	423.81	7045.04
	-18	180	95.49	137.75	69.08	-	-	36.80	57.80	448.74	7437.74
	-19	190	100.80	145.40	72.67	-	-	38.74	60.85	473.67	7830.44
	-20	200	106.10	153.05	76.27	-	-	40.68	63.90	498.60	8223.14
	-21	210	111.41	160.70	79.86	-	-	42.63	66.95	523.53	8615.84
	-22	220	116.71	168.36	83.45	-	-	44.57	70.00	548.46	9008.54
	-23	230	122.02	176.01	87.05	-	-	46.51	73.05	573.39	9401.24
	-24	240	127.32	183.66	90.64	-	-	48.45	76.11	598.32	9793.94
	-25	250	132.63	191.31	94.23	-	-	50.40	79.16	623.25	10186.64

Appendix D

Input time history

The input time history for this study is generated using artificial motion generation program SIMQKE. The Italian version of the program from University of Brescia. This program generates artificial bed rock motion based on some input parameters. Earthquakes can be generated for any of the four seismic zones of Italy (zone 1-4). These seismic zones are defined according to the value of the maximum ground acceleration a_g, whose probability of exceedance is 10% in 50 years. Spectrum type can be chosen either horizontal/vertical and SLU/SLD/elastic. Response spectrum can be generated for ground type A to E for 5% damping ratio. Now a random bedrock acceleration is generated for a given frequency or period. The total duration of the motion can also be specified (Chadha, 2015). The resulting time history can be exported as a (*.Txt) file. The magnitude of the peak acceleration can be scaled to any expected value in either SIMQKE or in DEEPSOIL.

For this study, the generated by selecting zone 3, soil type B, C, E, spectrum type "horizontal elastic" and frequency 2 Hz (period 0.5s). The duration of the motion is 20s. The generated motion is then scaled to 0.1g. (This motion is compared with several generated motions for other soil types and seismic zones and it is observed that the program generates same time history for all the cases for the given frequency and peak acceleration).

This acceleration time history can be used directly in DEEPSOIL and in PLAXIS 2D. In DEEPSOIL, it is done by simply clicking "Add" in the "Motion" tab and selecting the exported file from SIMQKE. Acceleration unit should be selected m/s^2 and time step should be specified. In PLAXIS 2D, the input time history is given in the bed rock as displacement boundary condition at the bottom. The x-component of the line displacement is set "prescribed" and assigned a value of 1.0m while y-component of the prescribed displacement is "fixed". Dynamic displacement of this line is defined by adding "DisplacementMultiplier_1" to "$Multiplier_x$". No dynamic displacement is assigned at "$Multiplier_y$". While assigning dynamic displacement, the signal type is selected "table". Input data type can be selected from three options i.e. displacement/velocity/acceleration. In this case, the available data type is acceleration history, therefore "acceleration" is chosen. Now the summary can be seen at the "selection explorer."

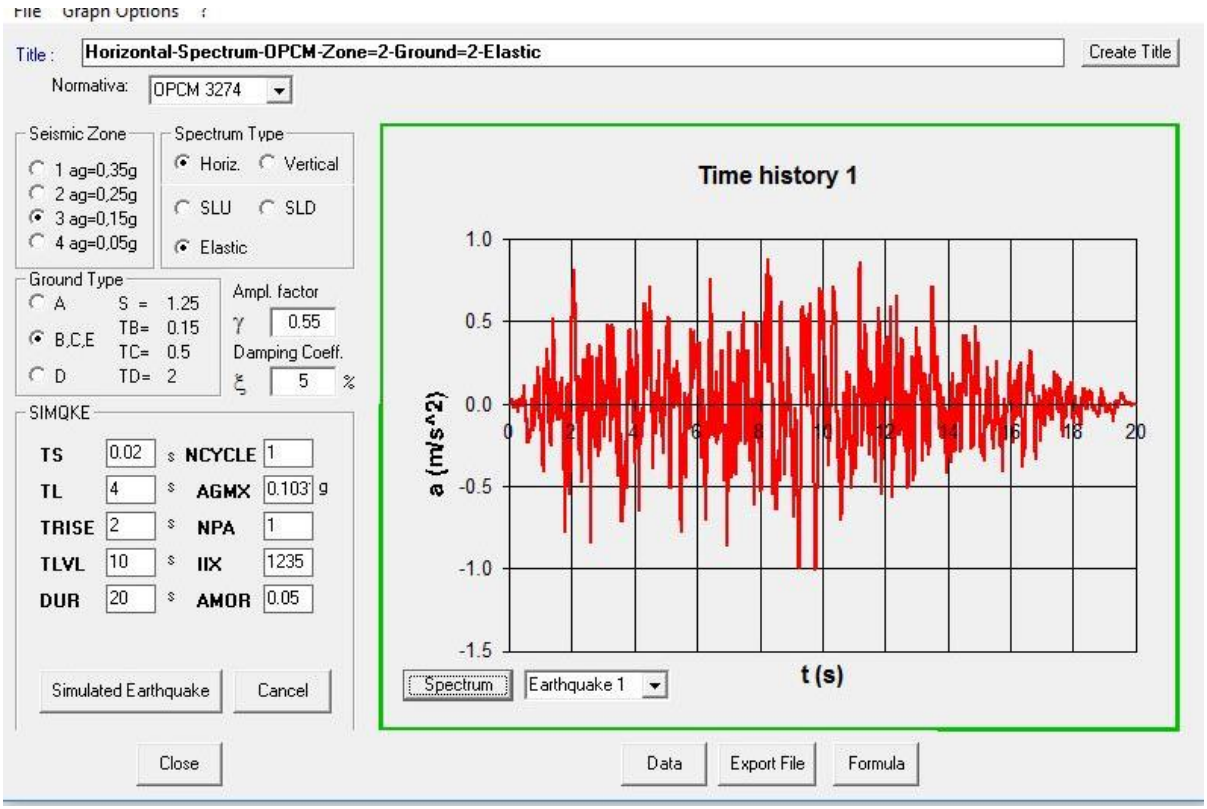

Figure D-1: Artificially generated time history by SIMQKE program. Where a_{gmax} = 0.1g

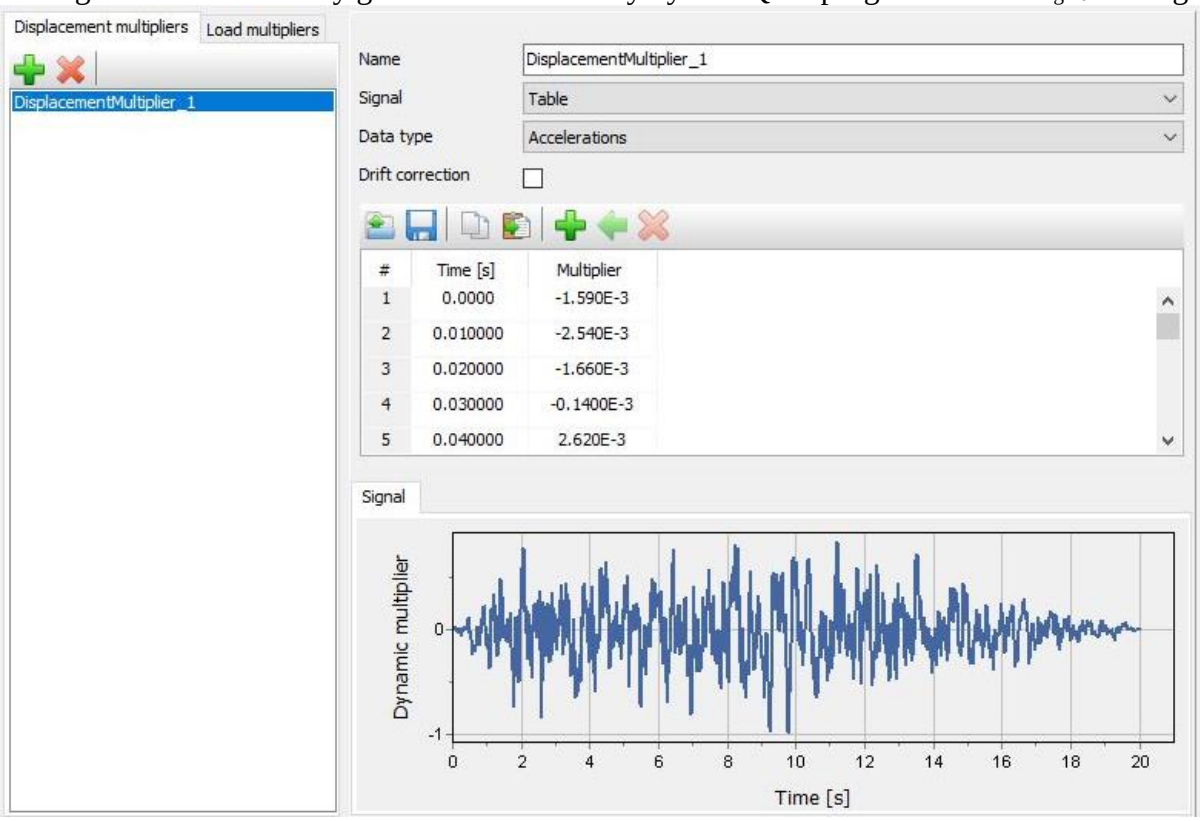

Figure D-2: Imported input motion in PLAXIS 2D

Appendix E

Calculation of amplitude factor.

Table E: Calculation chart of amplitude factor from theory and PLAXIS output

Frequency f	Angular frequency, ω	frequency ratio, r	Theoretical Solution, |Fω|	PLAXIS output |Fω|
0	0	0	1	-
1.5	9.42	0.5	1.41	1.24
3	18.84	1	12.73	10.84
6	37.69	2	0.985	2.1
9	56.54	3	4.24	5.1
12	75.39	4	0.95	1.5

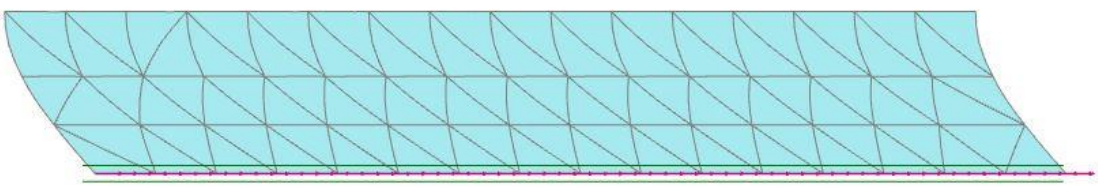

(a) Mode 1

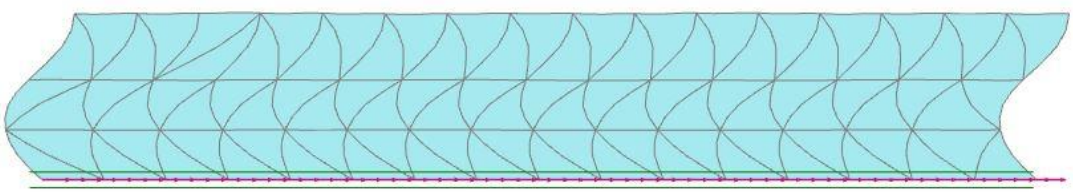

(b) Mode 2

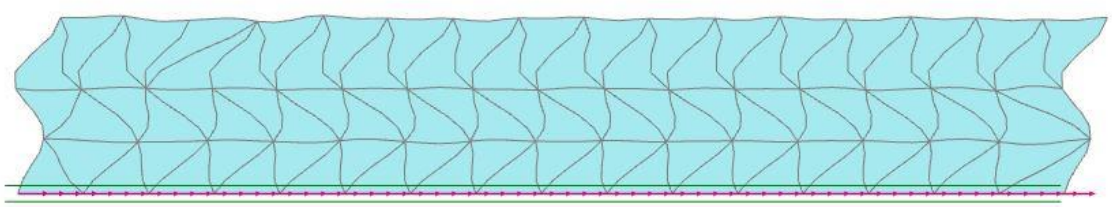

(c) Mode 3

Figure E: Mode shape of soil layer at different frequencies

Appendix F

Analysis in DEEPSOIL (Hashash, 2012):

STEPS OF ANALYSIS IN DEEPSOIL:

- ***Step 1 of 5: Analysis type selection:***

The Analysis starts with opening a new profile. At first the profile must be defined by selecting analysis options. Following specifications must be defined before proceeding to the next step (Hashash, 2012).

1. The analysis method:

- Frequency Domain
  1) Linear
  2) **Equivalent Linear**
- Time Domain
  1) Linear
  2) Nonlinear

Equivalent linear analysis is available in the frequency domain analysis. This option is chosen for the further analysis.

2. The type of input for shear properties:

- Shear Modulus (G_{max})
- **Shear Wave Velocity (V_s)** (Default selection)

3. The units to be used in analysis:

- English
- **Metric** (Metric selected)

4. The analysis type:

- **Total Stress Analysis** (applicable equivalent linear analysis in frequency domain)
- Effective Stress Analysis (Pore Water Pressure generation only)
  - Include PWP Dissipation (PWP generation and dissipation)

Effective stress option is only available for nonlinear analysis which can be performed under time domain.

5. The method to define the soil curve:

- For Equivalent Linear
  - **Discrete Points** (chosen for the analysis)
  - Pressure-Dependent Hyperbolic Model
- For Nonlinear
  - MRDF Pressure-Dependent Hyperbolic Model
  - Pressure-Dependent Hyperbolic Model

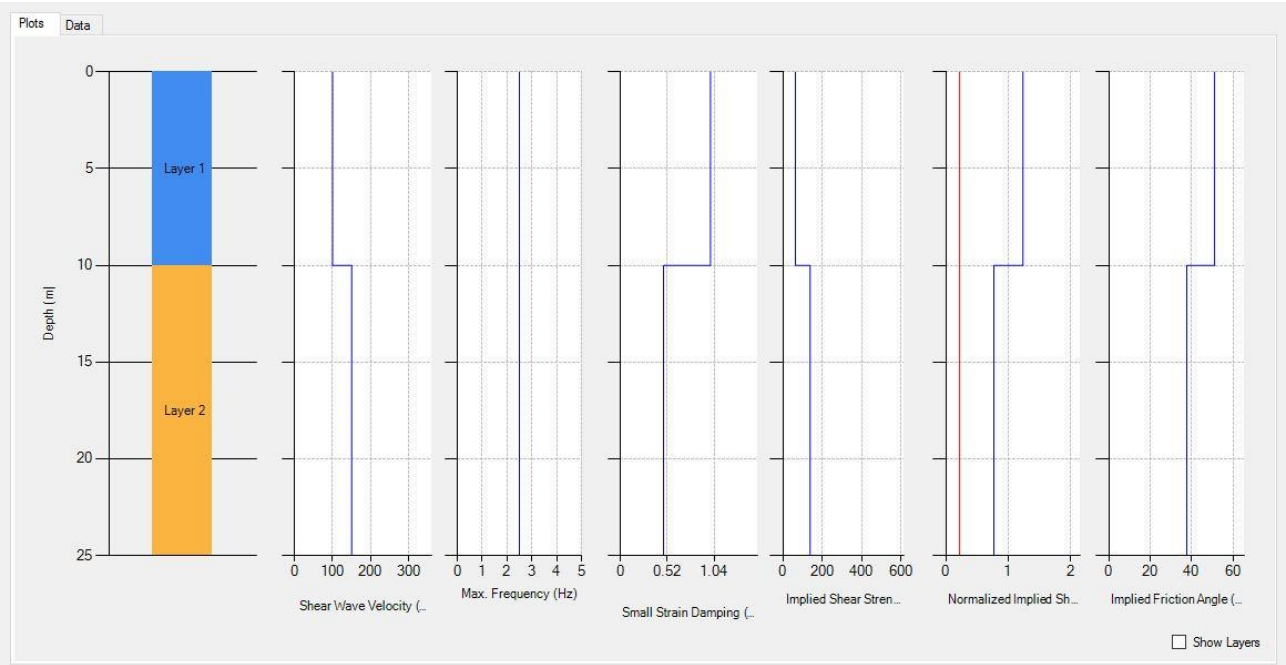

Figure F-1: DEEPSOIL input profile summary

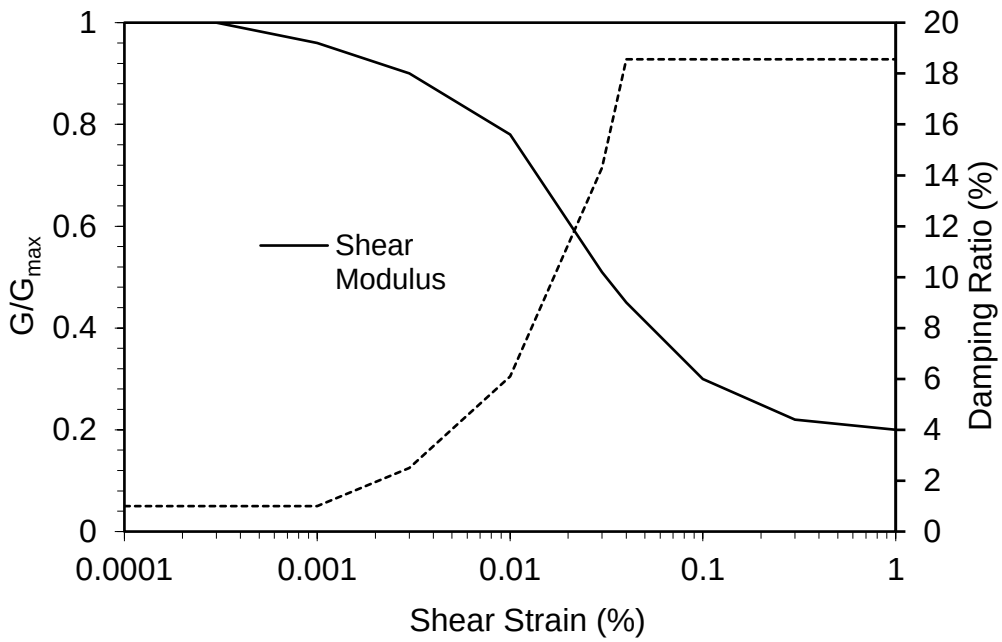

Figure F-2: Modulus reduction and damping curve for clay based on HSsmall model (described in section 2.2.1.2)

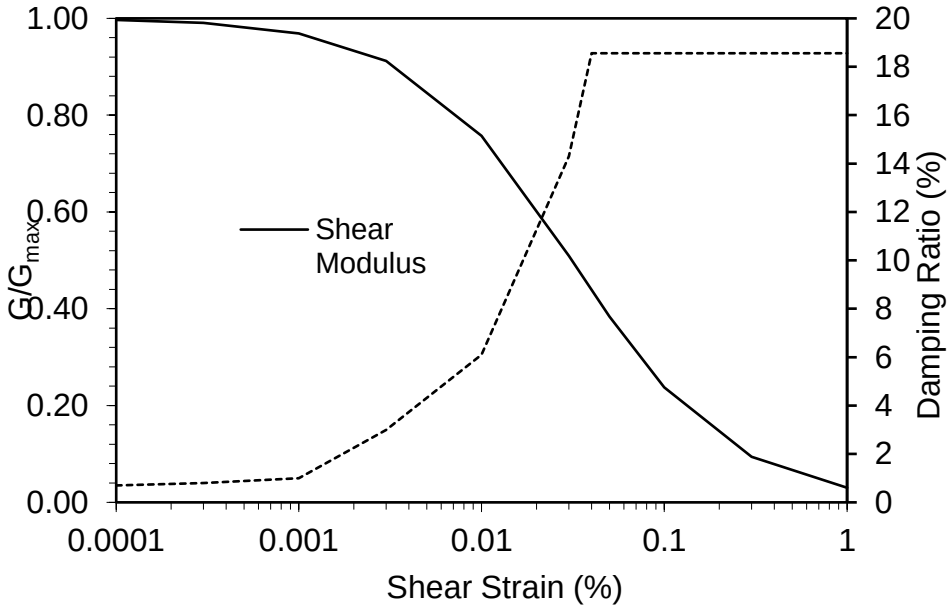

Figure F-3: Modulus reduction and damping curve for sand based on HSsmall model (described in section 2.2.1.2)

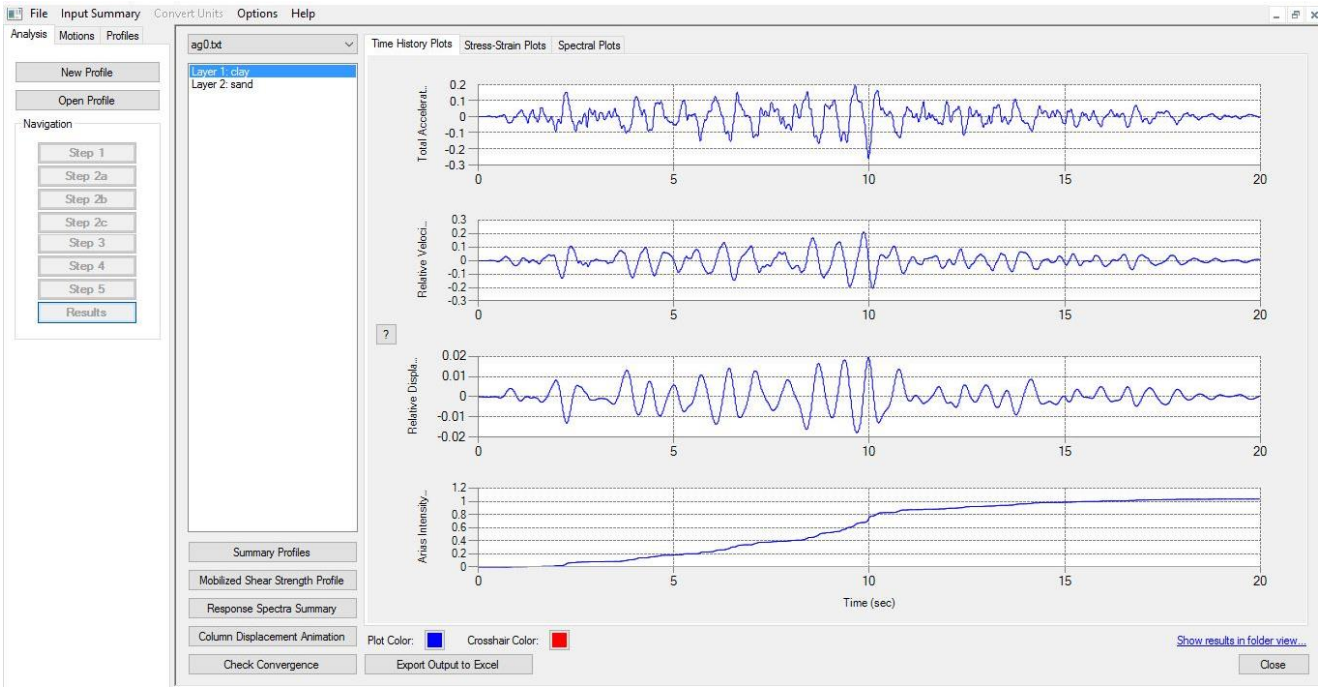

Figure F-4: Output summary from DEEPSOIL

Appendix G

Sample calculation of base shear.

Table G-1: Sample base shear calculation procedure for single-story structure with shallow foundation at step 1675

X [m]	Δx	τ_1 [kN/m²]	τ_{avg} [kN/m²]	F= τ_{avg}*Δx
-3.00		7.00		
-2.63	0.38	6.69	6.85	2.56
-2.25	0.38	7.05	6.87	2.57
-1.88	0.38	6.57	6.81	2.55
-1.50	0.38	4.01	5.29	1.98
-1.13	0.38	4.05	4.03	1.51
-0.75	0.38	4.66	4.35	1.63
-0.38	0.38	5.01	4.84	1.81
0.00	0.38	6.06	5.54	2.07
0.38	0.38	7.05	6.55	2.45
0.75	0.38	7.27	7.16	2.68
1.13	0.38	7.43	7.35	2.75
1.50	0.38	6.06	6.75	2.53
1.88	0.38	3.33	4.70	1.76
2.25	0.38	3.73	3.53	1.32
2.63	0.38	-0.84	1.44	0.54
3.00	0.38	-4.37	-2.61	-0.98
			Subtotal	29.79
	Shear force from 1m wall at both sides			13.13
				7
			Total (kN/m)	49.91

Table G-2: Sample base shear calculation procedure for single-story structure with pile support at step 1068

X [m]	Δx	τ_1 [kN/m²]	τ_{avg} [kN/m²]	F= τ_{avg}*Δx
-3.00		-0.17		
-2.62	0.38	3.36	1.59	0.60
-2.25	0.38	4.69	4.02	1.51
-1.87	0.38	4.04	4.36	1.64
-1.50	0.38	4.04	4.04	1.51
-1.12	0.38	4.86	4.45	1.67
-0.75	0.38	4.84	4.85	1.82
-0.37	0.38	4.50	4.67	1.75
0.00	0.38	4.69	4.59	1.72
0.38	0.37	5.16	4.93	1.85
0.75	0.37	4.95	5.05	1.89
1.13	0.37	4.73	4.84	1.81
1.50	0.37	5.48	5.11	1.91
1.88	0.37	5.39	5.43	2.04
2.25	0.37	6.17	5.78	2.16
2.63	0.37	6.29	6.23	2.33
3.00	0.37	10.04	8.16	3.06
			sum	29.29
	Shear force from 1m wall at both sides			6.28
				2.37
			Sum	37.94
	Shear force from,		Pile 1	17.24
			Pile 2	36.1
			Pile 3	-0.8
			Total force (kN/m)	90.48

Table G-3[1]: Sample shear force distribution along pile 1 (for single-story structure with pile support at step 1068)

z [m]	Q_{dyn} [kN/m]	$Q_{inertia}$ [kN/m]	$Q_{earthquakec}$= Q_{dyn}- $Q_{inertia}$
-1	-22.64	-5.45	-17.19
-1.39	-15.80	-4.82	-10.98
-1.78	-3.79	-4.07	0.27
-2.17	0.73	-3.21	3.93
-2.57	3.70	-2.28	5.98
-3.25	5.18	-1.13	6.31
-3.92	4.57	-0.33	4.90
-4.6	3.07	0.09	2.98
-5.28	0.98	0.28	0.69
-6.46	0.69	0.16	0.53
-7.64	-0.33	0.06	-0.40
-8.82	-0.27	0.01	-0.28
-10	0.16	0.00	0.16
-10	0.25	-0.01	0.27
-10.75	-0.61	-0.01	-0.60
-11.5	-0.19	-0.01	-0.19
-12.25	0.20	-0.01	0.21
-13	0.16	-0.01	0.16

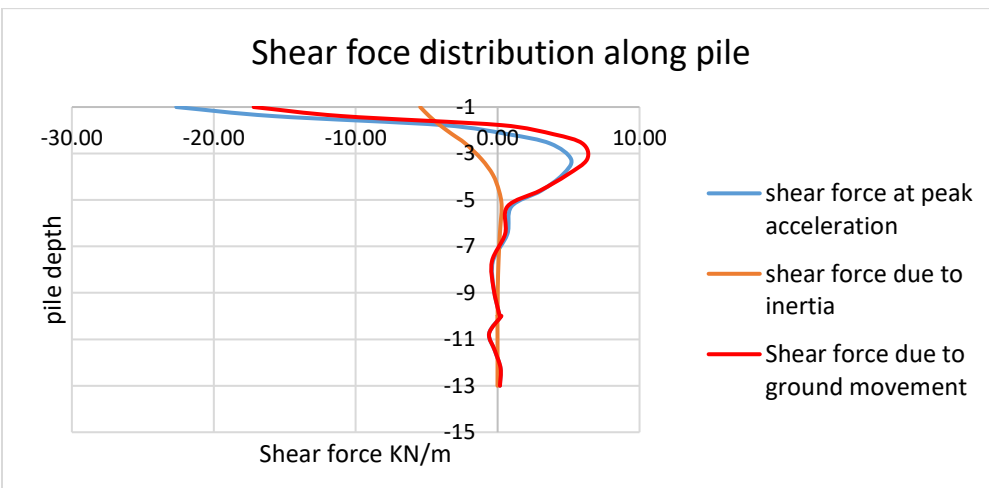

Figure G-1: Shear force distribution along pile 1

[1] Shear force at the pile head at any phase or time step can be directly read from PLAXIS output, hence, it is not necessary to calculate shear distribution for the piles for further calculation in this study.